2023

STAGE-STRUCTURED PREDATOR-PREY INTERACTIONS IN A WARMING WORLD: A CASE STUDY IN RIVERINE ROCK POOLS

Andrew T. Davidson
Virginia Commonwealth University

STAGE-STRUCTURED PREDATOR-PREY INTERACTIONS IN A WARMING WORLD: A CASE STUDY IN RIVERINE ROCK POOLS

A dissertation submitted in partial fulfillment of the requirements for the degree of Doctor of Philosophy at Virginia Commonwealth University.

by

Andrew T. Davidson
Bachelor of Science, Florida State University, 2013
Master of Science, Florida Atlantic University, 2016

Director: Dr. James R. Vonesh,
Assistant Director, Center for Environmental Studies

Virginia Commonwealth University
Richmond, Virginia
July 2023

Acknowledgements

This dissertation would not have been possible without the guidance, support, and assistance of many people. I would like to thank my advisor, Dr. James Vonesh, for his time spent guiding and encouraging me, and shaping me into the scientist I am today. I thank my dissertation committee members, Dr. Sal Agosta, Dr. Brian Byrd, Dr. Kristine Grayson, Dr. Elizabeth Hamman, and Dr. Derek Johnson, for the time and resources they dedicated to making this research possible and honing it into something I can be proud of. I would like to thank all of the past and present members of the Vonesh lab and Team Rock Pool, particularly Michael W. McCoy, C. Ryland Stunkle, and Josh T. Armstrong, for providing enthusiastic support with conducting this research and providing helpful feedback along the way. Last, but perhaps most importantly, I would like to thank my family and my wife, Jenn Davidson, for their immeasurable love, patience, and support along the way.

This dissertation was made possible with funding provided by the National Science Foundation, Award Numbers 1556686 and 1556743, and Virginia Commonwealth University's Integrative Life Sciences Doctoral Program.

Table of Contents

List of Figures

List of Tables

Abstract

STAGE-STRUCTURED PREDATOR-PREY INTERACTIONS IN A WARMING WORLD: A CASE STUDY IN RIVERINE ROCK POOLS

By Andrew T. Davidson, Master of Science

A dissertation submitted in partial fulfillment of the requirements for the degree of Doctor of Philosophy at Virginia Commonwealth University.

Virginia Commonwealth University, 2023

Major Director: Dr. James R. Vonesh,

Assistant Director, Center for Environmental Studies

Warming can impact predator-prey interactions through a variety of mechanisms. For example, warming can both alter the rate at which predators consume prey and the rate prey develop through vulnerable life stages. Thus, the overall effect of warming on consumer-resource interactions will depend upon the strength and asymmetry of warming effects on predator and prey performance. Here, we describe the consequences of these asymmetrical responses to temperature by first developing a simple stage-structured modeling framework, then applying that framework to predation of American rock pool mosquito larvae, *Aedes atropalpus*, by several common predators in riverine rock pools. We then relate our model's predictions about how warming will impact this predator-prey interaction to patterns of rock pool mosquito larval abundance across natural gradients of temperature and predation risk in riverine rock pools. Last, we discuss the consequences of warming for predation of rock pool mosquito larvae by

multiple predator species with different responses to temperature, as well as difficulties with detecting emergent multiple predator effects (MPEs) in a warming world. Our findings suggest that warming accelerated both larval mosquito development and increased dragonfly consumption of larvae. Model simulations suggest that differences in the magnitude and rate of predator and prey responses to warming determined the change in magnitude of the overall effect of predation on prey survival to adulthood. Specifically, we found that depending on which predator species prey were exposed to in the model, the net effect of warming was either an overall reduction or no change in short-term predator-prey interaction strength across a temperature gradient. These findings were mirrored by field observations of rock pool mosquito larvae, which were more abundant at warmer temperatures even in the presence of predators. Last, we found that warming poses a significant challenge when detecting emergent MPEs in multiple-predator systems under current methodologies. Our overall findings highlight a need for better mechanistic understanding of the differential effects of temperature on consumer-resource pairs to accurately predict how warming affects food web dynamics.

1. Stage-structured predator-prey interactions in a warming world: a modeling approach

1.1. Introduction

Climate change is predicted to have wide-ranging effects on the diversity, structure, and composition of ecological communities by modifying the processes and interactions that shape them (Mann et al. 1998; Hughes 2000; Brose et al. 2012). The consequences of warming are especially important for consumer-resource interactions such as predation, which may in turn have strong cascading effects on the dynamics of entire food webs (Petchey et al. 1999; Jochum et al. 2012; Lurgi et al. 2012). Increasing temperatures can have nonlinear impacts on short-term predation strength by modifying the rate at which predators forage for and attack prey (Brown et al. 2004; Rall et al. 2010) while decreasing the time it takes for them to handle and digest prey (Englund et al. 2011; Sentis et al. 2012). Because predation rates generally increase unimodally with temperature (as described by a thermal performance curve; Huey & Stevenson 1979; Huey & Kingsolver 1989) several studies have suggested that climate warming will usually increase short-term interaction strength for ectothermic predators and their prey within a biologically relevant temperature range (Hoekman 2010; Rall et al. 2010; Vucic-Pestic et al. 2010; Karban et al. 2015). Models suggest that this increase in predation pressure can have diverse consequences for community structure and function, including increasing (Fussmann et al. 2014) or decreasing (Vasseur & McCann 2005) community stability, increased top-down control (O'Connor et al. 2009; Hoekman 2010) and other context-dependent changes in community structure (Petchey et al. 2010; Amarasekare 2015; Davidson et al.. 2021).

However, these models make several important simplifying assumptions. Because thermal performance is typically unimodally related to temperature, performance in traits such as predator attack rates or handling times only increase with temperature up to a thermal optimum (T_{opt}), after which performance becomes energetically inefficient and declines (Angilletta 2006; Payne and Smith 2017). Most models assume that predators generally occupy habitats with temperatures that are on average below their thermal optimum, and therefore moderate increases in temperature will typically increase predation rates. In doing so, these models seldom consider – and often explicitly ignore – supraoptimal temperatures above which predation rates should instead decrease. It is also unclear how general these models' predictions are, given that thermal reaction norms are often species- or even population-specific (Dell et al. 2011; Payne and Smith 2017) and can be plastic in many organisms, allowing them to change on time scales within the lifespan of an individual organism (Angilletta 2009). Therefore, for a given predator species, the extent to which warming will increase or decrease the rate at which it forages for prey will depend on current and future habitat conditions, as well as the shape of its thermal performance curve (i.e., the rate of its response, its optimal temperature, etc.) for traits related to foraging (e.g., search rates, digestion, etc.; Englund et al. 2011; Dell et al. 2014).

Further, temperature does not exclusively affect predator physiology. Temperature can influence various elements of prey physiology, including but not limited to the prey's activity, body velocity, growth rate, and ontogeny (Ohlberger 2013; Dell et al. 2014; Payne and Smith 2017) – all traits which may directly or indirectly impact their encounter rate with and/or vulnerability to predators. For example, the rate at which predators consume their prey is often directly but nonlinearly related to prey body size. Predators typically require more time to handle and consume larger prey (Werner and Gilliam 1984; McCoy et al. 2011), and in some cases, prey can grow so large relative to their predators that they reach an eventual size refuge (Paine 1976). On the other hand, individual prey that are too small relative to their predators may go undetected or be undervalued by their predators (Peters 1983; Brose 2010; Vucic-Pestic et al. 2011). Similarly, many prey species, such as fish, amphibians, and insects, undergo ontogenetic niche shifts as they develop, and they may be subject to different sets of predators at different life stages (Werner and Gilliam 1984; Vonesh and Bolker 2005; Briones et al. 2012).

Prey therefore go through different periods of vulnerability to their predators throughout their lifespan, and by increasing growth and/or developmental rates (Brown et al. 2004; Davidowitz and Nijhout 2004), warming may also decrease predation strength by limiting the amount of time that individual prey spend at more vulnerable size or stage classes. Previous studies suggest that these types of temperature-driven changes in the prey's physiological rates can have effects on short-term predation strength that can counterbalance, or even exceed, the effects of temperature-driven changes in predator foraging rates on interaction strength (Culler et al. 2015; Davidson et al. 2021; but see also Pepi et al. 2018). Temperature therefore has the potential to impact predator-prey interactions by influencing both (1) predator traits, such as the rate at which predators forage for, capture, and digest their prey, and (2) prey traits, such as the window of time during which prey are vulnerable to their predators (Davidson et al. 2021). Thus, to accurately predict warming's impacts on predator-prey interactions, it is critical that we consider how temperature simultaneously influences traits that are relevant to the interaction in both predator and prey species (i.e., the shape of their thermal performance curves; Dell et al. 2014, Davidson et al. 2021; Fig. 1.1), as well as the relative importance of these traits in determining the outcome of the interaction.

Here, we explored how the temperature-dependence of predator and prey traits interact to shape predation strength across a thermal gradient using a simple mathematical model. In the model, we consider a predator-prey interaction with a prey species that has stage-based vulnerability as an example of a temperature-dependent prey trait that can influence prey survival in the presence of a predator. Specifically, we consider prey with a predator-vulnerable larval stage and a predator-invulnerable adult stage (Fig. 1.2). This pattern of predator vulnerability occurs in many species of insects and amphibians, where the aquatic larval stage may be subject to different predators than the terrestrial adult (Werner and Gilliam 1984; Vonesh and Bolker 2005). Previous studies suggest that asymmetries in the responses of these types of prey and their predators to temperature can cause changes in short-term interaction strength and predator-prey population dynamics under warming conditions (Culler et al. 2015; Davidson et al. 2021; Pepi et al. 2023). Here, we focused on exploring how short-term predation strength is affected by warming by using the model to explore interactions between stage-structured prey and predators with traits that had asymmetrical (1) rates of response to temperature or (2) optimal temperatures (Fig. 1.1).

1.2. Methods

1.2.1. *Modeling Framework*

To predict how warming will influence short-term interaction strength via its effects on both predator and prey traits, we developed a simple discrete time model (Fig. 1.2). Here, we will describe it in its simplest form, with a generic predator and prey whose thermal responses can be modified *in silico* to produce several simple scenarios to illustrate how temperature modifies these interactions. However, the model can also easily be parameterized using empirical data (as in Ch. 2, Davidson et al. 2021).

The model tracks the survivorship of a single cohort of prey as they develop from a predator-vulnerable stage (i.e., the larva in Fig. 1.2) to a predator-invulnerable stage (i.e., the adult in Fig. 1.2). At each time step, t, a proportion of the prey in the model transition from the predator-vulnerable stage to the predator-invulnerable stage according to a transition rate, r_{dev}.

Predation is incorporated into the model by removing a proportion, p, of the predator-vulnerable prey at each time step. The model runs until all prey have either reached the invulnerable stage, died, or been eaten by the predator – i.e., the model does not currently consider reproduction or long-term population dynamics. The end result is therefore the predicted number of prey from the initial cohort that survive to the predator-invulnerable stage for a given, constant rearing temperature. Model simulations can then be compared across a thermal gradient to predict how predation strength changes across that gradient as predator foraging rates and prey developmental rates change. While temperature can also lead to changes in the growth rates, body size, and developmental of predators with consequences for their consumption rates (Brown et al. 2004), the life history of predator species often operates on different (i.e., longer) time scales than their prey, and thus predation rates are considered static in the model.

To broadly explore the effects of temperature-driven changes in predation rates and prey development rates on the number of prey that survive to adulthood, we ran a series of simulations using the model. In these simulations, we manipulated elements of the predator and prey's response to temperature (i.e., their thermal performance curves) – specifically, (1) the rate at which both species responded to temperature and (2) their optimal temperatures.

1.2.2. Differences in the Rates of Response to Temperature

In the first set of simulations, we considered the effects of warming on a stage-structured predator-prey interaction in which both predator foraging and prey development rates share a thermal optimum but vary in the rate at which they respond to temperature. Variation in the rate of response to temperature occurs naturally between species and within different populations of the same species (Dell et al. 2011) but warming temperatures under climate change may exacerbate these differences between predators and their prey. To explore how this will impact overall short-term predation strength, we consider scenarios where both the predator and prey vary in the degree to which they exhibit either a gradual response to temperature across a broader gradient (i.e., a thermal generalist; the red line in Fig. 1.1a), or a rapid response to temperature within a narrow range (i.e., a thermal specialist; the blue line in Fig. 1.1a).

In these scenarios, we predicted that short-term predation strength (measured as how many prey from a cohort survived the larval stage to the invulnerable adult stage) would depend upon which species responded more readily to temperature. For example, as temperatures increase towards the peak of the thermal performance curve (i.e., from the left in Fig. 1.1), a thermal specialist prey's development rate exhibits a more rapid response to temperature than a thermal generalist predator's foraging rates do (Fig. 1.1a), so short-term predation strength should decrease as temperature rises, instead of increasing as many models assume. However, in the opposite scenario, where the prey is a thermal generalist and the predator is a thermal specialist, the opposite should be true – short-term predation strength should increase in line with general model predictions. Here, we consider only temperatures below both species' thermal optimum. Mean temperatures that substantially exceed that thermal optimum will likely have more detrimental effects on thermal specialists, which are adapted for a narrower range of temperatures (Addo-Bediako et al. 2000; Markle and Kozak 2018).

To simulate the effects of warming on interactions between predators and prey with different rates of response to temperature, we generated thermal performance curves for both the predator and prey using the Arrhenius equation (Brown et al. 2004):

$$(1) \quad rate = R_0 e^{-\frac{E_a}{kT}}$$

where R_0 is a species-specific scaling constant, E_a is activation energy, k is Boltzmann's constant (8.617e-5), and T is temperature, in degrees Celsius. The Arrhenius equation is widely used to describe the rising component (i.e., temperatures up to the optimum) of temperature-dependence of predation (Brown et al. 2004), but it is important to note that it does not include the decrease in performance seen at supraoptimal temperatures. Thus, here, we will only consider temperatures up to the optimum.

The shape of the Arrhenius curve is determined by several variables, but we chose to focus here on the parameter E_a, activation energy. From a biochemical perspective, activation energy is the minimum amount of energy required for biological reactions, such as those involved in metabolism, to occur (Brown et al. 2004). From a mathematical perspective, however, activation energy determines the rate at which trait performance increases with temperature, or its slope. Studies suggest that the mean value for activation energy across most animal taxa is around 0.65 eV (Brown et al. 2004; Savage et al. 2004; Dell et al. 2011), however it can vary between 0.2 and 1.2 eV (Dell et al. 2011). Therefore, to simulate predators and prey with varying thermal responses, we generated thermal performance curves with a range of values for activation energy between 0.2 and 1.2 eV (Fig. 1-3a. We determined values for R_0, the species-specific scaling constant, by solving Eqn. 1 numerically so that at the lowest temperature present in the model (20°C), r_{dev} and p were both equal to a baseline value of 0.025. As temperatures increased beyond that initial point in the model, r_{dev} and p increased according to their activation energy.

The model simulations were carried out in this way with different combinations of values for activation energy (E_a) for the predator and prey, thereby allowing for scenarios where the predator and prey responded in similar manners to temperature, or where either the predator or prey had a more rapid response to temperature. Using the model, we predicted the effects of increasing temperature and the rate of the predator and preys' thermal responses on prey survival, across a range of temperatures between 20 and 44°C, with a single predator present and a starting prey density of 1000 individuals.

1.2.3. Differences in Optimal Temperature

In the second set of scenarios, we considered how predation strength will be impacted if the predator's foraging rates and the prey's development rates have different optimal temperatures (Fig. 1.1b). Climate change is predicted to cause expansion and contraction of different species' ranges, as environmental conditions in different regions become more or less suitable to their needs (Parmesan 2006; Brown et al. 2016). This could cause invasion of novel predators or prey into previously unsuitable habitats for their thermal niche. In these situations, novel interactions could emerge between species that have strongly mismatched optimal temperatures for basic activities, such as foraging, growth, and development.

We predicted that under a warming climate, conditions will favor whichever species possesses the higher optimal temperature (as in Pepi et al. 2023). For example, as habitats warm, at certain temperatures the species with the higher thermal optimum may experience increasing trait performance (the red line in Fig. 1.1b) while cooler-adapted species instead experience declines in trait performance (the blue line in Fig. 1.1b). In this way, a warm-adapted predator moving into habitat occupied by cool-adapted prey may have stronger impacts on those prey as temperatures rise, whereas a cool-adapted predator may have weaker impacts on a warm-adapted prey moving into its range as temperatures rise.

To simulate how warming will influence these types of interactions, we generated thermal performance curves using a Gaussian curve instead of the Arrhenius equation (Angilletta 2006):

$$(2) \quad rate = ae^{-0.5(\frac{|T-T_{opt}|}{c})^2}$$

where a is the height of the curve's peak, T is temperature, T_{opt} is the curve's optimal temperature and c is the width of the curve. Gaussian curves are similar to an Arrhenius curve and have also been used to model thermal reaction norms, however, they allow for predictions of performance at supraoptimal temperatures.

Model simulations were carried out in a similar manner as described above, with a range of temperatures between 10 and 40°C, a single predator, and 1000 prey present initially (Fig. 1-3b). However, a and c were set to constant values (0.15 and 7.5, respectively), and T_{opt}, the optimal temperature, varied between 15 and 35°C for both the predator and its prey across simulations. This effectively created variation in the shape of the predator and prey's thermal response between simulations, as described by Eqn. 2 (and shown in Fig. 1.3b). Using these simulations, we generated predictions about how prey survival will vary with temperature under scenarios where predator foraging and prey development rates have similar optimal temperatures, or where either the predator or prey has a higher optimal temperature.

1.3. Results

1.3.1. Differences in the Rate of Response to Temperature

Temperature's effects on prey survival varied depending on the predator and prey's activation energy (E_a) for consumption and development, respectively (Fig. 1.4a). When the predator's response to temperature was substantially faster than the prey's (i.e., the predator had a higher activation energy than the prey), prey survival generally decreased as temperature increased (Fig. 1.4b; e.g., prey $E_a = 0.35$ eV and predator $E_a = 0.95$ eV). Conversely, when the prey responded more rapidly to changes in temperature than the predator (i.e., the prey had a higher activation energy than the predator), prey survival generally increased with temperature (Fig. 1.4b; e.g., prey $E_a = 0.95$ eV and predator $E_a = 0.35$ eV).

Temperature-driven increases or decreases in prey survival were roughly proportional depending on which species had the higher rate of response (Fig. 1.4b). For example, in scenarios where the prey's rate of response to temperature greatly outpaced the predator's (predator $E_a = 0.35$ eV; prey $E_a = 0.95$ eV), prey survival increased by a factor of 4.5X, from 128.1 individuals at 20°C to 579.0 individuals at 44°C. Similarly, in the opposite scenario (predator $E_a = 0.95$ eV; prey $E_a = 0.35$ eV) prey survival decreased by a factor of 3.9X, from 128.0 individuals at 20°C to 32.9 individuals at 44°C.

Because of these differences, scenarios in which the prey's activation energy was higher than the predator's tended to produce considerably larger net changes in the number of prey that survived across a temperature gradient (Fig. 1.4). For example, in the above two scenarios, when the prey's activation energy was higher than the predator's (predator $E_a = 0.35$ eV; prey $E_a = 0.95$ eV), an average of 450.9 more individual prey survived at the warmest temperatures (44°C) as compared to the coolest (20°C). On the other hand, when the predator's activation energy was substantially higher than the prey's (predator E_a = 0.95 eV; prey E_a = 0.35 eV), only 95.1 fewer prey survived on average at the warmest temperatures (44°C) as compared to the coolest (20°C).

1.3.2. Differences in Optimal Temperature

Temperature's effects on prey survival also varied depending on the optimal temperature (T_{opt}) for the predator's foraging rates and the prey's development rate (Fig. 1.5a). When the predator's T_{opt} was higher than the prey's, prey survival generally decreased as temperature increased (Fig. 1.5b; e.g., prey T_{opt} = 15°C and predator T_{opt} = 35°C). Conversely, when the prey's T_{opt} was higher than the predator's, prey survival generally increased with temperature (Fig. 1.5b; e.g., prey T_{opt} = 35°C and predator T_{opt} = 15°C). When both the predator and prey had similar rates of response to temperature, temperature had comparatively smaller effects on prey survival than when the rates of response were mismatched (Fig. 1.4b; Fig. 1.5b).

Unlike the model simulations where we manipulated rates of response to temperature, mismatches in optimal temperature led to symmetrical net changes in prey survival across a temperature gradient, regardless of which species had the higher optimal temperature. For example, in simulations where the predator's T_{opt} was lower than the prey's (prey T_{opt} = 35°C and predator T_{opt} = 15°C), an average of 913.6 prey survived at 10°C, while only an average of 4.4 prey survived at 40°C (a net decrease of 909.2 ind.; Fig. 1.5b). Similarly, when the predator's T_{opt} was higher than the prey's (prey T_{opt} = 15°C and predator T_{opt} = 35°C), an average of 4.4 prey survived at 10°C, while 913.6 prey survived on average at 40°C (a net increase of 909.2 ind.; Fig. 1.5b).

1.4. Discussion

Due to temperature's broad influence on organismal physiology, warming may impact ecological communities in ways that are challenging to predict. In the case of predator-prey interactions, this challenge stems partially from the fact that warming can affect both predator and prey traits in ways that may act in opposition to one another (Dell et al. 2014; Culler et al. 2015; Davidson et al. 2021). Thus, the net effect of warming on any given predator-prey interaction will depend on how both predator and prey respond to temperature. Here, we highlight the importance of considering temperature's impacts on both predator and prey physiology by providing further evidence that warming-driven changes in prey physiology can mitigate or even counteract warming-driven increases in predator foraging rates. To do so, we considered a simple predator-prey system in which temperature influences both predator foraging rates and the development rate of prey from a predator-vulnerable juvenile stage to a predator-invulnerable adult stage (as seen in many amphibian, reptile, and insect species; Werner and Gilliam 1984; McCoy et al. 2011).

Our model simulations suggested that warming can cause increases, decreases, or no change in prey survival depending on the joint effects of temperature on both predator and prey. For example, when prey development rate responded more rapidly to temperature than predator foraging rates did, prey survival increased with temperature (Fig. 1.4). When predator foraging rates responded more rapidly to temperature, the opposite occurred – prey survival decreased with temperature (Fig. 1.4). In nature, these scenarios could arise if one species was a thermal specialist while the other was a thermal generalist. Thus, it may be important to consider the thermal niche of predator and prey species when predicting how warming will impact different predator-prey interactions.

Warming is also predicted to drive migration of species from areas where conditions have become thermally unfavorable to regions better suited to their needs (Parmesan 2006; Brown et al. 2016). In these cases, species that are better adapted to warmer climates might be driven to habitats that were previously dominated by cool-adapted species. Depending on each species' thermal optimum, this may lead to situations where cool-adapted predators are exposed to warm-adapted prey, or vice versa. In these interactions, our model simulations suggested that the species with the higher thermal optimum will generally be favored. For example, warm-adapted prey tended to have greater survival when exposed to cool-adapted predators, whereas cool-adapted prey had poorer survival when exposed to warm-adapted predators (Fig. 1.5).

Importantly, the degree to which prey survival increased or decreased in our simulations depended on the type of mismatch that was present between the predator and prey's thermal niche. When both predator and prey shared a thermal optimum but differed in their rate of response to temperature, differences in that rate generally led to proportional increases or decreases in prey survival. For example, when the predator's activation energy was higher than the prey's, prey survival was halved at warmer temperatures relative to cooler ones, whereas when the prey's activation energy was higher, prey survival doubled across the temperature gradient (Fig. 1.4). This often resulted in substantially larger increases in prey survival in the latter scenarios than decreases in prey survival in the former scenarios. On the other hand, when the predator and prey had a similar rate of response to temperature but different optimal temperatures, changes in prey survival were symmetrical depending on which species had the higher optimal temperature (Fig. 1.5). Thus, cases where prey development responds more readily to temperature than predator foraging rates (due to thermal specialization or otherwise) may be biased towards greater net changes in prey survival than if predator foraging rates had the stronger temperature response.

Importantly, this study focuses on predicting how warming will impact short-term predation strength (i.e., the number of prey that survive a predator-vulnerable juvenile stage to a predator-invulnerable adult stage). It is thus unclear how long-term predator-prey population dynamics will be impacted by warming in these types of interactions. However, our findings are consistent with similar studies exploring the consequences of asymmetrical temperature responses for longer-term stage-structured predator-prey population dynamics. Specifically, Pepi et al. (2023) found that in interactions between predatory ants and caterpillar prey (*Formica lasioides* and *Arctia virginalis*, respectively) warmer conditions produced lower equilibrium densities of caterpillars, because *F. lasioides* possesses a higher optimal temperature. Thus, while Pepi et al. (2023) did not also explore asymmetries in the rate of response to temperature as we do here, we suspect that the short-term consequences of warming for these types of interactions may be similar in the long-term.

As the global climate shifts, the interactions that structure ecological communities are changing with it in ways that are often difficult to predict (Beveridge et al. 2010; Brose et al. 2012). Our simple models suggest that by modifying both predator foraging rates and prey development rates, increasing temperatures could in theory increase, decrease, or have no effect on short-term predator-prey interaction strength. While we focus here on stage-dependent predator-prey interactions where prey development rate is the primary temperature-dependent prey trait considered, other prey traits can also respond to temperature in ways that are relevant to their interaction with predators. For example, prey body velocity, growth rate, and behavior can all be influenced by temperature in ways that can affect their interactions with predators

(Angilletta 2009; Barton and Schmitz 2009; Dell et al. 2014). Thus, we stress the importance of incorporating an understanding of how both predator and prey traits respond to temperature when predicting the impacts of climate change on predator-prey interactions.

1.5. References

Addo-Bediako, A., Chown, S. L., & Gaston, K. J. (2000). Thermal Tolerance, Climatic Variability and Latitude. *Proceedings of the Royal Society B: Biological Sciences*, *267*(1445), 739–745.

Amarasekare, P. (2015). Effects of temperature on consumer-resource interactions. *Journal of Animal Ecology*, *84*(3), 665–679. https://doi.org/10.1111/1365-2656.12320

Angilletta Jr., M. J. (2009). *Thermal Adaptation: A Theoretical and Empirical Synthesis*. Oxford Academic.

Barton, B. T., & Schmitz, O. J. (2009). Experimental warming transforms multiple predator effects in a grassland food web. *Ecology Letters*, *12*(12), 1317–1325. https://doi.org/10.1111/j.1461-0248.2009.01386.x

Beveridge, O. S., Humphries, S., Petchey, O. L., Beveridge, O. S., Humphries, S., & Petchey, O. L. (2010). The interacting effects of temperature and food chain length on trophic abundance and ecosystem function. *Journal of Animal Ecology*, *79*(3), 693–700.

Briones, J. C., Tsai, C.-H., Nakazawa, T., Sakai, Y., Papa, R. D. S., Hsieh, C., & Okuda, N. (2012). Long-Term Changes in the Diet of *Gymnogobius isaza* from Lake Biwa, Japan: Effects of Body Size and Environmental Prey Availability. *PLoS ONE*, *7*(12). https://doi.org/10.1371/journal.pone.0053167

Brose, U., Dunne, J. A., Montoya, J. M., Petchey, O. L., Schneider, F. D., & Jacob, U. (2012). Climate change in size-structured ecosystems. *Proceedings of the Royal Society B: Biological Sciences*, *367*, 2903–2912.

Brown, J. H., Gillooly, J. F., Allen, A. P., Savage, V. M., & West, G. B. (2004). Toward a metabolic theory of ecology. *Ecology*, *85*(7), 1771–1789. https://doi.org/Doi 10.1890/03-9000

Brown, C. J., O'Connor, M. I., Poloczanska, E. S., Schoeman, D. S., Buckley, L. B., Burrows, M. T., Duarte, C. M., Halpern, B. S., Pandolfi, J. M., Parmesan, C., & Richardson, A. J. (2016). Ecological and methodological drivers of species' distribution and phenology responses to climate change. *Global Change Biology*, *22*(4), 1548–1560. https://doi.org/10.1111/gcb.13184

Culler, L. E., Ayres, M. P., & Virginia, R. A. (2015). In a warmer Arctic, mosquitoes avoid increased mortality from predators by growing faster. *Proceedings of the Royal Society B: Biological Sciences*, *282*(1815), 20151549. https://doi.org/10.1098/rspb.2015.1549

Davidowitz, G., & Nijhout, H. F. (2004). The Physiological Basis of Reaction Norms: The Interaction Among Growth Rate, the Duration of Growth and Body Size. *Integrative and Comparative Biology*, *44*(6), 443–449. https://doi.org/10.1093/icb/44.6.443

Davidson, A. T., Hamman, E. A., McCoy, M. W., & Vonesh, J. R. (2021). Asymmetrical effects of temperature on stage-structured predator–prey interactions. *Functional Ecology*, *35*(5). https://doi.org/10.1111/1365-2435.13777

Dell, A. I., Pawar, S., & Savage, V. M. (2011). Systematic variation in the temperature dependence of physiological and ecological traits. *Proceedings of the National Academy of Sciences*, *108*(26), 10591–10596. https://doi.org/10.1073/pnas.1015178108

Dell, A. I., Pawar, S., & Savage, V. M. (2014). Temperature dependence of trophic interactions are driven by asymmetry of species responses and foraging strategy. *Journal of Animal Ecology*, *83*(1), 70–84. https://doi.org/10.1111/1365-2656.12081

Englund, G., Öhlund, G., Hein, C. L., & Diehl, S. (2011). Temperature dependence of the functional response. *Ecology Letters*, *14*(9), 914–921. https://doi.org/10.1111/j.1461-0248.2011.01661.x

Fussmann, K. E., Schwarzmüller, F., Brose, U., Jousset, A., & Rall, B. C. (2014). Ecological stability in response to warming. *Nature Climate Change*, *4*(3), 206–210. https://doi.org/10.1038/nclimate2134

Hoekman, D. (2010). Turning up the heat: temperature influences the relative importance of top-down and bottom-up effects in pitcher plant inquiline communities. *Ecology*, *91*(10), 100521032119033. https://doi.org/10.1890/10-0260

Huey, R. B., & Kingsolver, J. G. (1989). Evolution of thermal sensitivity of ectotherm performance. *Trends In Ecology & Evolution*, *4*(5), 131–135. https://doi.org/10.1016/0169-5347(89)90211-5

Huey, R. B., & Stevenson, R. D. (1979). Integrating Thermal Physiology and Ecology of Ectotherms: A Discussion of Approaches. *American Zoologist*, *19*(1), 357–366.

Hughes, L. (2000). Biological consequences of global warming: is the signal already apparent? *Trends in Ecology & Evolution*, *15*(2), 56–61. https://doi.org/10.1016/S0169-5347(99)01764-4

Jochum, M., Schneider, F. D., Crowe, T. P., Brose, U., & O'Gorman, E. J. (2012). Climate-induced changes in bottom-up and top-down processes independently alter a marine ecosystem. *Philosophical Transactions of the Royal Society B: Biological Sciences*, *367,* 2962–2970. https://doi.org/10.1098/rstb.2012.0237

Karban, R., Grof-Tisza, P., Mcmunn, M., Kharouba, H., & Huntzinger, M. (2015). Caterpillars escape predation in habitat and thermal refuges. *Ecological Entomology*, *40*(6), 725–731. https://doi.org/10.1111/een.12243

Lurgi, M., López, B. C., & Montoya, J. M. (2012). Novel communities from climate change. *Philosophical Transactions of the Royal Society B: Biological Sciences*, *367*, 2913–2922. https://doi.org/10.1098/rstb.2012.0238

Mann, M. E., Bradley, R. S., & Hughes, M. K. (1998). Global-scale temperature patterns and climate forcing over the past six centuries. *Nature*, *392*(6678), 779–787. https://doi.org/10.1038/33859

Markle, T. M., & Kozak, K. H. (2018). Low acclimation capacity of narrow-ranging thermal specialists exposes susceptibility to global climate change. *Ecology and Evolution*, *8*(9), 4644–4656. https://doi.org/10.1002/ece3.4006

McCoy, M. W., Bolker, B. M., Warkentin, K. M., & Vonesh, J. R. (2011). Predicting Predation through Prey Ontogeny Using Size-Dependent Functional Response Models. *The American Naturalist*, *177*(6), 752–766. https://doi.org/10.1086/659950

O'Connor, M. I. (2009). Warming Strengthens an Herbivore-Plant Interaction. *Ecology*, *90*(2), 388–398. https://doi.org/10.1890/08-0034.1

Ohlberger, J. (2013). Climate warming and ectotherm body size - from individual physiology to community ecology. *Functional Ecology*, *27*, 991–1001. https://doi.org/10.1111/1365-2435.12098

Paine, R. T. (1976). Size-Limited Predation: An Observational and Experimental Approach with the Mytilus-Pisaster Interaction. *Ecology*, *57*(5), 858–873.

Parmesan, C. (2006). Ecological and evolutionary responses to recent climate change. In *Annual Review of Ecology, Evolution, and Systematics* (Vol. 37, pp. 637–669). https://doi.org/10.1146/annurev.ecolsys.37.091305.110100

Payne, N. L., & Smith, J. A. (2017). An alternative explanation for global trends in thermal tolerance. *Ecology Letters*, *20*(1), 70–77. https://doi.org/10.1111/ele.12707

Pepi, A., Grof-Tisza, P., Holyoak, M., & Karban, R. (2018). As temperature increases, predator attack rate is more important to survival than a smaller window of prey vulnerability. *Ecology*. https://doi.org/10.1002/ecy.2356

Pepi, A., Hayes, T., & Lyberger, K. (2023). Thermal asymmetries influence effects of warming on stage and size-dependent predator–prey interactions. *Theoretical Ecology*. https://doi.org/10.1007/s12080-023-00555-3

Petchey, O. L., McPhearson, P. T., Casey, T. M., & Morin, P. J. (1999). Environmental warming alters food web structure and ecosytem function. *Nature*, *402*, 69–72.

Peters, R. H. (1983). *The Ecological Implications of Body Size*. Cambridge University Press.

Rall, B. C., Vucic-Pestic, O., Ehnes, R. B., Emmerson, M. C., & Brose, U. (2010). Temperature, predator–prey interaction strength and population stability. *Global Change Biology*, *16*, 2145–2157. https://doi.org/10.1111/j.1365-2486.2009.02124.x

Savage, V. M., Gillooly, J. F., Brown, J. H., West, G. B., & Charnov, E. L. (2004). Effects of Body Size and Temperature on Population Growth. *The American Naturalist*, *163*(3), 429–441. https://doi.org/10.1086/381872

Sentis, A., Hemptinne, J.-L. L., & Brodeur, J. (2012). Using functional response modeling to investigate the effect of temperature on predator feeding rate and energetic efficiency. *Oecologia*, *169*(4), 1117–1125. https://doi.org/10.1007/s00442-012-2255-6

Vasseur, D. A., & McCann, K. S. (2005). A mechanistic approach for modeling temperature-dependent consumer-resource dynamics. *American Naturalist*, *166*(2), 184–198. https://doi.org/10.1086/431285

Vonesh, J. R., & Bolker, B. M. (2005). Compensatory larval responses shift trade-offs associated with predator-induced hatching plasticity. *Ecology*, *86*(6), 1580–1591. https://doi.org/10.1890/04-0535

Vucic-Pestic, O., Rall, B. C., Kalinkat, G., & Brose, U. (2010). Allometric functional response model: Body masses constrain interaction strengths. *Journal of Animal Ecology*, *79*(1), 249–256. https://doi.org/10.1111/j.1365-2656.2009.01622.x

Werner, E. E., & Gilliam, J. F. (1984). The Ontogenetic Niche and Species Interactions in Size-Structured Populations. *Annual Review of Ecology and Systematics*, *15*, 393–425.

1.6. Figures and Tables

Fig. 1.1. Example thermal performance curves for two different species: Species 1 (red) and Species 2 (blue). In the first example, a) trait performance in Species 1 has a stronger rate of response to temperature than in Species 2, which may occur due to a higher degree of thermal specialization in Species 1. In the second example, b) Species 1 and 2 have different optimal temperatures for trait performance. Specifically, Species 1 is more cool-adapted whereas Species 2 is more warm-adapted. In both scenarios, both species response to temperature in different ways, which can lead to changes in interaction strength if Species 1 is a predator of Species 2, or vice versa.

Fig. 1.2. A schematic of the simple mechanistic model used by this paper to describe and model temperature-driven changes in interaction strength when prey vulnerability to predators depends on life stage. Specifically, juvenile prey are vulnerable to predators, whereas adult prey are not. In the model, prey develop from a juvenile to adult life stage at a rate described by the parameter r_{dev}, but a proportion of juvenile prey are also consumed by the predator according to the rate p. Both r_{dev} and p can be manipulated in the model and described as functions of temperature, similar to those illustrated in Fig. 1.

Fig. 1.3. Thermal performance curves used to describe prey development rate (r_{dev}) and predation rate (p) in the stage-structured model. In panel a), the curves differ in the rate of response to temperature (E_a), while in panel b), the three curves differ in their optimal temperature (T_{opt}). In the subsequent sections, we ran two sets of simulations using a) combinations of each value of E_a for the predator and prey or b) combinations of each value of T_{opt} for the predator and prey species.

Fig. 1.4. Prey survival as predicted by the stage-structured model when the rates of response (E_a) of prey development (r_{dev}) and predation rate (p) were manipulated. Panel a) shows mean prey survival across the thermal gradient for different combinations of values for predator and prey E_a, while panel b) shows how prey survival changes across a temperature gradient for different combinations of values for predator and prey E_a.

Fig. 1.5. Prey survival as predicted by the stage-structured model when the optimal temperature (T_{opt}) of prey development (r_{dev}) and predation rate (p) were manipulated. Panel a) shows mean prey survival across the thermal gradient for different combinations of values for predator and prey T_{opt}, while panel b) shows how prey survival changes across a temperature gradient for different combinations of values for predator and prey T_{opt}.

Fig. 1.1.

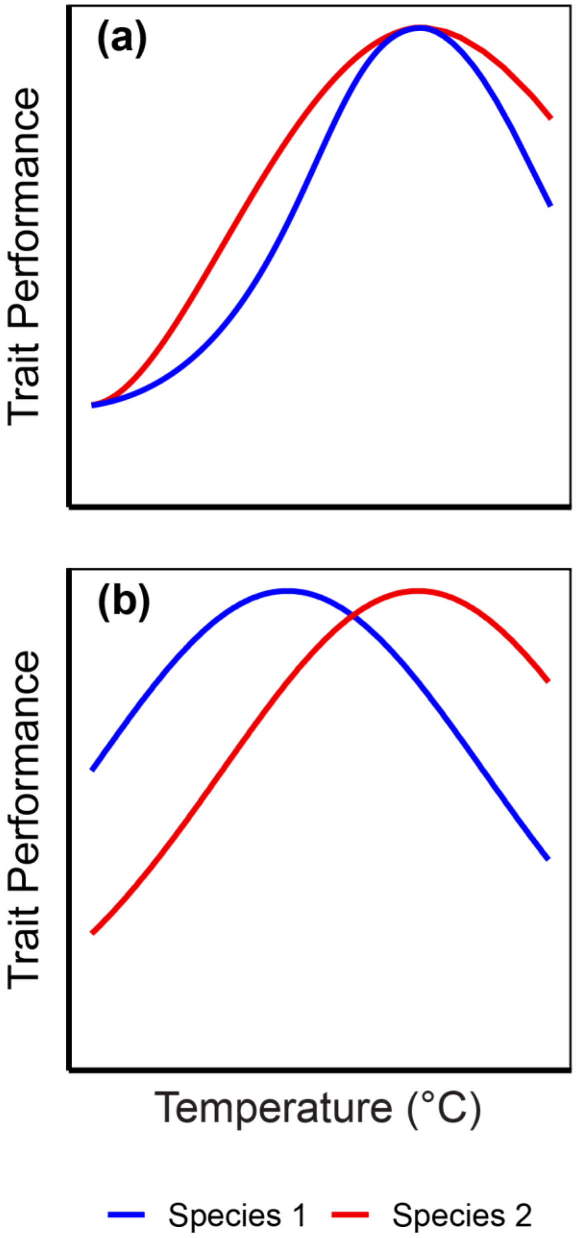
(a)
(b)
Trait Performance
Trait Performance
Temperature (°C)
Species 1
Species 2

Fig. 1.2.

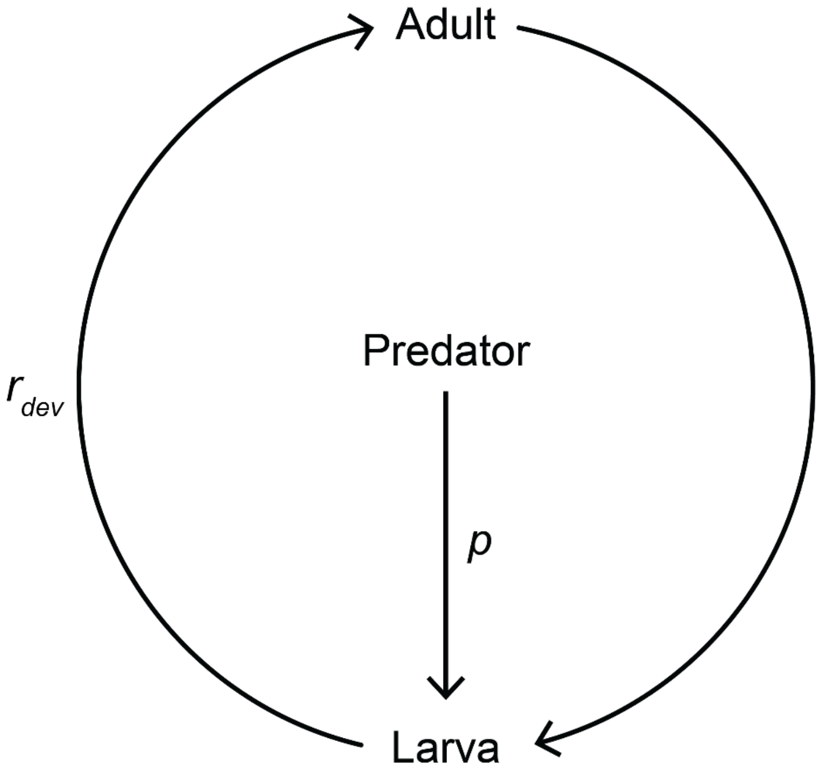

Fig. 1.3.

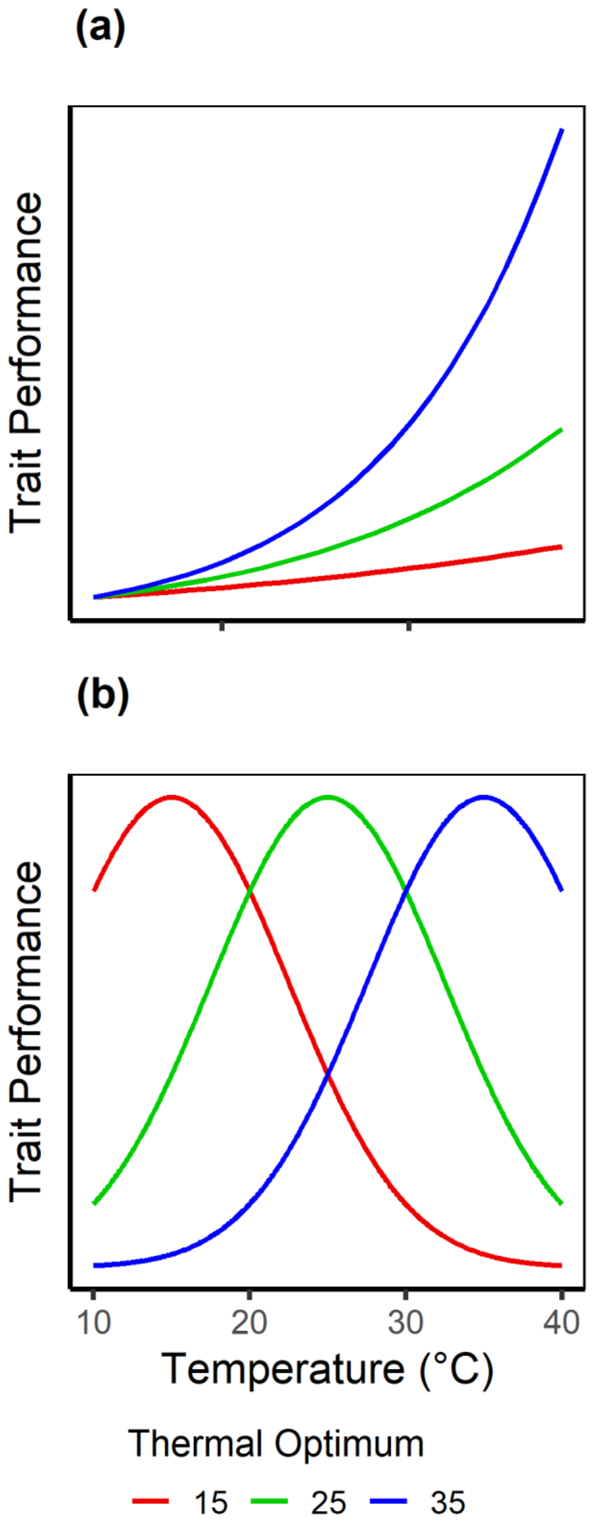
(a)
Trait Performance
(b)
Trait Performance
10
20
30
40
Temperature (°C)
Thermal Optimum
15
25
35

Fig. 1.4.

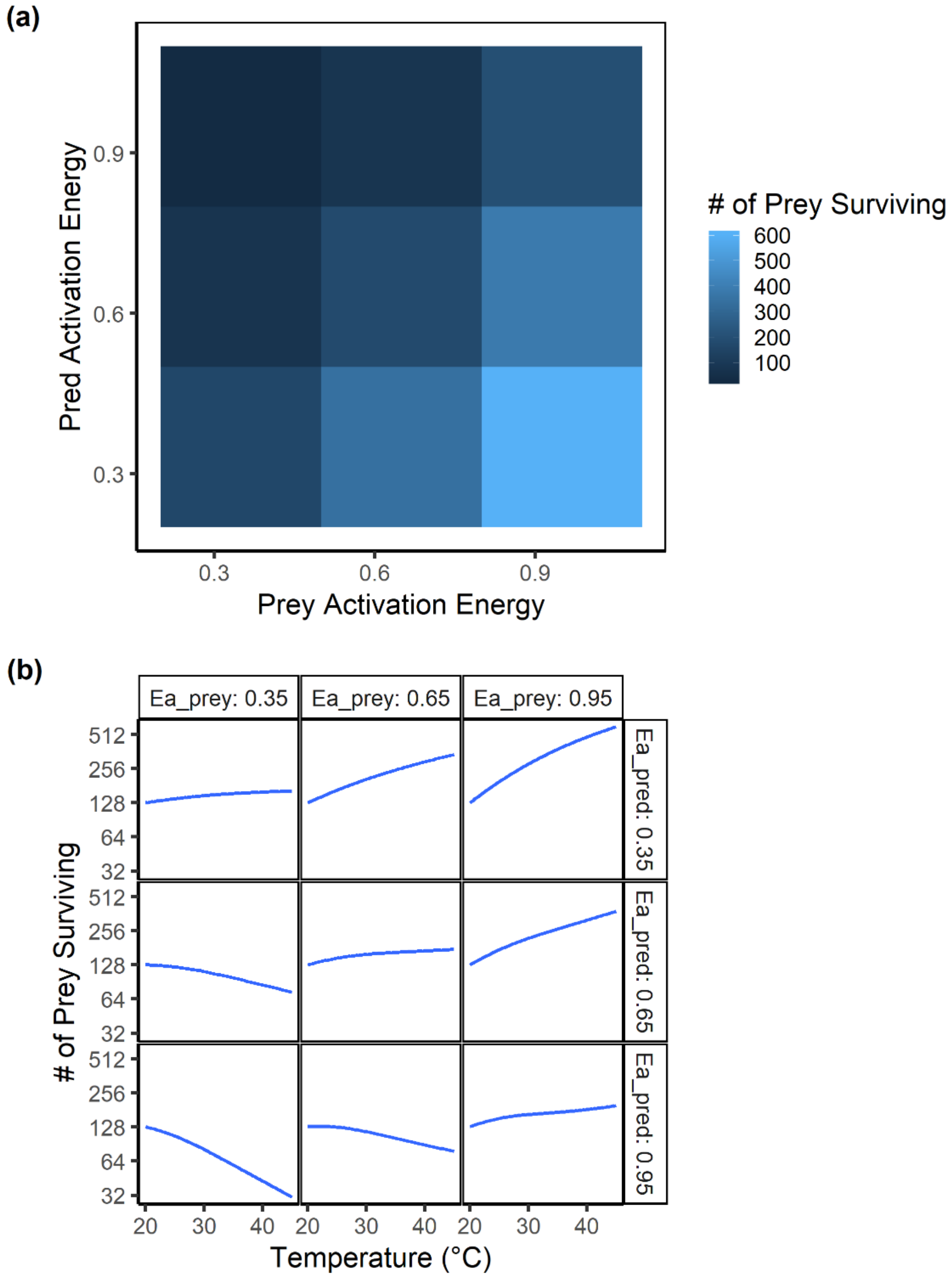

(a)
# of Prey Surviving
600
500
400
300
200
100
Pred Activation Energy
0.9
0.6
0.3
0.3
0.6
0.9
Prey Activation Energy
(b)
Ea_prey: 0.35
Ea_prey: 0.65
Ea_prey: 0.95
Ea_pred: 0.35
Ea_pred: 0.65
Ea_pred: 0.95
# of Prey Surviving
512
256
128
64
32
20
30
40
Temperature (°C)

Fig. 1.5.

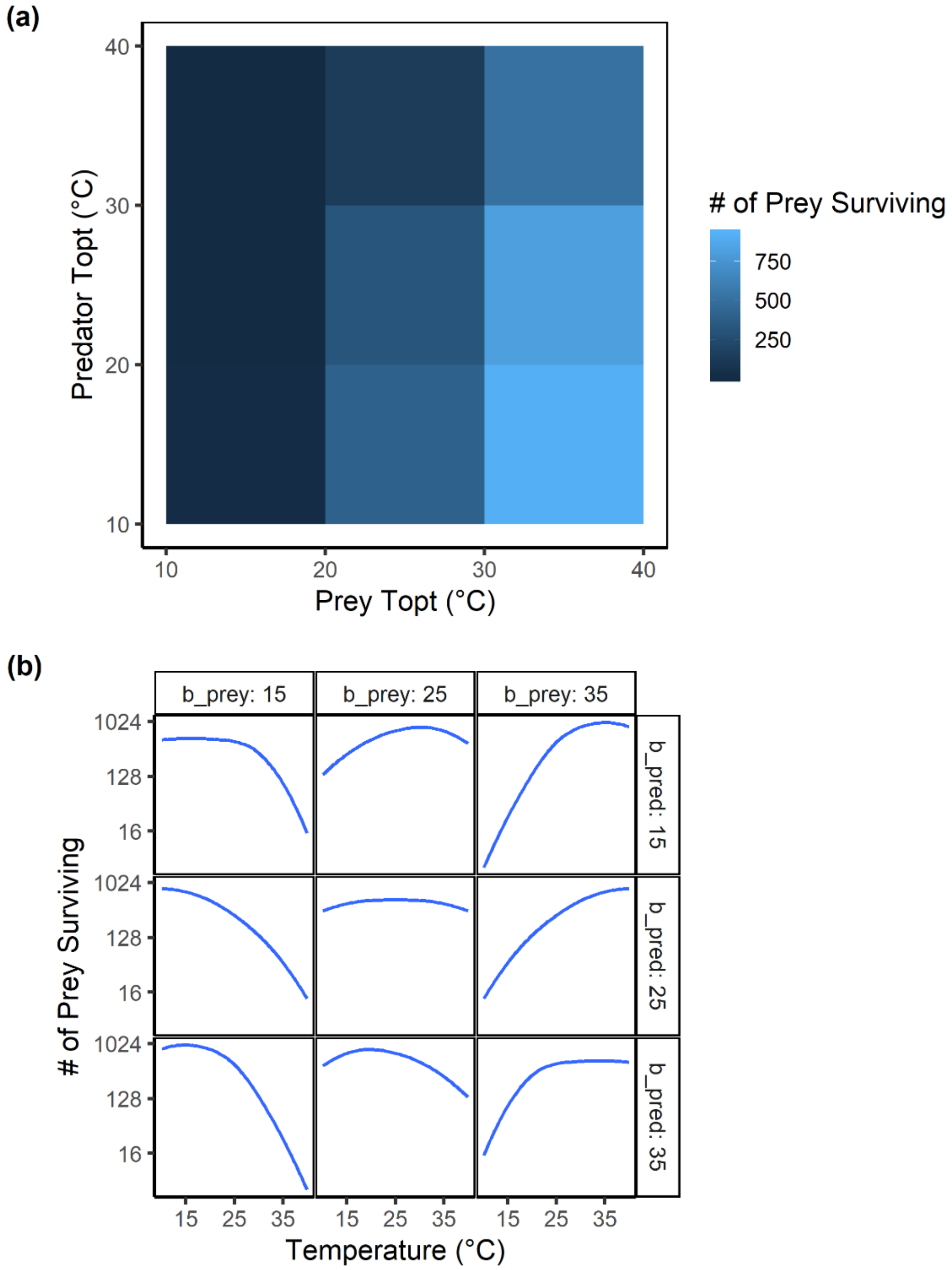
(a)
Predator Topt (°C)
40
30
20
10
Prey Topt (°C)
10
20
30
40
# of Prey Surviving
750
500
250
(b)
b_prey: 15
b_prey: 25
b_prey: 35
b_pred: 15
b_pred: 25
b_pred: 35
# of Prey Surviving
1024
128
16
Temperature (°C)
15
25
35

2. Asymmetrical effects of temperature on stage-structured predator-prey interactions

*This manuscript is published in Functional Ecology as Davidson et al. 2021 – see References.

2.1. Introduction

Temperature is a critical determinant of physiological rates in ectotherms, setting the pace at which those organisms perform necessary activities such as foraging, growth, and reproduction (Brown et al. 2004). Temperature therefore has repercussions for processes that shape ecological communities, particularly consumer-resource interactions (Petchey et al. 1999; Jochum et al. 2012; Lurgi et al. 2012). In predator-prey interactions between ectothermic animals, increasing temperatures can have nonlinear impacts on short-term interaction strength by modifying the rate at which predators forage (Brown et al. 2004; Rall et al. 2010), increasing predator attack rates on prey while decreasing the time it takes to handle prey (Englund et al. 2011; Sentis et al. 2012). Because foraging rates generally increase unimodally with temperature (as described by a thermal performance curve; Huey & Stevenson 1979; Huey & Kingsolver 1989), a number of studies have suggested that climate warming will usually increase short-term interaction strength for ectothermic predators and their prey within a biologically relevant temperature range (Hoekman 2010; Rall et al. 2010; Vucic-Pestic et al. 2010; Karban et al. 2015). Models suggest that this increase in interaction strength will have diverse consequences for community structure and function, including increasing (Fussmann et al. 2014) or decreasing (Vasseur and McCann 2005) community stability, increased top-down control (O'Connor et al. 2009; Hoekman 2010), and other context-dependent changes in community structure (Petchey et al. 2010; Amarasekare 2015).

Many models of warming's impacts on predator-prey systems rely on the assumption that warming will generally increase interaction strength, but in doing so, they fail to account for potential temperature effects on prey traits that are relevant to the predator-prey interaction (e.g., Dell et al. 2014). For example, many ectothermic animal species also undergo ontogenetic niche shifts, including insects, amphibians, reptiles, and fish, in the form of either shifts in habitat or resource use, or a complex life cycle with discrete life stages (Werner and Gilliam 1984). It is widely known that temperature can accelerate the rate at which organisms grow and develop to varying degrees (Kingsolver et al. 2011; Quinn 2017; Rebaudo & Rabhi 2018). This is crucial, because the vulnerability of many prey species to their predators strongly depends on prey body size and/or life stage (Werner & Gilliam 1984; McCoy & Bolker 2008; Brose 2010; McCoy et al. 2011), and thus, warming has the potential to narrow the window of time that prey spend in vulnerable periods of their ontogeny (McCoy et al. 2011). Therefore, warming can have both positive and negative impacts on prey survival (and thus short-term interaction strength), by simultaneously acting on both predator foraging rates and prey development rates. Predicting the direction and magnitude of temperature-driven changes in predator-prey interaction strength thus requires considering the thermal responses of both predator and prey traits (e.g., Hoekman 2010; Rall et al. 2010; Vucic-Pestic et al. 2010; Karban et al. 2015).

When predator and prey traits have different thermal responses, interaction strength may deviate from predictions that assume shared thermal response curves. For example, consider a simple system where a predator and prey share an optimal temperature for foraging and development, respectively, but differ in the rate and magnitude of their response to temperature (Fig. 2.1). If predator foraging traits respond more strongly than prey development, short-term interaction strength should increase with temperature, as previous theory predicts (Fig. 2.1, red lines; Dell et al. 2014). However, if prey development rate has a stronger response to temperature than predator foraging traits, short-term interaction strength may actually decrease across a thermal gradient, with more prey surviving at warmer temperatures than cooler ones (Fig. 2.1, blue lines; Dell et al. 2014)., Lastly, the effects of temperature on prey survival may be equivocal when predator and prey traits respond similarly, resulting in no change in interaction strength (Fig. 2.1, green lines). Interaction strength may also change if predator and prey traits respond to temperature asymmetrically in other ways beyond the rate or magnitude of their response – e.g., if predator and prey differ in the optimal temperatures for their respective traits (Dell et al. 2014).

Temperature-driven changes in size- or stage-dependent predator-prey interaction strength are therefore likely to be driven by the thermal responses of both predator and prey species – when predator and prey respond asymmetrically to temperature, warming is expected to influence interaction strengths. We are aware of only two case studies exploring this prediction and their results were disparate, finding that warming caused an increase (Pepi et al. 2018) and a decrease (Culler et al. 2015) in interaction strength on stage-structured prey (caterpillars and mosquito larvae, respectively). Here, we reconcile these two results under one hypothesis using existing theory, and argue that the consequences of warming for size- and stage-structured predator-prey interactions are understudied, particularly given the abundance of organisms with ontogenetic changes in niche or body size. Elements of the response to temperature for specific traits, such as the rate or magnitude of response or its optimal temperature, generally vary both between species and within populations of the same species (Angilletta 2009; Dell et al. 2011). Thus, mismatches between the predator and prey's thermal responses are likely very common in size- and/or stage-structured interactions, and failing to account for how traits of both interactors respond to temperature may lead to unreliable predictions about how warming will impact predator-prey systems (Fig. 2.1).

To facilitate better incorporation of both predator and prey thermal responses into predictive models, we present a combined experimental and modeling framework for predicting how interaction strength varies with temperature for prey that have a predator-invulnerable life stage. Using experiments, we derive metrics of the temperature-dependence of predator foraging rates (i.e., the functional response; Holling 1959) and prey developmental rates to parameterize a discrete time model that predicts prey recruitment to an invulnerable stage (i.e., within a single generation) as a function of temperature. Both metrics are widely used in the literature, however, the consequences of increasing temperature for both processes on predator-prey interaction strength are seldom considered together. Attempts to describe the temperature-dependence of growth and development date back well over 50 years (Quinn 2017), and usage of the functional response forms the foundation of many models of predator-prey population dynamics (e.g., Yodzis and Innes 1992, McCann 2011).

Functional responses additionally provide a flexible approach to describing predator foraging rates under varying contexts, such as resource density, prey body size, and/or temperature (Englund et al. 2011; McCoy et al. 2011; Sentis et al. 2012). This is particularly important because the effects of prey density and temperature on foraging rates are very rarely linear (Jeschke et al. 2004; Brown et al. 2004), and the use of a linear model can thus lead to over- or under-estimates of predator foraging. These nonlinearities are also critical determinants of the coexistence of predator-prey pairs (Murdoch 1969; Kalinkat et al. 2013) and the long-term stability of food webs (Brose et al. 2006). Evidence suggests that prey density and temperature have both independent and potentially interactive effects on predation rates, which can be described mathematically by components of the functional response, such as the predator's attack rate (*a*), which includes searching for and capturing prey, and handling time (*h*), which includes processing and digestion of prey (Holling 1959; Sentis et al. 2012; Uzsko et al. 2017). Thus, functional responses provide a robust, standardized, and mechanistically-focused approach for exploring warming's effects on predator-prey interactions. Further, the use of temperature- and density-dependent functional response models (or other similar approaches) to describe predator foraging rates will be necessary for future models of the consequences of warming for long-term predator-prey population dynamics in these systems.

Using the model, we demonstrate the different ways that short-term predator-prey interaction strength can change across a thermal gradient, and how these changes are determined by the relative thermal-dependence of predator and prey traits. We also demonstrate the consequences of failing to account for thermally-mediated changes in the traits of both species, using a case study consisting of dragonfly nymph predators (*Erythemis simplicicollis* and *Pachydiplax longipennis*) feeding on mosquito larva prey (*Aedes atropalpus*). Understanding how warming influences these interactions may be especially important for predicting how warming will impact predator control of prey that vector diseases or are agricultural pests (Whitehorn & Yacoub 2019).

2.2. Methods

2.2.1. Study System

Riverine rock pools are small, discrete aquatic ecosystems formed by erosion in the bedrock of rocky, fast-flowing rivers around the world (Ortega et al. 2014; Pelletier et al. 2015; Ren et al. 2016; Schiesari et al. 2018). Submerged only during high flows, they may become seasonally isolated from the river, but continue to hold water for weeks to years (Jocqué et al. 2010), forming numerous discrete habitat patches that are colonized by a diverse suite of aquatic organisms (Ren et al. 2016). Rock pools are an ideal study site for research on warming and its effects on biodiversity because these pools naturally exhibit a wide range of temperatures both within and between pools. During the summer months, daily maximum temperatures in rock pools often exceed air temperatures due to heat retention by the surrounding bedrock, peaking over 40°C. By contrast, in the winter months, pools often freeze over. Pool temperatures also vary spatially depending on their proximity to trees and other sources of shade. For example, pool diel temperature profiles collected from June 10th to June 29th 2019 (n = 28) showed that daily average pool temperature varied by 8.7°C across pools (24.8 ± 0.4°C to 33.5 ± 0.9°C), and variation in temperatures within pools ranged an average of 11.9 ± 0.7°C across the course of the day (means ± std. errors; Vonesh lab unpublished data). Additionally, pools are often numerous where they are found, and their relatively small size (ranging from ~700 mL to ~9300 L) allows for rapid data collection across many pools. The rock pool system on the south side of Belle Isle in Richmond, VA, USA are the subject of a long-term project monitoring the biodiversity of over 700 independent pools, with data dating back to 2009.

Larvae of the North American rock pool mosquito, *Ae. atropalpus*, are endemic in the rock pools of Belle Isle and along the Atlantic coast of the United States. *Ae. atropalpus* is not considered to be an important vector of disease due to its ability to produce eggs without a blood meal (i.e., autogenously; Bowen et al. 1994). While *Ae. atropalpus* is the most common species present at the Belle Isle field site, a variety of other mosquito species also inhabit the pools, including several *Culex* and *Aedes* spp. One such species, *Ae. japonicus*, is an invasive species and known vector of diseases such as West Nile Virus (Kaufman & Fonseca 2014), and temperature has been suggested as an important driver of its interactions with *Ae. atropalpus* in its invaded range (Byrd et al. 2019). Common predators of mosquito larvae in rock pools include Libellulid dragonfly nymphs *Pantala* spp., *E. simplicicollis* and *P. longipennis*. Dragonfly nymphs are widely regarded as important predators of mosquito larvae, providing regulation of mosquito pests by reducing larval survival to emergence (Corbet 1999; Saha et al. 2012; Benelli et al. 2016).

Temperature has broad and well-known impacts on both players in this interaction, altering the foraging rates of dragonflies (Gresens et al. 1982; Frances & McCauley 2018; Herrera et el. 2018) and the development and survivorship of both taxa (Dodson et al. 2012; Ciota et al. 2014; McCauley et al. 2015). Interactions between dragonfly nymphs and *Ae. atropalpus* in rock pools are likely to occur under a wide variety of thermal contexts. *Ae. atropalpus* larvae are present in rock pools throughout the majority of the year, from mid-March to mid-November (Vonesh lab unpublished data), and dragonfly nymphs are present nearly year-round, in some cases even overwintering. The abundances of both taxa typically peak during July and August (Vonesh lab unpublished data).

Given this context, we analyzed the effects of warming on the interaction between the predatory dragonfly nymphs *E. simplicicollis* and *P. longipennis,* and *Ae. atropalpus* prey, using a series of experiments and a mathematical model.

2.2.2. Temperature Dependence of Development Rates

We measured the response of *Ae. atropalpus* development rates to temperature by rearing *Ae. atropalpus* larvae at one of five constant temperatures in environmental chambers (Percival Scientific Model I-30VL; access provided by the University of Richmond, Richmond, VA). Rearing temperatures included 20°C, 24°C, 28°C, 32°C, and 36°C, with a 14L:10D photoperiod.

Larvae were simultaneously hatched from rehydrated eggs that had been harvested from a laboratory colony of adults, originally collected as larvae earlier in the summer. The eggs were hatched in a 0.02% weight-per-volume solution of brewer's yeast in deionized water. We randomly assigned 10 larvae each to a total of 50 150mL cups, each filled to a standardized water volume of 100mL, and 10 cups each were randomly assigned to each environmental chamber (n = 10 per temperature treatment).

During the course of the experiment, we fed the larvae ad libitum on a mixture of brewer's yeast and desiccated beef liver powder, dissolved in 10mL of water. Larvae were fed different amounts of each food source depending on their age, to provide appropriate nutrition. On the first day, all larvae received 5mg of brewer's yeast. On subsequent days, any cups with primarily first instar larvae were provided 2.5mg of brewer's yeast and 2.5mg of liver powder; and cups with primarily second instar and later larvae were provided 5mg of liver powder. Feeding ceased when all larvae in the cup had pupated.

Experiments performed inside environmental chambers are often pseudoreplicated at the chamber level, such that all of the replicates within a treatment are placed inside of the same chamber (Hurlbert 1984). To avoid this, every other day, the cups were briefly removed from their assigned environmental chamber, the water in the cups was replaced with 100mL of fresh deionized water to avoid fouling, and the chambers were randomly reassigned a new temperature. The cups were placed into the chamber that corresponded to their treatment temperature after the chambers had warmed or cooled to their newly assigned temperatures. While the experiment ran, we collected data daily on larval mortality and the number of larvae at each instar. Any adult mosquitoes that emerged were removed from the cup, scored, and frozen.

Using nonlinear least squares estimation, we fit temperature-dependent models to larval development rate (i.e., the number of larvae that emerged per day) using the Arrhenius equation (Brown et al. 2004; Quinn 2017):

$$(1) \quad r_{dev} = ce^{b/(T+273.15)}$$

where r_{dev} is the rate at which larvae developed to adulthood (days^{-1}); T is temperature (°C); and c and b are fitted constants.

We modeled daily larval mortality rate as a logistic function of temperature, using nonlinear least squares estimation:

$$(2) \quad m = \frac{1}{1 + e^{-r_m(T-T_0)+\,m_0}}$$

where m is the daily per-capita mortality rate; T is temperature (°C); and r_m, m_0, and T_0 are fitted constants.

Temperature Dependence of the Functional Response

Different groups of organisms respond to temperature differently, and the response of a given trait to temperature is often species-specific, or even population-specific within the same species (Angilletta 2009; Dell et al. 2011). Because we hypothesized that overall short-term interaction strength would depend on the relative change in both the predator's feeding rates and the prey's development rates, we assessed the response of two different predators to temperature. Specifically, we measured the foraging rates of two dragonfly nymphs (*Pachydiplax* and *Erythemis*) on *Ae. atropalpus* as a function of temperature and prey density. Using these data, we fit a functional response model that simultaneously estimates the effects of temperature and prey density on the number of prey the predator consumes (as in Uszko et al. 2020). Libellulid dragonfly nymphs are common aquatic predators of mosquito larvae (Corbet 1999) and both species co-occur with *Ae. atropalpus* in its natural habitat: riverine rock pools (Vonesh lab unpublished data).

We measured the functional response of both dragonfly nymph species across the same set of constant temperatures (20°C, 24°C, 28°C, 32°C, and 36°C) with the same photoperiod (14L:10D) in the environmental chambers described above. We measured feeding rates for both dragonfly nymph species on five densities of *Ae. atropalpus* larvae: 10, 20, 40, 60, and 80. To reduce the number of treatments needed to estimate the full factorial functional response surface, we subsampled temperature and density treatment combinations using a response surface design (McCoy & Bolker 2008). This resulted in 13 treatments, each of which was replicated between 3-4 times for both nymph species (see Fig. S2.1; McCoy et al. 2011). This design allowed us to measure predator foraging rates across a broad range of temperatures and prey densities, in turn allowing us to describe the nonlinear effects of both variables on foraging via the functional response. To address concerns regarding pseudoreplication, the experiment ran in two blocks on subsequent days, with 2 replicates of each treatment running on the first day, and the remainder running on the second day. Between blocks, we randomly re-assigned each environmental chamber to a new temperature.

Functional response experiments were conducted using third instar *Ae. atropalpus* larvae. Four days prior to each block, we hatched *Ae. atropalpus* larvae from rehydrated eggs, using the same protocol described in the development experiment. The larvae were reared at a constant 28°C in plastic larval rearing trays filled with 600mL of a 0.02% weight-per-volume solution of brewer’s yeast in deionized water, with a stocking density of ~1000 eggs per tray. The larvae were fed once daily with 25mg each of brewer’s yeast and liver powder for first instar larvae, and 50mg of liver powder for later instar larvae. We reared the larvae in this way until the majority of the larvae (>80%) had reached their third instar. While the mosquito larvae were developing, we collected late instar *Erythemis* (mean head capsule width ± std. error = 4.03 ± 0.10 mm) and *Pachydiplax* (mean head capsule width ± std. error = 3.80 ± 0.09 mm) nymphs from two local ponds. We brought the nymphs into the lab three days prior to their block and held them there at room temperature (~22°C). The nymphs were fed to satiation on the first day of their captivity using live brine shrimp (*Artemia* spp.), after which they were starved for the remaining 48hrs prior to the experiment.

The experiment was conducted in a series of 950mL cups, filled to a standardized volume of 800mL of deionized water. We added four small (<4cm diameter) river rocks and a 10cm tall plastic aquarium plant to each cup to increase habitat complexity and provide the nymphs structure to cling to. We randomly assigned each cup to a predator species (either *E. simplicollis* or *Pd. longipennis*), temperature (20°C, 24°C, 28°C, 32°C, or 36°C), and larval density (10, 20, 40, 60, or 80). The cups were added to the environmental chamber with their corresponding temperature, allowing the water temperature to equilibrate overnight (~24 hrs) before the study organisms were added.

The day of the experiment, we placed the mosquito larvae into the deli cups at their assigned densities and left them in the chambers for an hour to allow the larvae time to acclimate. At the same time, the dragonfly nymphs were added to the chambers in 150mL cups (1 nymph per cup) so that both the predator and prey could acclimate separately before the experiment ran. After an hour had passed, we added a single nymph to each deli cup, and the nymphs were allowed to feed on the mosquito larvae for a full 24 hours. At the end of the 24-hour period, we removed all of the dragonfly nymphs and counted the remaining mosquito larvae in each cup. We photographed each nymph and the surviving larvae from its cup and used

ImageJ software to determine the head width of the nymph and the average body size of the surviving mosquito larvae, and weighed the wet mass (mg) of a subsample of 25 of the remaining dragonflies per species. Predator wet mass is necessary to estimate the temperature-dependence of handling time (see Eqn. 5 below), so we weighed the nymphs 24-48 hours after the experiment to allow time for digestion and more accurately estimate the weight of an "average" individual of the species.

To determine the temperature-dependence of *Erythemis* and *Pachydiplax* feeding rates on *Ae. atropalpus* prey, we used maximum likelihood estimation to estimate Type II functional responses by fitting Rogers random predator equation (Rogers 1972) to our data:

$$(3) \quad N = N_0 - \frac{W(ahN_0 e^{-a(t-hN_0)})}{ah}$$

where N is the number of prey eaten after time t (24hrs), N_0 is the initial number of prey, a is attack rate, h is handling time, and W is the Lambert's W function (McCoy & Bolker 2008).

Because the rate at which a predator forages for (a) and consumes (h) prey are temperature-dependent, we used the following equations to model attack rate and handling time (see Sentis et al. 2012). Attack rate (a) was described as a unimodal function of temperature in Celsius (T) as:

$$(4) \quad a = b(T - T_{min})(T_{max} - T)^{1/2}$$

where b is a fitted constant, and T_{min} and T_{max} are the predator's lower and upper thermal bounds for activity, respectively (Briere et al. 1999; Sentis et al. 2012). Handling time (h) was modelled as a power function of temperature in Celsius (T) and predator body mass in mg (M) as:

$$(5) \quad h = h_0 M^{b_h} e^{E_{h/k(T+273.15)}}$$

where h_0 is a fitted constant, b_h is an allometric scaling exponent (0.75; Brown et al. 2004), E_h is the activation energy for the rate-limiting enzyme-catalyzed biochemical rate of metabolism (eV), and *k* is Boltzmann's constant ($8.62 \cdot 10^{-5}$ eV K^{-1}) (i.e., the Arrhenius equation; Brown et al. 2004).

Estimates of the lower and upper temperature thresholds for activity (T_{min} and T_{max}, respectively) were only available in the literature for *Pachydiplax*, for which T_{max} is 41.7°C (Garten & Gentry 1976). A meta-analysis of the upper thermal limits of Libellulid dragonfly nymphs found a median value for T_{max} around 42.2°C (given as CT_{max} in Dallas & Rivers-Moore 2012), so we used this value to approximate T_{max} for *Erythemis*.

Lower temperature thresholds for activity (T_{min}) are poorly studied in Odonata; however, a study of dragonfly nymph growth showed that for the few species that have been studied, growth halts at temperatures of around 10°C (Suhling et al. 2015). Therefore, we set the value of T_{min} to 10°C for both *Erythemis* and *Pachydiplax*. Due to a lack of data on these parameters, we also performed a sensitivity analysis for T_{min} and T_{max} and found that they did not strongly change the shape of the temperature-dependent functional response fits as long as the values chosen for T_{min} and T_{max} were within a biologically relevant range (between 4-40°C) and were not within a degree of the range of temperatures used in our study (20-36°C; analysis not shown).

2.2.3. Temperature Dependence of Predator-Prey Interaction Strength

To predict how warming will influence short-term interaction strength for different predator-prey pairs, we developed a mathematical model. The model unites the results from the previous two experiments in order to predict the number of *Ae. atropalpus* larvae that survive to adulthood in the presence of one nymph of either *Erythemis* or *Pachydiplax* as a function of temperature. The model also allows us to disentangle the effects of temperature on the predator's foraging rates and the prey's developmental rates, allowing us to assess the effects of temperature-driven changes in these rates on prey survival either together or independently *in silica.*

The model takes the form of a stage-based discrete-time model (Fig. 2.2), where the survivorship of a starting density of mosquito larvae (i.e., a cohort) is tracked as they develop to adulthood as a function of time, *t*, as:

$$(6) \quad N_{j,t} = N_{j,t-1} + r_{dev}N_{j-1,t-1} - r_{dev}N_{j,t-1}$$

where *j* is the developmental stage of the larvae (i.e., instar); and r_{dev} is the proportion of larvae that move to the next instar at time *t*. Mosquito larvae possess four developmental instars as well as a pupal stage, and thus they have five stages to move through before reaching adulthood (j = 5; Fig. 2.2). Thus, r_{dev} is calculated by solving Eqn. 1 (i.e., development rate from hatch to eclosion) and scaling that rate up by a factor of five.

At each time step, a proportion of the prey move to the next instar according to r_{dev} (as in Eqn. 6); then, a fraction of them die due to predation, *p*, and background mortality, *m*:

$$(7) \quad N_t = (1 - m - p) \sum_{j=1}^{5} N_{j,t}$$

m is calculated by solving Eqn. 2 (i.e., temperature-dependent mortality) and *p* is calculated by solving Eqn. 3 (i.e., the functional response) and expressing the number of prey that are consumed (N_0 - N) as a proportion of the initial number of prey (N_0) at that time step. Thus, each time step involves solving both Eqn. 6 and Eqn. 7 sequentially to determine what instar (*j*) each of the remaining larvae are in, and how many larvae from each instar are either consumed by a predator or die due to background mortality. We assume that each of these processes are constant across all instars – i.e., that an individual larva's chances of developing to the next instar (r_{dev}), dying due to background mortality (*m*), or being eaten by the dragonfly nymph (*p*) do not depend on its current developmental stage. Any individuals for which $j = 5$ are considered to be adults, which are immune to predation by dragonfly nymphs and are scored as having survived the larval period.

We simulated the predator-prey interaction for a starting prey density of 300 larvae across a range of temperatures between 20-36°C. The model ran for a total of thirty time-steps to allow ample time for any surviving prey to move through the full course of their development. To account for uncertainty in our estimation of the functional response parameters, we replicated this process by randomly resampling the fitted parameters *b*, *h0*, and *Eh* from a distribution determined by their standard error for a total of 3,000 replicated model runs.

Using the model, we ran three sets of simulations to independently demonstrate the effects of temperature on prey survivorship when 1) only the predator's thermal performance is considered; 2) only the prey's thermal performance is considered; or 3) both predator and prey thermal performance is considered. In the first scenario, predator feeding rates (*p*) were allowed to vary with temperature (as described by Eqn. 3-5) while prey development and mortality rates were held constant across the temperature gradient by calculating the development rate where $T = 20°C$ (Eqn. 1-2). In the second scenario, prey development (r_{dev}) and mortality rates (*m*) were allowed to vary with temperature (as described by Eqn. 1-2) while predator foraging rates were held constant across the temperature gradient by calculating the functional response where $T = 20°C$ (Eqn. 3-5). In the final scenario, both predator feeding rates and prey development rates were allowed to vary in parallel with temperature (Eqn. 1-5), as they necessarily would in a natural or experimental setting.

2.2.4. Model Sensitivity Analysis

To demonstrate the importance of using mechanistic models to describe key processes in our model (e.g., predation rates and prey development rates), we conducted a sensitivity analysis to highlight the effects of our choice of functional response model on the overall model's predictions about prey recruitment to adulthood. Previous studies of the effects of temperature on predation have modeled the effects of temperature and prey density on predator foraging rates in various ways, in some cases using linear functions to describe these relationships (e.g., a Type I functional response) where nonlinear relationships are generally more common in nature (e.g., a Type II or III functional response to describe density-dependence, or a hump-shaped or Arrhenius function to describe temperature-dependence; Jeschke et al. 2004; Sentis et al. 2012; Uzsko et al. 2017). To demonstrate the importance of appropriately modeling the independent and interactive effects of temperature and density on predator foraging rates, we considered the consequences of modeling predation rates using a Type I instead of Type II functional response for our model's predictions.

The primary difference between a Type I and Type II functional response is the inclusion of a parameter capturing the handling time (*h* in Eqn. 3) of the predator in the Type II equation, which describes time spent by the predator processing and digesting prey once prey have been located and captured (Holling 1959). Its addition results in the characteristic "saturating" function that a Type II functional response captures. Importantly, because handling times describe predominantly biochemical processes such as digestion, they are an important component of the temperature-dependence of predation (Brown et al. 2004; Sentis et al. 2012). Thus, to simulate the effects of using a Type I instead of a Type II functional response, we manipulated the predator's handling time in our model by applying a scaling constant between

0.01 and 2 to handling time (*h*) in Eqn. 3. A smaller scaling constant (< 1) reduces handling time, in effect making the functional response more closely resemble a linear, Type I functional response, whereas a larger scaling constant (> 1) increases the amount of time needed by the predator to handle its prey. We ran the full stage-dependent predator-prey model described above using this approach to explore how temperature and the inclusion of handling time (as in a Type II functional response) influenced prey recruitment to adulthood.

2.3. Results

2.3.1. Temperature-Dependence of Development Rates

Temperature had strong and nonlinear impacts on the rate at which *Ae. atropalpus* larvae developed, halving their development time from 13.9 ± 0.1 (mean ± std. error) days at 20°C to 6.9 ± 0.2 days at 36°C (Fig. 2.3a; Table 2.1). Background mortality also increased with temperature nonlinearly. While mortality was roughly constant across the majority of the temperature gradient (mean proportion of dead individuals ± standard error = 14% ± 0.1% from 20-32°C), the majority of larvae (74% ± 4%) reared at 36°C died (Fig. 2.3b; Table 2.1).

2.3.2. Temperature-Dependence of the Functional Response

Feeding rates were nonlinearly related to temperature and prey density for both predator species (Fig. 2.4, Table 2.2). Feeding rates increased across the temperature gradient, such that they were lowest at 20°C and highest at 36°C. However, the two species differed in the extent to which their feeding rates increased with temperature. *Erythemis* nymphs were highly temperature sensitive, consuming approximately 81.3% more larvae at 36°C as compared to 20°C for the highest densities tested (N_0 = 80; Fig. 2.4a, 2.4c). By comparison, *Pachydiplax* nymphs were less responsive to temperature, consuming only approximately 35.0% more prey across the temperature range at the highest densities tested (N0 = 80; Fig. 2.4b, 2.4d). Mean wet masses (measured 24-48 hours after the experiment) for *Pachydiplax* were 68.7 ± 5.9 mg (mean ± std. error), while *Erythemis* nymphs weighed on average 114.2 ± 7.5 mg (mean ± std. error).

2.3.3. Temperature-Dependence of Predator-Prey Interaction Strength

Average model predictions for *Ae. atropalpus* survivorship varied both across a temperature gradient and depending on the predator species present. Additionally, our predictions changed depending on whether only the predator's thermal response was considered, only the prey's thermal response was considered, or both were considered. In simulations where only the predator was allowed to respond to temperature, prey survival decreased monotonically with temperature. The number of surviving adults decreased from 34.3 ± 0.7 ind. at 20°C to 1.3 ± 0.1 ind. at 36°C for *Erythemis* (Fig. 2.5a, red line), and from 56.3 ± 1.4 ind. at 20°C to 12.4 ± 0.4 ind. at 36°C for *Pachydiplax* (Fig. 2.5b, red line). In simulations where only prey development and mortality were allowed to vary with temperature, prey survival increased unimodally with temperature. The number of surviving adults increased from 34.3 ± 0.7 ind. at 20°C to 92.9 ± 1.1 ind. at 33°C for *Erythemis* (Fig. 2.5a, blue line), and from 56.2 ± 1.4 ind. at 20°C to 93.3 ± 1.8 ind. at 33°C for *Pachydiplax* (Fig. 2.5b, blue line). Regardless of the predator species present, survival decreased once temperatures lethal to the prey were reached (≥ 34°C; Fig. 2.5, blue lines).

By contrast, in simulations where both predator and prey trait responses to temperature were considered, accelerated development rates buffered prey survivorship to adulthood against the effects of higher predator feeding rates, regardless of the predator present (Fig. 2.5, green lines). The number of surviving adults increased unimodally, from 34.3 ± 0.7 ind. at 20°C to 39.3 ± 0.8 ind. at 26°C for *Erythemis* (Fig. 2.5a, green line), and from 56.3 ± 1.4 ind. at 20°C to 77.4 ± 1.7 ind. at 33°C for *Pachydiplax* (Fig. 2.5b, green line). This suggests that when both the predator and the prey possess traits that are both thermally responsive and relevant to the predator-prey interaction, prey survivorship will increase for both of the interactions we studied.

The overall shape of this relationship and the extent to which prey survivorship increased also differed between the two predators. On average, simulated prey survivorship for *Ae. atropalpus* reared in the presence of *Erythemis* increased modestly, gaining ~14.6% more adult mosquitoes from 20°C to 26°C (Fig. 2.5a, green line). However, projected *Ae. atropalpus* survivorship in the presence of *Pachydiplax* improved by over twice that proportion, increasing by ~37.5% from 20°C to 33°C (Fig. 2.5b, green line). In both cases, as temperatures approached 36°C, *Ae. atropalpus* survivorship dropped rapidly due to high rates of temperature-dependent background mortality.

2.3.4. Model Sensitivity Analysis

Prey survival to adulthood as predicted by the model depended strongly on predator handling time, and thus the form of the functional response we used to model predation rates (Fig. 2.6). Handling times that were smaller than those initially fit to our data (i.e., scaling coefficients below 1) caused the model to predict very low prey survival compared to unmanipulated values for handling time (i.e., a scaling coefficient of 1), whereas larger values for handling time (i.e., scaling coefficients above 1) resulted in comparatively greater prey survival.

This likely occurred for two reasons. First, reducing handling times in effect shortened the amount of time that the predator needed to spend processing and digesting individual prey. As a result, the predator had more time to spend actively foraging and attacking other prey, resulting in an overall increase in predation rates. Second, reducing handling time caused the relationship between prey density and predator foraging rates to become more linear, as in a Type I functional response. This relationship is generally saturating in a Type II functional response. Thus, when prey densities are high relative to the densities at which a Type II response's predation rates would level off (i.e., above the asymptote), a Type I functional response may greatly overestimate predation rates.

Manipulating handling time had the secondary effect of changing the effects of temperature on prey survival (Fig. 2.6). Handling time includes components such as the processing and digestion of prey, many of which are largely biochemical in nature and thus known to be temperature-sensitive (Brown et al. 2004). Because temperature itself thus influences handling time, temperature had a larger effect on prey survival when handling times were also larger (i.e., scaling coefficients above 1), and a smaller effect on prey survival when handling times were smaller (i.e., scaling coefficients below 1). Thus, opting to describe predator foraging rates using functional forms that discount handling time or remove it altogether (e.g., a Type I functional response) may result in the loss of a key mechanism by which temperature influences predation rates.

Overall, the results of our sensitivity analysis suggest that using an inappropriate model to describe predator foraging rates may hamper our ability to draw predictions about how warming will impact short-term interaction strength across a full, biologically-relevant range of temperatures and prey densities. Importantly, because handling time describes in part both the temperature- and density-dependence of foraging, our findings suggest that the effects of temperature on predator foraging cannot be accurately predicted across all levels of prey density using models that do not also account for the effects of prey density on foraging, and vice-versa. Selecting the most appropriate models may be challenging, though, because the relationship between temperature, prey density, and predator foraging rates does not exhibit the same functional form across all predator-prey pairs (Holling 1959; Englund et al. 2011; Uzsko et al. 2017). However, functional response models can account for this by providing us with a means to choose the most appropriate models (e.g., Eqn. 3-5) for our data on a case-by-case basis.

2.4. Discussion

Predator-prey population dynamics are the product of a series of often interdependent factors that collectively influence the rate at which predators consume prey, including (but not limited to) the density of the prey (Holling 1959; Rogers 1972) and the body size and life stage of individual prey (Peters 1983; Werner and Gilliam 1984; Brose 2010), each of which may affect predation rates in a nonlinear fashion. As the field of ecology has shifted its view towards predicting how warming will impact ecological communities, recent studies have come to appreciate that temperature is yet another determinant of predator-prey interactions (e.g., Englund et al. 2011; Sentis et al. 2014; Bideault et al. 2019). Previous studies have often ignored the importance of the temperature-dependence of prey traits in these interactions, instead focusing on the predator's thermal response alone (O'Connor 2009; Hoekman 2010; Rall et al. 2010; Vucic-Pestic et al. 2010; Karban et al. 2015), and in doing so have suggested that increases in mean temperature will primarily increase predator-prey interaction strength by producing "hungrier" predators (e.g., Fig. 2.5, red lines). Here, we add to a growing body of evidence (e.g., Dell et al.

2014; Culler et al. 2015; Pepi et al. 2018) that instead suggests that differential temperature responses in predator and prey traits can produce a wide range of changes in short-term interaction strength across a thermal gradient.

We found that all three of the species we studied responded to temperature in ways that are relevant to the two predator-prey interactions we highlight here. By using a broad range of both prey densities and temperatures, we show that dragonfly foraging rates increased nonlinearly with temperature and density, and the effects of temperature on foraging became more pronounced as prey density increased (Fig. 2.4). Previous work suggests that temperature-driven increases in predation are common in many ectothermic predators, including dragonflies (e.g., Gresens et al. 1982; Eck et al. 2014; Herrera et el. 2018). However, despite similarities between predators (both are Libellulid dragonflies that co-occur in much of their geographic range), the extent to which foraging increased with temperature differed between the two species. *Erythemis* consumed on average 81.3% more mosquito larvae at the warmest temperatures compared to the coolest temperatures, but *Pachydiplax* consumed only 35% more larvae. Our finding that changes in temperature altered predation rates was expected – previous work suggests that the majority of ectothermic predators have higher feeding rates at warmer temperatures, until temperatures exceed a species-specific optimum (Englund et al. 2011; Sentis et al. 2012; Uiterwaal and Delong 2020). There is also considerable variation in the extent to which ectothermic organisms respond to temperature, both within and across habitat types and taxonomic groups (Dell et al. 2011). While these findings are thus not novel by themselves, they allow us to illustrate, using our model, how differences in the extent to which predator species respond to temperature may then influence predation on a shared prey species via the prey's own thermal response (Fig. 2.5). Further, our experimental findings (Fig. 2.4) and sensitivity analysis (Fig. 2.6) together highlight the value of using mechanistic models such as the functional response, which can capture both the independent and interactive effects of temperature and density on predator foraging rates.

Prey development was highly sensitive to warming. Across this ecologically relevant temperature gradient, *Ae. atropalpus* development rates were cut in half, dramatically reducing the amount of time they spend vulnerable to dragonfly nymph predators. Accelerated development rates with similar magnitudes are widely documented in mosquito larvae (e.g., Ciota et al. 2014), thus our finding that warming reduces the effectiveness of larval predators by reducing exposure to larval stage predators (as in Culler et al. 2015) may apply more broadly across mosquito taxa, including species that are important disease vectors. While our study's use of larval mosquitoes and their predators is thus compelling on its own, recognizing the role of temperature sensitive development for modulating the strength of predator-prey interactions will be important for many taxa. Ontogenetic niche shifts are ubiquitous, occurring in a variety of organisms such as fish, reptiles, amphibians, and most invertebrates (Werner and Gilliam 1984). Given that the effects of temperature on development are thought to be general in ectotherms (Brown et al. 2004), it is likely that many species with stage-dependent variation in their vulnerability to predators could benefit from warmer temperatures in a similar fashion. Thus, accounting for the thermal responses of both predator and prey traits is critical for estimating changes in interaction strength as the climate warms.

Our model simulations demonstrate that prey suppression depends on asymmetry in the species-specific thermal responses of both predator and prey (Fig. 2.5). We find the net effect of warming on predator and prey performance for our study species is reduced short-term interaction strength, because temperature-driven changes in prey development rates either exceeded or counterbalanced the corresponding change in predator feeding rates. Failure to account for the thermal response of both predator and prey performance, however, can yield very different predictions about how these types of interactions will change as the climate warms. For example, consider how the expectations for predation in our study system would change if we focused solely on predator or prey temperature dependence (Fig. 2.5). In June 2019, the average daily temperature of rock pools in our study system at Belle Isle, Richmond, VA ranged from ~25°C to ~34°C. If we consider only the temperature dependence of the predators, across this gradient we predict a decrease in prey survival by ~28% with *Pachydiplax* predators, or ~73% with *Erythemis* predators (Fig. 2.5, red lines). If we consider only the temperature dependence of the prey, on the other hand, we predict the opposite – an increase in prey survival of 24% with *Pachydiplax* or 55% with *Erythemis* (Fig. 2.5, blue lines). When both mechanisms are considered, however, we predict a 14% increase in prey survival with *Pachydiplax*, and a ~25% decrease with *Erythemis* (Fig. 2.5, green lines). Therefore, given the implications of our model, and the ubiquity of temperature-dependence in functional responses (Englund et al. 2011; Uiterwall and Delong 2020) and development rates (Brown et al. 2004) between the discrete life stages observed in many taxa (Werner and Gilliam 1984), we suggest that asymmetries in the responses of both predator and prey performance to temperature are widespread, and likely to be a crucial determinant of how warming will change predator-prey interaction strength.

We suggest that our modeling approach provides a useful theoretical framework for predicting warming's effects on predator-prey interactions. Specifically, using data from simple short-term laboratory experiments, we developed empirical models that can be used to mechanistically explore the effects of nonlinearities introduced by temperature- and density-dependence on short-term predator-prey interaction strengths. We focused here on understanding the temperature-dependence of functional responses, development, and growth rates, because it broadens our ability to consider temperature driven interactions over short time scales and may ultimately shed insights about long term predator-prey population dynamics for a wide variety of taxa.

However, temperature has important effects on other relevant life history traits such as body size, longevity, and fecundity (e.g., McCoy and Gillooly 2008; Delatte et al. 2009; Ciota et al. 2014) in mosquitos and other ectotherms. Temperature has well-known positive impacts on the growth rates of ectotherms, but negative impacts on their adult body size (Atkinson 1994; Daufresne et al. 2009; Gardner et al. 2011). Previous work has suggested that accounting for temperature-mediated changes in body sizes may further weaken overall predation rates by altering the ratio of predator to prey body size (Bideault et al. 2019). Additionally, while we do not include predator development and growth in our model, by shortening the predator's developmental period, temperature could alter the duration and timing of prey exposure to predators across different life stages, and these effects could be modulated depending on the seasonality of the species in play. Thus, while our model (and previous studies, e.g., Culler et al. 2015) predicts that the ability of predators to suppress prey could become weaker as temperatures rise, it will be important to take a holistic, whole life cycle approach to predicting how warming will influence the spread of individual species.

Lastly, it is important to note that the model's use of short-term experiments carried out under constant temperature regimes to parameterize the temperature-dependence of predator and prey traits is a simplification. Daily variation in temperature is ubiquitous, and it is known to influence the shape of an organism's thermal performance curve (Kingsolver et al. 2015). Accounting for temperature variation may be especially important given that warming is not only expected to influence average temperatures, but also the frequency and magnitude of extreme temperature events (Fischer and Knutti 2015), which may be relevant for rock pools and many other systems.

As the climate warms, the interactions that link ecological communities are changing with it, and the consequences of these changes for community structure and function are often difficult to predict (Beveridge et al. 2010; Brose et al. 2012; Rodríguez-Castañeda 2013). Our model suggests that by modifying predator foraging rates and prey development rates, increasing temperatures could in theory increase, decrease, or have no effect on predator-prey interaction strength. However, when parameterized for these two predator-prey exemplars, we observe a net decrease in prey suppression because prey recruitment is driven largely by prey temperature-dependence, rather than predator temperature-dependence. This result contrasts with previous work which only considered predator temperature- dependence, including many attempts to model warming's impacts on predator-prey population dynamics (O'Connor et al. 2009; Hoekman 2010; Karban et al. 2015).

This study also expands upon previous work on temperature's effects on stage-dependent predation (e.g., Culler et al. 2015; Pepi et al. 2018) by incorporating functional response models as a means of estimating predator foraging rates. In doing so, we provide a flexible modeling framework that simultaneously considers the nonlinear impacts of temperature, prey density, and their interaction on predator foraging rates, which will be necessary for determining the long-term effects of warming on stage-structured predator-prey population dynamics (Murdoch 1969; Kalinkat et al. 2013). Given the wide variety of relevant traits that are altered by temperature, and the overall lack of generality in the way that different species respond to temperature (Angilletta 2009; Dell et al. 2011), it is challenging to draw broad conclusions about how warming will influence predator-prey systems as a whole. However, as we demonstrate in this study, the use of robust and well-established general models of predator and prey traits (e.g., functional response and development models) provides a useful and necessary way of incorporating and comparing the different mechanisms by which warming can modify these interactions.

2.5. References

Amarasekare, P. (2015). Effects of temperature on consumer-resource interactions. *Journal of Animal Ecology*, *84*(3), 665–679. https://doi.org/10.1111/1365-2656.12320

Angilletta Jr., M. J. (2009). *Thermal Adaptation: A Theoretical and Empirical Synthesis*. Oxford Academic.

Atkinson, D. (1994). Temperature and Organism Size—A Biological Law for Ectotherms? *Advances in Ecological Research*, *25*, 1–58. https://doi.org/10.1016/S0065-2504(08)60212-3

Benelli, G., Jeffries, C. L., & Walker, T. (2016). Biological control of mosquito vectors: Past, present, and future. *Insects*, *7*(4), 1–18. https://doi.org/10.3390/insects7040052

Beveridge, O. S., Humphries, S., Petchey, O. L., Beveridge, O. S., Humphries, S., & Petchey, O. L. (2010). The interacting effects of temperature and food chain length on trophic abundance and ecosystem function. *Journal of Animal Ecology*, *79*(3), 693–700.

Bideault, A., Loreau, M., & Gravel, D. (2019). Temperature Modifies Consumer-Resource Interaction Strength Through Its Effects on Biological Rates and Body Mass. *Frontiers in Ecology and Evolution*, *7*(February), 1–11. https://doi.org/10.3389/fevo.2019.00045

Bowen, M. F., Davis, E. E., Haggart, D., & Romo, J. (1994). Host-seeking behavior in the autogenous mosquito Aedes atropalpus. *Journal of Insect Physiology*, *40*(6), 511–517. https://doi.org/10.1016/0022-1910(94)90124-4

Briere, J.-F., Pracros, P., le Roux, A.-Y., & Pierre, J.-S. (1999). A novel rate model of temperature-dependent development for arthropods. *Environmental Entomology*, *28*(1), 22–29.

Brose, U. (2010). Body-mass constraints on foraging behaviour determine population and food-web dynamics. *Functional Ecology*, *24*(1), 28–34. https://doi.org/10.1111/j.1365-2435.2009.01618.x

Brose, U., Jonsson, T., Berlow, E. L., Warren, P. H., Banasek-Richter, C., Bersier, L.-F., Blanchard, J. L., Brey, T., Carpenter, S. R., Blandenier, M.-F. C., Cushing, L., Dawah, H. A., Dell, T., Edwards, F. K., Harper-Smith, S., Jacob, U., Ledger, M. E., Martinez, N. D., Memmott, J., … Cohen, J. E. (2006). Consumer-Resource Body-Size Relationships in Natural Food Webs. *Ecology*, *87*(10), 2411–2417.

Brose, U., Dunne, J. A., Montoya, J. M., Petchey, O. L., Schneider, F. D., & Jacob, U. (2012). Climate change in size-structured ecosystems. *Proceedings of the Royal Society B: Biological Sciences*, *367*, 2903–2912.

Brown, J. H., Gillooly, J. F., Allen, A. P., Savage, V. M., & West, G. B. (2004). Toward a metabolic theory of ecology. *Ecology*, *85*(7), 1771–1789. https://doi.org/Doi 10.1890/03-9000

Byrd, B. D., Sither, C. B., Goggins, J. A., Kunze-Garcia, S., Pesko, K. N., Bustamante, D. M., Sither, J. M., Vonesh, J. R., & O’meara, G. F. (2019). Aquatic thermal conditions predict the presence of native and invasive rock pool Aedes (Diptera: Culicidae) in the southern Appalachians, U.S.A. *Journal of Vector Ecology*, *44*(1), 30–39.

Ciota, A. T., Matacchiero, A. C., Kilpatrick, A. M., & Kramer, L. D. (2014). The Effect of Temperature on Life History Traits of Culex Mosquitoes. *Journal of Medical Entomology*, *51*(1), 55–62. https://doi.org/10.1109/TMI.2012.2196707.Separate

Corbet, P. S. (1999). *Dragonflies: Behaviour and Ecology of Odonata*. Comstock Publishing Associates.

Culler, L. E., Ayres, M. P., & Virginia, R. A. (2015). In a warmer Arctic, mosquitoes avoid increased mortality from predators by growing faster. *Proceedings of the Royal Society B: Biological Sciences*, *282*(1815), 20151549. https://doi.org/10.1098/rspb.2015.1549

Dallas, H. F., & Rivers-Moore, N. A. (2012). Critical Thermal Maxima of aquatic macroinvertebrates: Towards identifying bioindicators of thermal alteration. *Hydrobiologia*, *679*(1), 61–76. https://doi.org/10.1007/s10750-011-0856-4

Daufresne, M., Lengfellner, K., & Sommer, U. (2009). Global warming benefits the small in aquatic ecosystems. *Proceedings of the National Academy of Sciences*, *106*(31), 12788–12793. https://doi.org/10.1073/pnas.0902080106

Davidson, A. T., Hamman, E. A., McCoy, M. W., & Vonesh, J. R. (2021). Asymmetrical effects of temperature on stage-structured predator–prey interactions. *Functional Ecology*, *35*(5). https://doi.org/10.1111/1365-2435.13777

Delatte, H., Gimonneau, G., Triboire, A., & Fontenille, D. (2009). Influence of Temperature on Immature Development, Survival, Longevity, Fecundity, and Gonotrophic Cycles of *Aedes albopictus* , Vector of Chikungunya and Dengue in the Indian Ocean. *Journal of Medical Entomology*, *46*(1), 33–41. https://doi.org/10.1603/033.046.0105

Dell, A. I., Pawar, S., & Savage, V. M. (2011). Systematic variation in the temperature dependence of physiological and ecological traits. *Proceedings of the National Academy of Sciences*, *108*(26), 10591–10596. https://doi.org/10.1073/pnas.1015178108

Dell, A. I., Pawar, S., & Savage, V. M. (2014). Temperature dependence of trophic interactions are driven by asymmetry of species responses and foraging strategy. *Journal of Animal Ecology*, *83*(1), 70–84. https://doi.org/10.1111/1365-2656.12081

Dodson, B. L., Kramer, L. D., & Rasgon, J. L. (2012). Effects of larval rearing temperature on immature development and West Nile virus vector competence of *Culex tarsalis*. *Parasites & Vectors*, *5*(1), 199. https://doi.org/10.1186/1756-3305-5-199

Eck, B., Byrne, A., Popescu, V. D., Harper, E. B., & Patrick, D. A. (2014). Effects of water temperature on larval amphibian predator-prey dynamics. *Herpetological Conservation and Biology*, *9*(2), 301–308.

Englund, G., Öhlund, G., Hein, C. L., & Diehl, S. (2011). Temperature dependence of the functional response. *Ecology Letters*, *14*(9), 914–921. https://doi.org/10.1111/j.1461-0248.2011.01661.x

Fischer, E. M., & Knutti, R. (2015). Anthropogenic contribution to global occurrence of heavy-precipitation and high-temperature extremes. *Nature Climate Change*, *5*(6), 560–564. https://doi.org/10.1038/nclimate2617

Frances, D. N., & McCauley, S. J. (2018). Warming drives higher rates of prey consumption and increases rates of intraguild predation. *Oecologia*, *187*(3), 585–596. https://doi.org/10.1007/s00442-018-4146-y

Fussmann, K. E., Schwarzmüller, F., Brose, U., Jousset, A., & Rall, B. C. (2014). Ecological stability in response to warming. *Nature Climate Change*, *4*(3), 206–210. https://doi.org/10.1038/nclimate2134

Garten, C. T. Jr., & Gentry, J. B. (1976). Thermal Tolerance of Dragonfly Nymphs II. Comparison of Nymphs from Control and Thermally Altered Environments. *Physiological Zoology*, *49*(2), 206–213.

Gresens, S. E., Cothran, M. L., & Thorp, J. H. (1982). The Influence of Temperature on the Functional Response of the Dragonfly Celithemis fasciata (Odonata: Libellulidae). *Oecologia*, *53*(3), 281–284. https://doi.org/10.1007/BF00388999

Herrera, E. Q., Casas, J., Dangles, O., & Pincebourde, S. (2018). Temperature effects on ballistic prey capture by a dragonfly larva. *Ecology and Evolution*, *8*(8), 4303–4311. https://doi.org/10.1002/ece3.3975

Holling, C. S. (1959). The components of predation as revealed by a study of small-mammal predation of the european pine sawfly. *The Canadian Entomologist*, *91*(5), 293–320.

Huey, R. B., & Kingsolver, J. G. (1989). Evolution of thermal sensitivity of ectotherm performance. *Trends In Ecology & Evolution*, *4*(5), 131–135. https://doi.org/10.1016/0169-5347(89)90211-5

Huey, R. B., & Stevenson, R. D. (1979). Integrating Thermal Physiology and Ecology of Ectotherms: A Discussion of Approaches. *American Zoologist*, *19*(1), 357–366.

Hurlbert, S. H. (1984). Pseudoreplication and the Design of Ecological Field Experiments. *Ecological Monographs*, *54*(2), 187–211.

Jeschke, J. M., Kopp, M., & Tollrian, R. (2004). Consumer-food systems: Why type I functional responses are exclusive to filter feeders. *Biological Reviews of the Cambridge Philosophical Society*, *79*(2), 337–349. https://doi.org/10.1017/S1464793103006286

Jochum, M., Schneider, F. D., Crowe, T. P., Brose, U., & O’Gorman, E. J. (2012). Climate-induced changes in bottom-up and top-down processes independently alter a marine ecosystem. *Philosophical Transactions of the Royal Society B: Biological Sciences*, *367*, 2962–2970. https://doi.org/10.1098/rstb.2012.0237

Jocqué, M., Vanschoenwinkel, B., & Brendonck, L. (2010). Freshwater rock pools: A review of habitat characteristics, faunal diversity and conservation value. *Freshwater Biology*, *55*(8), 1587–1602. https://doi.org/10.1111/j.1365-2427.2010.02402.x

Kalinkat, G., Schneider, F. D., Digel, C., Guill, C., Rall, B. C., & Brose, U. (2013). Body masses, functional responses and predator-prey stability. *Ecology Letters*, *16*(9), 1126–1134. https://doi.org/10.1111/ele.12147

Karban, R., Grof-Tisza, P., Mcmunn, M., Kharouba, H., & Huntzinger, M. (2015). Caterpillars escape predation in habitat and thermal refuges. *Ecological Entomology*, *40*(6), 725–731. https://doi.org/10.1111/een.12243

Kaufman, M. G., & Fonseca, D. M. (2014). Invasion Biology of Aedes japonicus japonicus (Diptera: Culicidae). *Annual Review of Entomology*, *59*, 31-49. https://doi.org/10.1007/s11103-011-9767-z.Plastid

Kingsolver, J. G., Arthur Woods, H., Buckley, L. B., Potter, K. A., MacLean, H. J., & Higgins, J. K. (2011). Complex life cycles and the responses of insects to climate change. *Integrative and Comparative Biology*, *51*(5), 719–732. https://doi.org/10.1093/icb/icr015

Kingsolver, J. G., Higgins, J. K., & Augustine, K. E. (2015). Fluctuating temperatures and ectotherm growth: Distinguishing non-linear and time-dependent effects. *Journal of Experimental Biology*, *218*(14), 2218–2225. https://doi.org/10.1242/jeb.120733

Lurgi, M., López, B. C., & Montoya, J. M. (2012). Novel communities from climate change. *Philosophical Transactions of the Royal Society B: Biological Sciences*, *367*, 2913–2922. https://doi.org/10.1098/rstb.2012.0238

McCauley, S. J., Hammond, J. I., Frances, D. N., & Mabry, K. E. (2015). Effects of experimental warming on survival, phenology, and morphology of an aquatic insect (Odonata). *Ecological Entomology*, *40*(3), 211–220. https://doi.org/10.1111/een.12175

McCoy, M. W., & Bolker, B. M. (2008). Trait-mediated interactions: Influence of prey size, density and experience. *Journal of Animal Ecology*, *77*(3), 478–486. https://doi.org/10.1111/j.1365-2656.2008.01372.x

McCoy, M. W., Bolker, B. M., Warkentin, K. M., & Vonesh, J. R. (2011). Predicting Predation through Prey Ontogeny Using Size-Dependent Functional Response Models. *The American Naturalist*, *177*(6), 752–766. https://doi.org/10.1086/659950

McCoy, M. W., & Gillooly, J. F. (2008). Predicting natural mortality rates of plants and animals. *Ecology Letters*, *11*(7), 710–716. https://doi.org/10.1111/j.1461-0248.2008.01190.x

Murdoch, William, W. (1969). Switching in General Predators : Experiments on Predator Specificity and Stability of Prey Populations. *Ecological Monographs*, *39*(4), 335–354.

O'Connor, M. I. (2009). Warming Strengthens an Herbivore-Plant Interaction. *Ecology*, *90*(2), 388–398. https://doi.org/10.1890/08-0034.1

Ortega, J. A., Gómez-Heras, M., Perez-López, R., & Wohl, E. (2014). Multiscale structural and lithologic controls in the development of stream potholes on granite bedrock rivers. *Geomorphology*, *204*, 588–598. https://doi.org/10.1016/j.geomorph.2013.09.005

Pelletier, J. D., Sweeney, K. E., Roering, J. J., & Finnegan, N. J. (2015). Controls on the geometry of potholes in bedrock channels. *Geophysical Research Letters*, *42*(3), 797–803. https://doi.org/10.1002/2014GL062900

Pepi, A., Grof-Tisza, P., Holyoak, M., & Karban, R. (2018). As temperature increases, predator attack rate is more important to survival than a smaller window of prey vulnerability. *Ecology*. https://doi.org/10.1002/ecy.2356

Petchey, O. L., Brose, U., & Rall, B. C. (2010). Predicting the effects of temperature on food web connectance. *Philosophical Transactions of the Royal Society B: Biological Sciences*, *365*(1549), 2081–2091. https://doi.org/10.1098/rstb.2010.0011

Petchey, O. L., McPhearson, P. T., Casey, T. M., & Morin, P. J. (1999). Environmental warming alters food web structure and ecosytem function. *Nature*, *402*, 69–72.

Peters, R. H. (1983). *The Ecological Implications of Body Size*. Cambridge University Press.

Quinn, B. K. (2017). A critical review of the use and performance of different function types for modeling temperature-dependent development of arthropod larvae. *Journal of Thermal Biology*, *63*(May 2016), 65–77. https://doi.org/10.1016/j.jtherbio.2016.11.013

Radzio, T. A., & O’Connor, M. P. (2017). Behavior and temperature modulate a thermoregulation–predation risk trade-off in juvenile gopher tortoises. *Ethology*, *123*(12), 957–965. https://doi.org/10.1111/eth.12695

Rall, B. C., Vucic-Pestic, O., Ehnes, R. B., Emmerson, M. C., & Brose, U. (2010). Temperature, predator–prey interaction strength and population stability. *Global Change Biology*, *16*, 2145–2157. https://doi.org/10.1111/j.1365-2486.2009.02124.x

Rebaudo, F., & Rabhi, V. B. (2018). Modeling temperature-dependent development rate and phenology in insects: review of major developments, challenges, and future directions. *Entomologia Experimentalis et Applicata*, *166*(8), 607–617. https://doi.org/10.1111/eea.12693

Ren, H., Yuan, X., Yue, J., Wang, X., & Liu, H. (2016). Potholes of mountain river as biodiversity spots: Structure and dynamics of the benthic invertebrate community. *Polish Journal of Ecology*, *64*(1), 70–83. https://doi.org/10.3161/15052249PJE2016.64.1.007

Rodríguez-Castañeda, G. (2013). The world and its shades of green: A meta-analysis on trophic cascades across temperature and precipitation gradients. *Global Ecology and Biogeography*, *22*(1), 118–130. https://doi.org/10.1111/j.1466-8238.2012.00795.x

Rogers, D. (1972). Random Search and Insect Population Models. *Journal of Animal Ecology*, *41*(2), 369–383.

Saha, N., Aditya, G., Banerjee, S., & Saha, G. K. (2012). Predation potential of odonates on mosquito larvae: Implications for biological control. *Biological Control*, *63*(1), 1–8. https://doi.org/10.1016/j.biocontrol.2012.05.004

Savage, V. M., Gillooly, J. F., Brown, J. H., West, G. B., & Charnov, E. L. (2004). Effects of Body Size and Temperature on Population Growth. *The American Naturalist*, *163*(3), 429–441. https://doi.org/10.1086/381872

Schiesari, L., Monteiro, A. S., Ilha, P., Pope, N., & Corrêa, D. T. (2018). The ecology of a system of natural mesocosms: Rock pools in the Atlantic Forest. *Freshwater Biology*, *March*, 1–11. https://doi.org/10.1111/fwb.13118

Sentis, A., Hemptinne, J. L., & Brodeur, J. (2014). Towards a mechanistic understanding of temperature and enrichment effects on species interaction strength, omnivory and food-web structure. *Ecology Letters*, *17*(7), 785–793. https://doi.org/10.1111/ele.12281

Sentis, A., Hemptinne, J.-L. L., & Brodeur, J. (2012). Using functional response modeling to investigate the effect of temperature on predator feeding rate and energetic efficiency. *Oecologia*, *169*(4), 1117–1125. https://doi.org/10.1007/s00442-012-2255-6

Stahlschmidt, Z. R., & Adamo, S. A. (2013). Warm and cozy: Temperature and predation risk interactively affect oviposition site selection. *Animal Behaviour*, *86*(3), 553–558. https://doi.org/10.1016/j.anbehav.2013.06.009

Suhling, F., Suhling, I., & Richter, O. (2015). Temperature response of growth of larval dragonflies – an overview. *International Journal of Odonatology*, *18*(1), 15–30. https://doi.org/10.1080/13887890.2015.1009392

Uiterwaal, S. F., & Delong, J. P. (2020). Functional responses are maximized at intermediate temperatures. *Ecology*. https://doi.org/10.1002/ecy.2975

Vasseur, D. A., & McCann, K. S. (2005). A mechanistic approach for modeling temperature-dependent consumer-resource dynamics. *American Naturalist*, *166*(2), 184–198. https://doi.org/10.1086/431285

Vucic-Pestic, O., Rall, B. C., Kalinkat, G., & Brose, U. (2010). Allometric functional response model: Body masses constrain interaction strengths. *Journal of Animal Ecology*, *79*(1), 249–256. https://doi.org/10.1111/j.1365-2656.2009.01622.x

Werner, E. E., & Gilliam, J. F. (1984). The Ontogenetic Niche and Species Interactions in Size-Structured Populations. *Annual Review of Ecology and Systematics*, *15*, 393–425.

Whitehorn, J., & Yacoub, S. (2019). Global warming and arboviral infections. *Clinical Medicine, Journal of the Royal College of Physicians of London*, *19*(2), 149–152. https://doi.org/10.7861/CLINMEDICINE.19-2-149

Yodzis, P., & Innes, S. (2016). Body Size and Consumer-Resource Dynamics. *The American Naturalist*, *139*(6), 1151–1175.

2.6. Figures and Tables

Fig. 2.1. A conceptual diagram illustrating how the temperature-dependence of different predator and prey traits can combine to influence the number of prey that survive across a temperature gradient. In the figure, the predator and prey have the same thermal optimum, but the rate of their response to temperature varies. As temperature increases, (a) prey development time decreases, limiting their window of vulnerability to predators; but (b) predator foraging rates increase, thereby increasing the number of prey that are consumed during that window. Depending on the shape of these relationships relative to one another (a-b) – i.e., the thermal performance curve of predator foraging rate and prey development rate to temperature – (c) prey survivorship can decrease (red lines), remain the same (green lines), or increase (blue lines).

Fig. 2.2. A conceptual diagram of the stage-based discrete time model used to predict how temperature influences the predator-prey interaction. Mosquito larvae possess four discrete developmental instars, a pupa stage, and an adult stage. The model starts with a freshly hatched cohort of first instar larvae of a given initial density, N_0. As time passes, a proportion of the larvae develop through a series of j developmental stages to adulthood (total $j = 5$), informed by their development rate, d; a proportion of the larvae, m, die due to background mortality; and a proportion, p, die to predation. Each of these three parameters – d, p, and m – are described as functions of temperature, allowing the model to predict the number of prey that survive to adulthood (N_{surv}) at different constant temperatures.

Fig. 2.3. The temperature-dependence of *Ae. atropalpus* (a) development rate to adulthood (shown as development time) and (b) daily mortality rate. Shaded areas indicate the 95% confidence interval of the fitted relationships described in Eqn. 1-2.

Fig. 2.4. The functional response of a) *Erythemis* nymphs and b) *Pachydiplax* nymphs feeding on *Ae. atropalpus* larvae, as a function of initial prey density (a-b) and temperature (c-d). Data were measured at a range of constant temperatures from 20°C to 36°C. Functional responses were fit accounting for depletion, with attack rate and handling time modeled as functions of temperature as described in Eqn. 3-5.

Fig. 2.5. Predicted survivorship of a cohort of 300 *Ae. atropalpus* larvae in the presence of either: a) one *Erythemis* nymph or b) one *Pachydiplax* nymph, as a function of temperature (°C). The blue lines depict model simulations where prey development is allowed to vary with temperature, but predator feeding rates are fixed at a low temperature ($T = 20$°C). The red lines depict simulations where predator feeding rates are allowed to vary with temperature, but prey development rates are fixed at an intermediate level ($T = 20$°C). Lastly, the green lines depict simulations where both rates are allowed to vary along the temperature gradient. Lines represent average larval survivorship across 3,000 replicated simulations. Shaded regions represent the 95% confidence interval. These simulations are analogous to the theoretical scenarios depicted in Fig. 1c, highlighted using corresponding colors. Contrasting the three simulated “treatments” highlights how focusing only on either predator or prey responses to temperature yields very different predictions than when both are considered together.

Fig. 2.6. Predicted survivorship of a cohort of 300 *Ae. atropalpus* larvae in the presence of either: a) one *Erythemis* nymph or b) one *Pachydiplax* nymph, as a function of temperature (°C) and the scaling coefficient applied to handling time (h). Handling times were manipulated by multiplying them by a scaling constant, with values above or below 1 resulting in longer or shorter handling times, respectively, than those fit using data generated by our functional response experiment. Shorter handling times (scaling coefficients below 1) also resulted in a

more linear functional response fit (i.e., closer to a Type I, where $h = 0$), to demonstrate the consequences of ignoring the density-dependence of predation on overall model predictions.

Table 2.1. Parameter estimates for models describing the temperature-dependence of *Ae. atropalpus* development rate and mortality rate. Model equations are given in Eqn 1 and 2. Residual standard error for development rate was 0.602, and 0.0158 for mortality rate.

Table 2.2. Log-transformed parameter estimates for models describing the temperature-dependence of the functional response of two dragonfly nymphs, *Erythemis simplicicollis* and *Pachydiplax longipennis*. Functional response equations are given in Eqns 3-5.

Fig. 2.1.

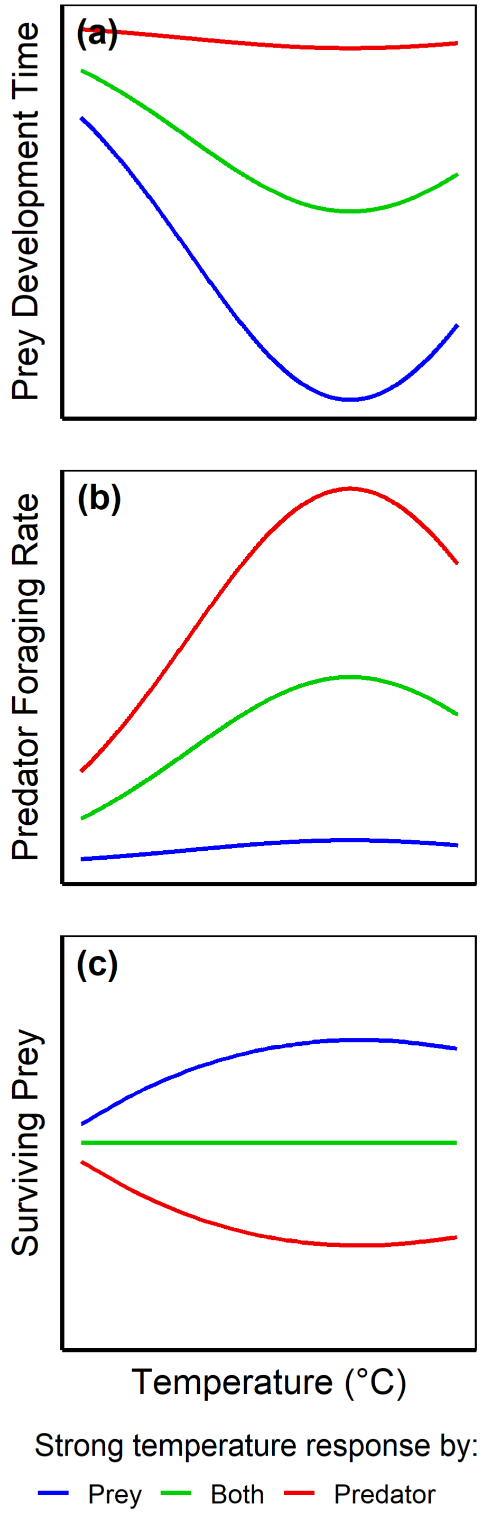
(a)
Prey Development Time
(b)
Predator Foraging Rate
(c)
Surviving Prey
Temperature (°C)
Strong temperature response by:
Prey
Both
Predator

Fig. 2.2.

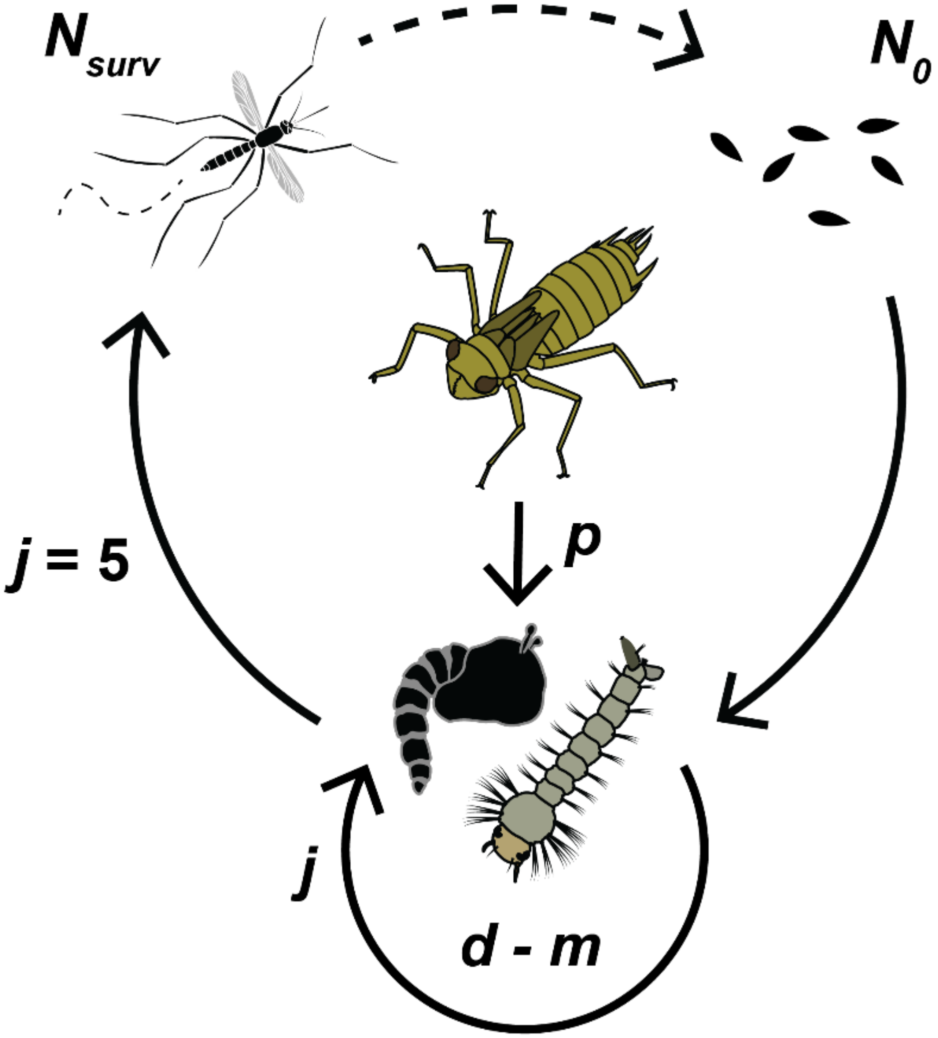

Fig. 2.3.

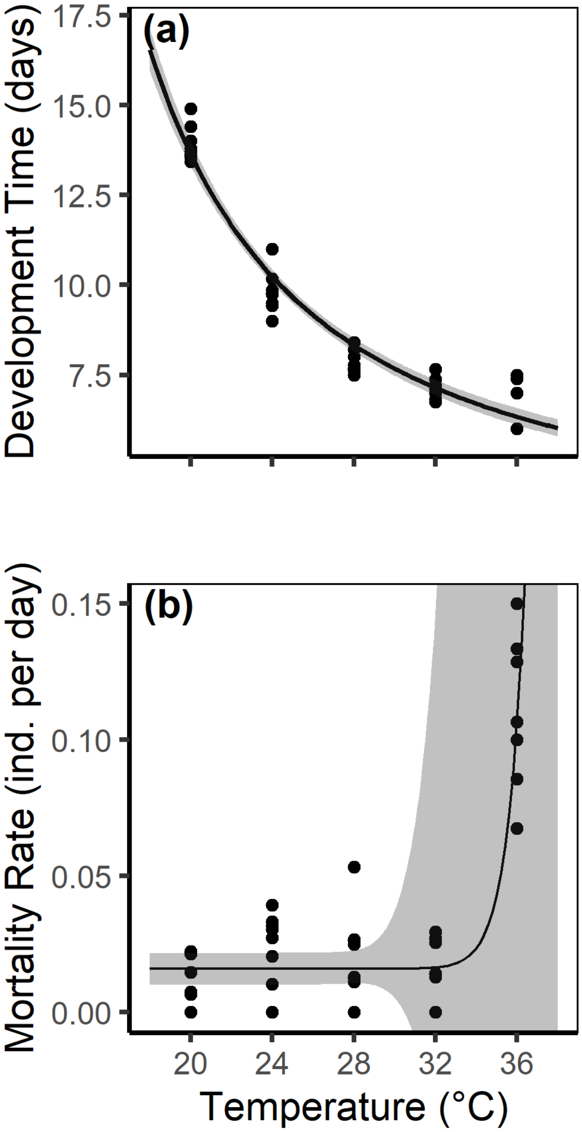
(a)
Development Time (days)
17.5
15.0
12.5
10.0
7.5
(b)
Mortality Rate (ind. per day)
0.15
0.10
0.05
0.00
20
24
28
32
36
Temperature (°C)

Fig. 2.4.

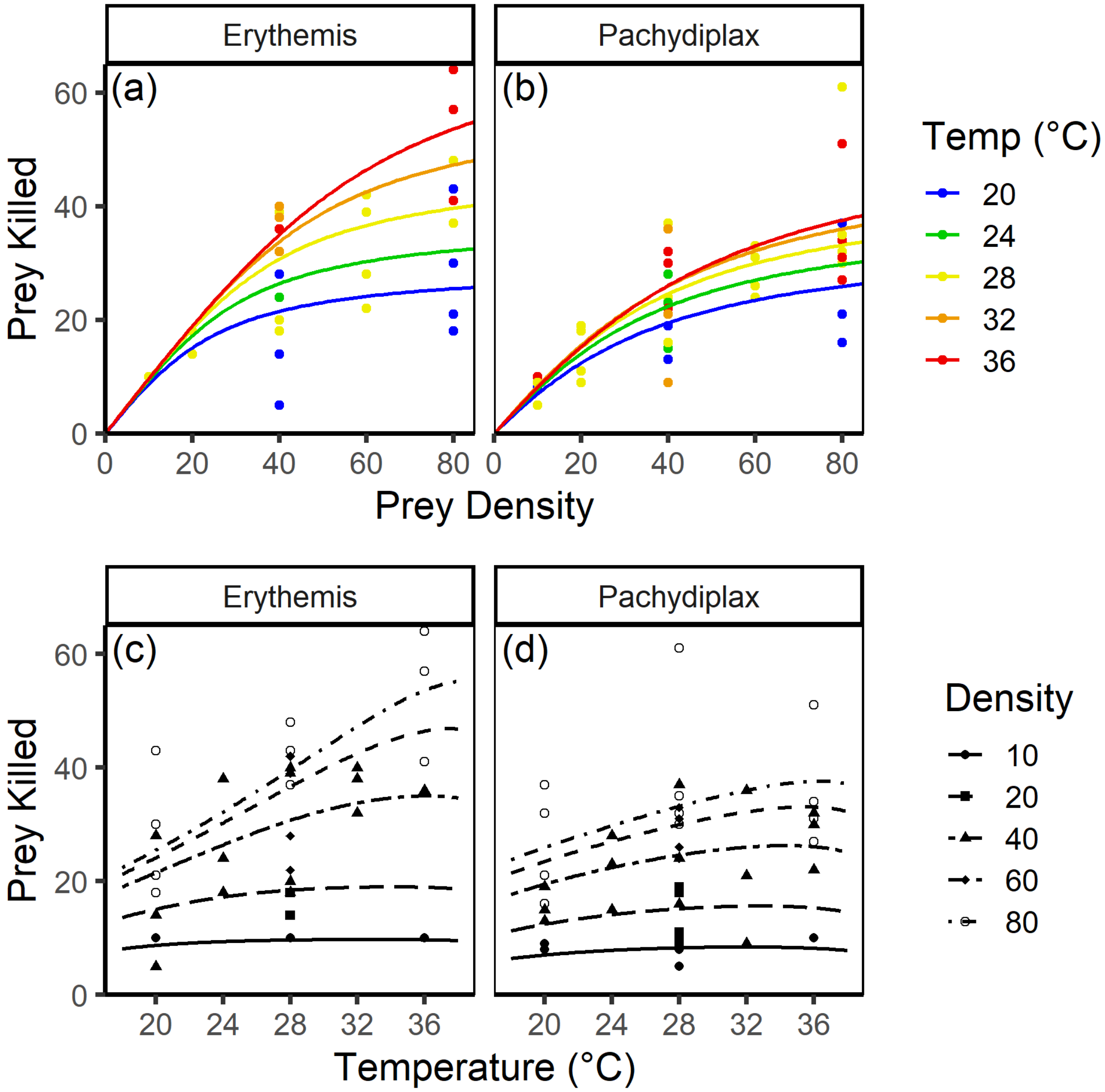

Erythemis
Pachydiplax
(a)
(b)
Prey Killed
0
20
40
60
Prey Density
80
Temp (°C)
20
24
28
32
36
Erythemis
Pachydiplax
(c)
(d)
Prey Killed
Temperature (°C)
Density
10
20
40
60
80

Fig. 2.5.

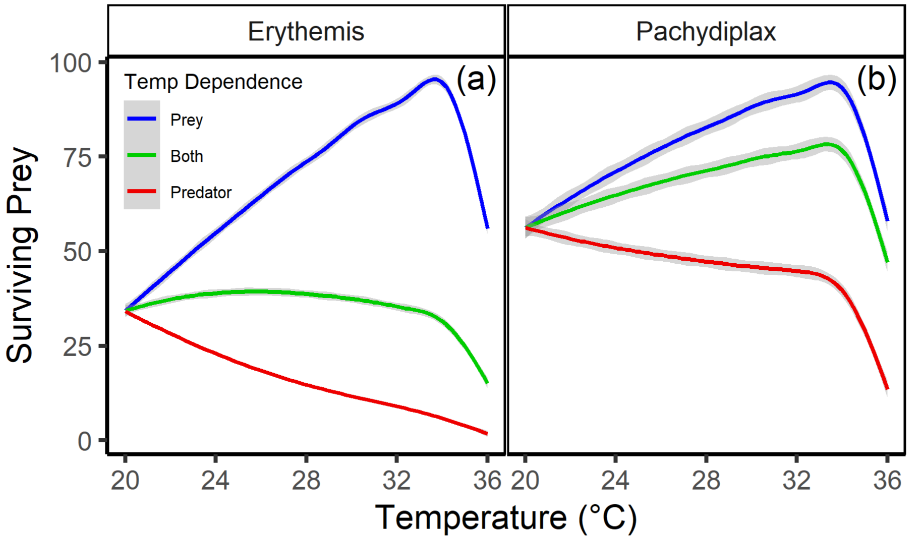
Erythemis
Pachydiplax
(a)
(b)
Temp Dependence
Prey
Both
Predator
Surviving Prey
100
75
50
25
0
20
24
28
32
36
Temperature (°C)

Fig. 2.6.

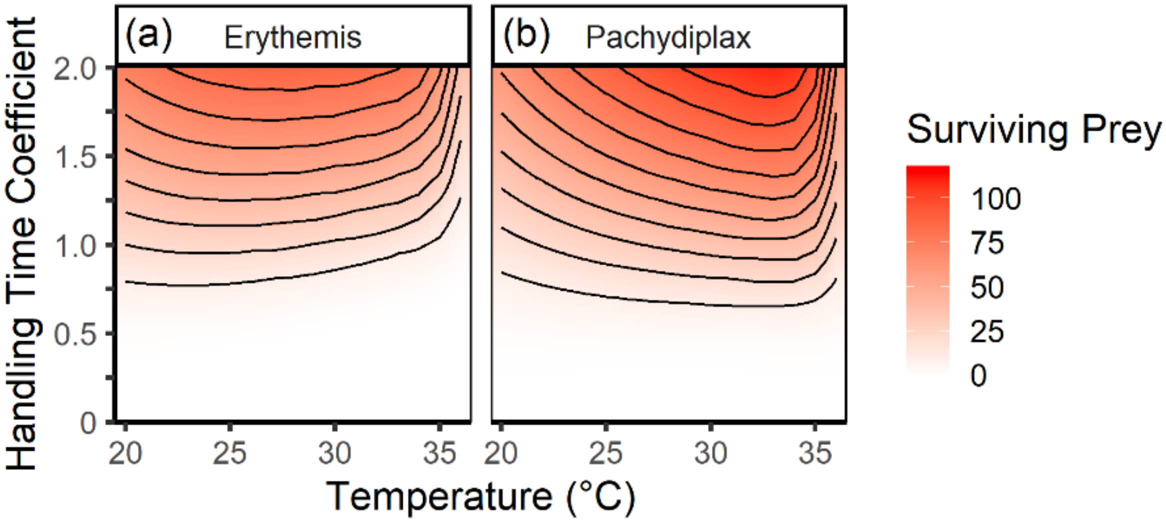
(a) Erythemis
(b) Pachydiplax
Handling Time Coefficient
2.0
1.5
1.0
0.5
0
20
25
30
35
Temperature (°C)
Surviving Prey
100
75
50
25
0

Table 2.1.

	Parameter	Estimate	Std. Error	*p* value
Development Rate	c	0.412	0.0197	<0.001
	b	-34.526	1.125	<0.001
Mortality Rate	T_0	37.776	3.421	<0.001
	m_0	0.0159	0.003	<0.001
	r_m	1.290	2.495	0.608

Table 2.2.

	Parameter	Estimate	Std. Error	*p* value
Erythemis	*b*	-2.791	0.116	<0.001
	h0	-25.0	0.493	<0.001
	E_h	-0.785	0.028	<0.001
Pachydiplax	*b*	-3.433	0.119	<0.001
	h0	-15.409	1.570	<0.001
	E_h	-1.518	0.186	<0.001

2.7. Supplementary Materials

Fig. S2.1. The response surface design used to collect data on the temperature-dependence of the functional response. Each number represents the number of replicates for the given temperature and prey density combination**.**

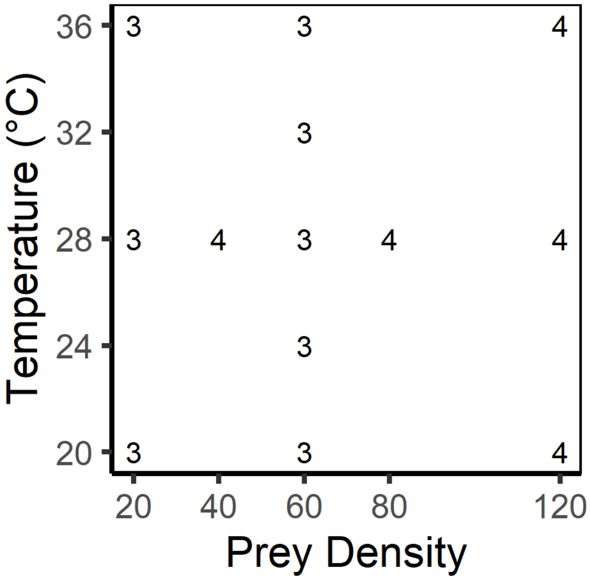

3. Warming and top-down control of stage-structured prey: linking theory to patterns in natural systems

*This manuscript is in review at Ecology, accepted pending minor revisions.

3.1. Introduction

Predators are key drivers of the structure and function of ecosystems by regulating the behavior, abundance, and population dynamics of prey species (Paine 1980; Oksanen et al. 1981; Power 1996). By suppressing prey populations, predators can stabilize food webs from the top-down (Oksanen et al. 1981; Leibold 1996; Estes et al. 2011) and provide valuable ecosystem services such as agricultural pest control or regulation of species that are vectors for disease (e.g., Bianchi et al. 2006; Begg et al. 2017; Tschumi et al. 2018). However, rising temperatures associated with climate change are expected to influence predator-prey interactions in ways that may jeopardize the ecological services they provide. Despite substantial research in the field (e.g., Rall et al. 2010; Brose et al. 2012; Romero et al. 2018), the consequences of rising temperatures on the outcomes of predator prey interactions remain somewhat unclear. This is in part because temperature sets the pace of a broad range of organism-level processes (e.g., metabolism, growth, reproduction, and mortality), which can have varied impacts on the way that predators and their prey interact (Brown et al. 2004; Rall et al. 2010; Dell et al. 2011).

Temperature has well-known nonlinear effects on predator foraging rates. Early attempts to quantify the relationship between temperature and foraging often invoked enzyme kinetics to model temperature effects using power relationships such as the Arrhenius equation (Brown et al. 2004). More recent studies suggest that predator foraging rates are often unimodal functions of temperature, increasing to a maximum before declining at high temperatures (Englund et al.

2011; Sentis et al. 2012; Uiterwaal and Delong 2020). Importantly, specific elements of the shape of this relationship, such as the rate of the predator's response to temperature or its inflection point (sometimes called the optimal temperature or T_{opt}) are not universal among predators (Dell et al. 2011; Uiterwaal and Delong 2020). Because of this, warming can either increase or decrease predation strength, depending upon both environmental context (e.g., current and future temperatures) and the predator species under consideration (e.g., its optimal temperature and rate of response).

Predicting warming's effects on predator-prey interactions is further complicated by the fact that warming does not solely impact predator physiology – it can also influence prey in ways that shape the outcome of their interactions with predators. For example, warmer conditions can increase prey body velocity, which can reduce predator capture success and foraging efficiency (Dell et al. 2014). Temperature also sets the pace of prey growth and development (Kingsolver et al. 2011; Quinn 2017), which can reduce the amount of time prey spend in predator-vulnerable life stages (Culler et al. 2015; Pepi et al. 2018; Davidson et al. 2021) or body sizes (Ohlberger 2013). By impacting both predator and prey traits, warming can thus cause either increases or decreases in short-term predation strength, depending on its relative impacts on predator and prey physiology (Dell et al. 2014).

Accurately predicting how warming will impact predator-prey interactions therefore requires accounting for multiple, often nonlinear effects of temperature on both predator and prey physiology. Studies have attempted to do so by drawing on data-driven theoretical models and laboratory experiments to describe temperature's effects on predator-prey interactions mechanistically (e.g., Rall et al. 2010; Sentis et al. 2012; Dell et al. 2014). However, these studies have generated a myriad of sometimes contradictory predictions about how warming-driven changes in predation will impact communities, such as increased (Fussmann et al. 2014) or decreased (Vasseur and McCann 2005) community stability, increased top-down control (O'Connor 2009; Hoekman 2010), and other context-dependent changes in community structure (Petchey et al. 2010; Amarasekare 2015). This stems in part from necessary but sometimes contradictory simplifying assumptions by these models, such as considering only temperatures below the predator's optimum (e.g., Brown et al. 2004; Dell et al. 2011; Price et al. 2012) and/or ignoring potentially important effects of temperature on prey physiology (e.g., prey body velocities, growth and development rates; Dell et al. 2014; Pepi et al. 2018; Davidson et al. 2021). Moreover, most models rely only on data collected in tightly controlled laboratory experiments (Dell et al. 2011), which may limit predictions to small spatiotemporal scales and a limited range of environmental contexts. Therefore, it is unclear how general our understanding of temperature effects on predation are, as well as how they fit into the broader context of the ecosystems they occur in.

While the general insights we have gained from existing studies are valuable, they may thus fail to capture context-dependent outcomes that are likely common in nature but difficult to predict. Nevertheless, these model-derived inferences provide testable hypotheses that can help us identify both theory concurrence and gaps in knowledge that can direct future research before additional warming occurs. Here, we field-test the predictions yielded by a model parameterized from controlled laboratory experiments (Fig. 3.1; but see also Ch. 2, Davidson et al. 2021) by evaluating the congruence of model predictions and field data collected from hundreds of natural riverine rock pools. To field-test our model, we: 1) quantified temperature variation across 755 rock pools distributed over 0.6 km^2; 2) parameterized our empirical model (Fig. 3.1a) using predators and prey from the same rock pool system (Fig. 3.1b) to quantitatively predict how short-term predation strength would vary across this thermal gradient (Fig. 3.1c); and 3) evaluated model predictions using patterns in the abundance of prey across naturally occurring gradients of both temperature and predator abundance across rock pools (Fig. 3.1d).

3.2. Methods

3.2.1. Characterizing Temperature Variation in Riverine Rock Pools

Riverine rock pools are commonly formed by hydrologic erosion along rivers with fast flow and rocky riverbeds (Ortega et al. 2014; Pelletier et al. 2015). Rock pools are particularly well suited for this research because they can be numerous, vary in size and other traits that contribute to their thermal conditions, and can be considered as relatively discrete communities, linked by aerial or flooding-driven colonization (Ren et al. 2016; Stunkle et al. 2021). Because rock pools are typically small and numerous within a given stretch of river, they can be surveyed rapidly and likely exhibit less spatial variability in their conditions than other more diffuse study systems, such as ponds or lakes. Here, we focus on interactions in rock pools between a common predator-prey pair: dragonfly nymphs of the genus *Pantala*, feeding on North American rock pool mosquito larvae (*Aedes atropalpus*).

To determine how temperature affects predation of *Ae. atropalpus* by *Pantala* nymphs *in situ*, we first characterized temperature variation across a system of riverine rock pools (total n = 755, spread across a ~0.6 km^2 study site) on the south side of Belle Isle on the James River in Richmond, VA, USA (37°31’44.98” N, 77°27’9.14” W). To do so, we deployed a series of water temperature data loggers (HOBO Pendant® Model MX2201) in randomly selected pools during the summer of 2021 (May – July). Data loggers were weighted using steel hardware nuts so that they would sink to the bottom of the pools.

We deployed probes for an eight-hour period each sampling date, beginning at 6:30AM and ending at 2:30PM. Based on pilot data, these sampling times allowed us to capture daily minimum and maximum pool temperatures while also monitoring the pools to prevent loss of data and data loggers due to theft or tampering by the general public. In total, we collected temperature data every 2-3 weeks in this manner from 155 unique pools across 4 sampling dates. A total of 36 pools were randomly selected for more than one sampling date, resulting in a total n of 203 data points.

To characterize the thermal environment of individual pools across the landscape, we developed a series of predictive general linear mixed models (GLMMs), which separately described the daily maximum temperature (T_{max}), minimum temperature (T_{min}), and temperature variation (measured as the coefficient of variation) within individual pools. These metrics were described using the following physical characteristics of the pools: 1) the average depth of the pool (cm), as estimated by measuring depth in four randomly selected locations within each pool; 2) its surface area (cm^2), as estimated by measuring the length and width of the pool along its longest axes and calculating the surface area of an ellipsoid ($A = \pi ab$); 3) the percentage of the pool that was shaded by surrounding vegetation or rock (as estimated using a canopy densiometer); and 4) the maximum temperature of the James River on the date of sampling (°C; using data collected and made available by the USGS from the Cartersville, VA river gage, approx. ~50 miles upstream).

Prior to model fitting, we checked for collinearity among covariates using the ggpairs function in the R package *GGally* (Schloerke et al. 2021). To aid in model fitting and to make model coefficients easier to directly compare to one another, we standardized all predictor variables by converting them into Z-scores prior to constructing the models. We then constructed a series of models in the R package *glmmTMB* (Brooks et al. 2017) using all possible combinations of the predictor variables above as fixed effects, with a random effect term for individual pools to account for non-independence of resampled pools and other characteristics of pools that we did not quantify (hereafter referred to as Pool ID).

From these candidate models, we compared their sample size corrected Akaike information criterion (AICc; Burnham and Anderson 2002; Brewer et al. 2016) scores as provided by the R package *glmmTMB* and considered the most appropriate model(s) to be within ΔAICc of 2.0 of the lowest AICc score. If multiple models were within ΔAICc of 2.0, we averaged the models (Dormann et al. 2018) using the R package MuMIn (Barton 2016). We calculated marginal and conditional pseudo r^2 values for all models using the R package *performance* (Nakagawa and Schielzeth 2013; Lüdecke et al. 2021). We also checked for multicollinearity among covariates in each model by calculating the variance inflation factor (VIF) of each covariate.

We subsequently predicted T_{max}, T_{min}, and the coefficient of variation for temperature across the whole landscape (n = 775 pools) using either the top or averaged model, holding maximum river temperature constant at its mean value (27.0°C). In the following section, we used the predicted values of $\mathrm{T_{max}}$ as a predictor of mosquito larval abundance across the rock pool landscape. In doing so, we consider these estimates as reflective of the relative thermal environment that organisms in each individual pool experience (i.e., not necessarily absolute predictions of pool temperature), in part because daily average temperatures could not be assessed given the 8-hr sampling window. It is also important to note that to collect this data set, we placed temperature loggers at the bottom of rock pools. Thus, these estimates more accurately describe the warmest temperature that organisms in a pool experience in the coolest parts of a pool (i.e., a thermal refuge). Dragonfly and mosquito larvae are both mobile organisms, capable of moving around their habitat to thermoregulate, and thus could be exposed to warmer temperatures within the pools. Thus, this model constitutes a conservative estimate of differences in temperature that organisms experience between pools.

3.2.2. Predicting Predator Effects Across a Thermal Gradient

Having characterized temperature variation across the rock pool landscape, we then generated predictions about how that thermal variation would affect predator-prey interactions in rock pools, using methodology from Davidson et al. (2021). As in Davidson et al. (2021), we consider predation of *Ae. atropalpus* mosquito larvae, but while Davidson et al. (2021) focused on dragonfly nymphs of the species *Pachydiplax longipennis* and *Erythemis simplicicollis*, we instead focus here on the most common genus in the system: *Pantala* spp. (Davidson pers. obs.).

In this predator-prey interaction, warming increases dragonfly nymph feeding rates but also accelerates mosquito larval development to adulthood. Because *Pantala* nymphs can only feed on the aquatic larval stage of *Ae. atropalpus*, this effectively shrinks the window of time that predators can feed on individual mosquito larvae. Thus, depending on temperature's effects on these two opposing processes, temperature can have varied effects on short-term predation strength (Dell et al. 2014; Davidson et al. 2021). For example, if predator feeding rates increase with temperature but mosquito larval development is relatively insensitive to temperature, short-term predation strength should increase (e.g., Pepi et al. 2018). However, if the opposite is true, and mosquito larvae exhibit a stronger response to temperature than their predators, interaction strength may decrease due to a shortened window of prey vulnerability (e.g., Culler et al. 2015; Davidson et al. 2021). Lastly, if the two species are equally impacted by temperature, there may be no change in interaction strength with warming. Based on previous work conducted in this system using similar predator-prey pairs (Davidson et al. 2021), we expected that *Pantala* predation of mosquito larvae would be weaker in warmer pools.

To quantify our predictions about how warming will influence dragonfly nymph predation of mosquito larvae within our system, we followed the modeling procedures described in Davidson et al. (2021). This approach first requires quantifying the temperature-dependence of predator feeding rates, prey development rates, and prey background mortality. We used parameter estimates published in Davidson et al. (2021) to model the temperature-dependence of *Ae. atropalpus* larval development using the Arrhenius equation (Brown et al. 2004, Quinn 2017) and prey mortality using a logistic function of temperature (see Davidson et al. 2021 for parameter estimates and equations). These parameter estimates were fit using data collected by rearing mosquito larvae from hatch to adulthood in environmental chambers (Percival Scientific Model I-30VL) set to one of five constant temperatures (20, 24, 28, 32, and 36°C) and a 14L:10D photoperiod (see Davidson et al. 2021 for specific methods).

In a separate laboratory experiment, we estimated the temperature-dependent functional response of *Pantala* nymphs on *Ae. atropalpus* larvae. We measured the temperature-dependent functional response of *Pantala* spp. on *Ae. atropalpus* using five constant temperature treatments (20, 24, 28, 32, and 36°C) and five starting prey density treatments (20, 40, 60, 80, and 120 larvae). A response surface design was employed to reduce the number of treatment combinations required to estimate the functional response (Fig. S3.1; McCoy et al. 2011; Davidson et al. 2021). This resulted in 13 treatment combinations with between 6-8 replicates each, for a total n of 83. Temperature manipulations were accomplished by using the same environmental chambers described above (Percival Scientific Model I-30VL) set to a 14L:10D photoperiod.

Prior to the experiment, *Ae. atropalpus* larvae were reared from eggs produced by a laboratory colony. Larvae were fed on a diet of brewer's yeast and liver powder (see Davidson et al. 2021) and allowed to grow to third instar in plastic larval rearing trays filled with 600 mL of deionized water, at a constant temperature of 28°C. *Pantala* nymphs were wild caught from riverine rock pools, fed to satiation on live brine shrimp (*Artemia* spp.), and then starved for 48hr prior to the experiment.

Mosquito larvae were added to experimental arenas consisting of a 950mL cup filled to a standardized volume of 800mL of deionized water, with four small (<4cm diameter) river rocks and a 10 cm tall plastic aquarium plant to provide habitat complexity and a structure for the dragonfly nymphs to cling to. Cups were randomly assigned to one of the treatment combinations described above and placed in the corresponding environmental chamber for 1hr so that the larvae could acclimate to their new surroundings and temperature. During this time, *Pantala* nymphs were also randomly assigned treatment combinations and placed in the corresponding environmental chamber in separate small 150mL cups to acclimate. After the hour had passed, we introduced a single *Pantala* nymph to each cup and allowed it to feed for 1hr, after which we removed the nymph and counted the surviving larvae.

As in Davidson et al. 2021, we fit a Type II functional response to the resulting data using the Rogers random predator equation (Rogers 1972):

$$(1) \quad N = N_0 - \frac{W\left(ahN_0 e^{-a(t-hN_0)}\right)}{ah}$$

where N is the number of prey eaten after time t (1hr), N_0 is the initial number of prey, a is the attack rate, h is the handling time, and W is the Lambert's W function (McCoy and Bolker 2008).

We allowed temperature to influence both the predator's attack rate (a) and handling time (h). For attack rate (a), we used the following unimodal function of temperature in Celsius (T):

$$(2) \quad a = b(T - CT_{min})(CT_{max} - T)^{1/2}$$

where b is a fitted constant, and CT_{min} and CT_{max} are the predator's lower and upper thermal bounds for activity, respectively (Briere et al. 1999; Sentis et al. 2012). These bounds vary from species to species and are not always readily available in the literature, so we used general estimates of the upper and lower thermal limit of Libellulid dragonflies (CT_{max} = 42.2°C, from Dallas and Rivers-Moore 2012; and CT_{min} = 10°C, from Suhling et al. 2015).

For handling time (h), we used the following form of the Arrhenius equation, where h depends on temperature in Celsius (T) and predator body mass in mg (M):

$$(3) \quad h = h_0 M^{b_h} e^{E_h/k(T+273.15)}$$

where h_0 is a fitted constant, b_h is an allometric scaling exponent (0.75; Brown et al. 2004), E_h is the activation energy for the rate-limiting enzyme-catalyzed biochemical rate of metabolism (eV) and k is Boltzmann's constant ($8.62 * 10^{-5}$ eV/K; Brown et al. 2004). On average, *Pantala* nymphs used in our experiment weighed approximately 401.6 mg.

Using these estimates for the temperature-dependence of predator feeding rates (Table 3.1) and prey development and mortality rates, and the stage-structured model outlined in Davidson et al. (2021), we predicted the number of *Ae. atropalpus* larvae that will survive from hatching to adulthood in the presence of a single *Pantala* nymph across a wide gradient of temperatures. Simulations were run as described in Davidson et al. 2021, using a starting prey density of 300 larvae and a temperature gradient of 20 to 36°C. Unlike in Davidson et al. 2021, the functional response of *Pantala* was measured over the course of an hour instead of a full 24 hours to avoid excessive depletion of prey during the experiment. For the purposes of this simulation, we assumed that the overall form and temperature-dependence of the functional response would be approximately the same across a 24-hr period, due to predator satiation.

To account for uncertainty in our estimates of the functional response parameters, simulations were replicated 3000 times, with each replicate using different values for the fitted parameters b, h_0, and E_h that had been randomly resampled from a distribution determined by their standard error.

3.2.3. Assessing Mosquito and Dragonfly Distributions Across the Landscape

To evaluate our model's predictions and determine how temperature and predation interactively influence prey populations in natural rock pools, we paired the pool-level estimates of T_{max} described above with data describing the distribution and abundance of both mosquito larvae and dragonfly nymphs in randomly selected rock pools across the landscape during the summer of 2021. We collected and quantified both organisms in each pool using 15.2 x 12.1 cm aquatic dip nets. To standardize sampling effort, we swept the pools using the nets nine times each, where a "sweep" was approximately 25 cm long. We spread sampling efforts within pools across three separate regions – the water column, sides, and bottom of the pool – each of which received three sweeps.

While pools were selected randomly, there was partial spatiotemporal overlap with the pools selected for temperature sampling above. In total, we collected 355 samples across 232 unique pools, and these samples included 75 of the pools that were selected for temperature data collection as described above. Sampling was spread across 21 different sampling dates during the months of May through September.

Using the temperature estimates from the model described above, we constructed a generalized linear mixed model with a negative binomial error structure using the R package *glmmTMB* (Brooks et al. 2017). The model described mosquito larval abundance in each pool as a function of the fixed effects of predicted T_{max} and the presence or absence of dragonfly nymphs, and a sampling date level random effect. As before, predicted temperature values were standardized by converting them into Z-scores to aid with model fitting and comparisons between models. Initial data exploration and model assessment using the R package *DHARMa* (Hartig 2022) suggested that the data were overdispersed and zero-inflated. Thus, while models with other structures and combinations of variables were considered and assessed using these same procedures, the final model that we present here (i.e., the one that best accounted for these issues) is a hurdle (i.e., zero-truncated) model. This model employed a two-step process to describe 1) the probability of mosquito larvae being absent as a function of dragonfly nymph presence, and 2) the abundance of mosquito larvae when they are present using a negative binomial conditional model consisting of the fixed and random effects described above. As before, we considered the top model to be within ΔAICc of 2.0, and if multiple models fit this criterion, we used model averaging to account for this. We calculated marginal and conditional pseudo r^2 values for this model using the R package *performance* (Nakagawa and Schielzeth 2013; Lüdecke et al. 2021).

In the final data set, some pools at the extreme high and low ends of the temperature gradient had no mosquito larvae but may have had predators present. We excluded such pools ($n = 17$) from the final analyses, because in these cases it would be difficult if not impossible to infer whether the absence of mosquito larvae was due to predator presence or temperature extremes (final $n = 338$). For the purposes of this model, we also assumed that dragonfly nymphs were randomly distributed across the landscape, and thus independent of temperature or other factors. This assumption was based on the tendency of some dragonfly species, including *Pantala flavescens*, to oviposit across a broad range of potential larval habitat patches (i.e., spatial risk spreading; Schenk et al. 2004). Previous research in this study system also suggests that dragonfly abundance primarily depends upon the number of days that have passed since the pool was last flooded by the river instead of other abiotic factors (Stunkle et al. 2021, see also Table S3.1), which we accounted for by randomly sampling across the field season.

3.3. Results

3.3.1. Temperature Variation in Rock Pools

We found considerable variation in rock pool temperatures, both between and within pools (Fig. 3.2). Daily maximum pool temperatures (T_{max}) across all sampling dates and pools averaged 31.7 ± 0.3 °C (mean ± std. err) but varied considerably across the landscape (Fig. 3.2a, 3.2d). For example, the largest difference in T_{max} between pools occurred on 6/24/2021, where the pool with the highest T_{max} peaked at 39.6 °C, while the pool with the lowest T_{max} peaked at only 21.6 °C (a difference of 18.0 °C). The model with the lowest AICc described T_{max} as a function of the fixed effects pool depth (cm), the percent of the pool that was shaded by surrounding vegetation, and maximum river temperature on the day that temperature data was collected (°C), and the random effect Pool ID (Table S3.2; marginal pseudo-r^2 = 0.45, conditional pseudo-r^2 = 0.87). Pools that were deeper (coeff. estimate = -1.95, 95% CI: -2.41 to -1.49) and shadier (coeff. estimate = -1.39, 95% CI: -1.85 to -0.92) generally had cooler daily maximum temperatures, while pools overall reached higher maximums on days where the daily maximum river temperature was also warmer (coeff. estimate = 1.65, 95% CI: 1.35 to 1.95).

Daily minimum pool temperatures (T_{min}) were also variable across the landscape, but to a lesser extent (Fig. 3.2b). The average T_{min} across all sampling dates and pools was 24.3 ± 0.2 °C. The largest difference in T_{min} across pools occurred on 5/20/2021, where the pool with the highest T_{min} reached a low of 23.4 °C, whereas the pool with the lowest T_{min} reached a low of 15.8 °C (a difference of 7.6 °C). Four models were within ΔAICc of 2.0. The averaged model for T_{min} predicted that pools that were shadier (coeff. estimate = -0.29, 95% CI: -0.48 to -0.10) and had higher surface area (coeff. estimate = -0.33, 95% CI: -0.52 to -0.15) generally had cooler minimum temperatures, while deeper pools (coeff. estimate = 0.54, 95% CI: 0.35 to 0.72) or pools sampled on days when the river was warmer (coeff. estimate = 2.72, 95% CI: 2.55 to 2.90) had warmer minimum temperatures (Table S3.3; pseudo-r^2 = 0.89). The pool-level random effect was excluded from this analysis due to the occurrence of singular gradients in the data set.

The daily range of temperatures within rock pools (measured as $T_{max} – T_{min}$) across all sampling dates was 7.4 ± 0.3 °C (Fig. 3.2c). Some pools experienced large fluctuations in temperature throughout the day, with ranges as large as 19.6 °C, while others experienced ranges as small as 0.5 °C during the same sampling date. There were three models for the coefficient of variation of temperature within ΔAICc of 2.0. The averaged model suggested that pools that were deeper (coeff. estimate = -0.030, 95% CI: -0.04 to -0.02) and shadier (coeff. estimate = -0.012, 95% CI: -0.02 to -0.005) had somewhat less variability in temperature, while days with higher river temperatures (coeff. estimate = -0.019, 95% CI: -0.02 to -0.01) led to somewhat greater variability in temperature overall (Table S3.4; marginal pseudo-r^2 = 0.39, conditional pseudo-r^2 = 0.82).

3.3.2. Temperature Effects on Predation in Silico

Our stage-structured model (Figs. 3.3-3.4) suggested that warmer conditions may increase *Ae. atropalpus* larval survival to adulthood in the presence of *Pantala* nymphs, because mosquito larval development (Fig. 3.3a-b) was more strongly affected by temperature than *Pantala* nymph feeding rates were (as in Davidson et al. 2021; Fig. 3.3c-d, Table S3.5). However, sustained high temperatures (≥ 33.0°C) caused mass mortality of *Ae. atropalpus* larvae in our experimental setting (Fig. 3.3b) and subsequently, our model (Fig. 3.4). We ultimately predicted that *Pantala* nymphs would have a weaker effect on the abundance of *Ae. atropalpus* larvae in warmer rock pools (Fig. 3.4c).

We also predicted that extreme high temperatures may eventually cause lower abundances of *Ae. atropalpus* larvae due to temperature-dependent mortality, however, we were uncertain how warm pools would need to be to observe this effect for two primary reasons. First, larval development and mortality rates were measured experimentally using constant temperatures, which are not directly comparable to observed and estimated field conditions (which were based on T_{max}). Additionally, during the experiment, larval mortality was typically late in development, usually during their final molt from the pupa to adult stage (i.e., eclosion). Thus, temperature-dependent mortality may not be obvious from point estimates of larval abundance.

3.3.3. Temperature Effects on Predation in Situ

Mosquito larvae were present in 50.1% (n = 178) of pools surveyed, while dragonfly nymphs were present in 24.2% (n = 86). Of those occurrences, both species overlapped in only 7.0% of pools surveyed (n = 25). Observational data suggests that while other species of mosquito larvae (e.g., *Culex* spp. and *Anopheles* spp.) and dragonfly nymphs (e.g., *E. simplicicollis* and *P. longipennis*) were sometimes present, the species observed were *Ae. atropalpus* and *Pantala* spp. in most cases (>90% of occurrences).

Two models describing mosquito abundance were within ΔAICc of 2.0, so model averaging was used to produce the final model. The resulting model suggested that the distribution of mosquito larvae across the landscape was driven by a combination of predicted T_{max} (Figs. 3.2a, 3.2d), the presence of dragonfly nymph predators, the interaction between the two, and the number of days since the pool was last inundated by the river (see Stunkle et al. 2021), with a random effect of sampling date (Fig. 3.5, Table S3.6; marginal pseudo-r^2 values for the component models = 0.351 and 0.364, conditional pseudo-r^2 values = 0.384 and 0.402).

Our model suggested that there was a lower probability of mosquito larvae being present in pools where dragonfly nymphs were present (Fig. 3.5a; zero-inflation model: coeff. estimate = 0.88, 95% CI: 0.29 to 1.46), which varied depending on the random effect of sampling date. When mosquito larvae were present, their abundance was higher in warmer pools (Fig. 3.5b; as approximated by T_{max}; conditional model: coeff. estimate = 0.48, 95% CI: 0.16 to 0.81), but their abundance was much lower in pools with higher dragonfly nymph abundance (conditional model: coeff. estimate = -2.30, 95% CI: -3.35 to -1.25). However, there was an interaction between these terms, such that the negative effect of dragonfly nymph abundance on mosquito larvae abundance was weaker when pools were warmer (Fig. 3.5b-c; conditional model: coeff. estimate =1.03, 95% CI: 0.14 to 1.93). Mosquito abundance increased slightly the longer it had been since the pool was last inundated by the river (conditional model: coeff. estimate = 0.14, 95% CI: -0.21 to 0.49). Estimates of the random effect of sampling date were -0.25 (95% CI: -

0.63 to 0.12) and 3.97 (95% CI: 3.41 to 4.54) in the zero-inflation and conditional model, respectively.

3.4. Discussion

Predicting the impacts of warming on predator-prey interactions remains challenging, in part because temperature has broad, often nonlinear and/or context-dependent effects on key elements of both predator and prey physiology. A considerable amount of research over the past few decades has focused on gaining a mechanistic understanding of how temperature impacts species interactions such as predation, via a combination of theory, controlled experiments, and modeling (e.g., Brown et al. 2004; Rall et al. 2010; Dell et al. 2014). These approaches are often designed using broadly applicable methodology, making them valuable tools for exploring and comparing the impacts of warming on predation across different species and systems, especially in systems where it is impractical or outright impossible to meaningfully manipulate thermal conditions *in situ*. However, these approaches often use experiments conducted on short time scales (e.g., functional responses measured in hours or days, single-generation development rates), focus on only one interacting pair of species, and may selectively include or exclude certain important system-specific contexts (e.g., Vasseur and McCann 2005; Amarasekare 2015; Davidson et al. 2021). Thus, the accuracy of their predictions and their long-term importance for broader ecosystem structure and function remain unclear.

Here, we attempted to bridge this gap by leveraging natural thermal variation in a system of riverine rock pools to assess one such set of predictions (Fig. 3.1; Davidson et al. 2021). To do so, we 1) characterized natural thermal variation across rock pools (Fig. 3.2), 2) predicted how that thermal variation should impact predation of mosquito larvae by dragonfly nymphs within the system (Figs. 3.3-3.4), and 3) looked for evidence for or against our predictions by examining patterns in the natural abundance of prey across gradients of both temperature and predator abundance (Fig. 3.5). Our initial model-derived predictions suggested that warmer conditions would result in weaker predator control of mosquito larvae, because for our focal taxa, warming has a stronger impact on prey development, shrinking the window of time in which predators can consume them (Figs. 3.3-3.4; Davidson et al. 2021). This prediction was corroborated by field patterns of mosquito larval abundance across a broad thermal gradient (Fig. 3.5).

Thermal conditions in rock pools varied considerably but generally depended upon the physical and abiotic characteristics of the pool (Fig. 3.2). Daily maximum temperatures and temperature variation in individual pools were driven by pool depth and the presence of overlying shade (e.g., trees and overhanging rocks), while minimum temperatures depended upon pool surface area and depth. While many studies have characterized the thermal conditions of larger aquatic systems, such as ponds, lakes, and sections of rivers or streams (e.g., Lamoureux et al. 2006, Sohrabi et al. 2017), rock pools are particularly well suited to studying the effects of water temperature on aquatic organisms. Rock pools are generally small and can be numerous where they occur, allowing for rapid sampling and high replication as compared to larger systems, such as streams, ponds, or lakes (Jocqué et al. 2010; Schiesari et al. 2018; Stunkle et al. 2021). Additionally, pools are relatively small and thus have relatively spatially consistent temperatures and few thermal refugia. Consequently, measured and predicted temperatures are likely closer to those experienced by the organisms themselves, as compared to larger aquatic systems. Pool temperatures can also be described using relatively simple models consisting of abiotic characteristics that are easily measured and unlikely to vary considerably across time.

We generated predictions about how this thermal variation would impact a key predator-prey interaction in rock pools using the approach described here and in Davidson et al. (2021). To do so, we parameterized a simple stage-structured model describing the interaction between *Pantala* spp. dragonfly nymph predators and *Ae. atropalpus* mosquito larval prey, using a series of laboratory experiments. Experimental and modeling results suggested that *Ae. atropalpus* development rates are highly sensitive to temperature, halving across the thermal gradient used (Fig. 3.3a). However, constant temperatures above 34°C were too warm for the larvae to tolerate and resulted in high mortality rates (Fig. 3.3b). By comparison, *Pantala* spp. feeding rates were relatively insensitive to temperature (Fig. 3.3c-d). Taken together, our model (Fig. 3.4) suggested that warmer conditions would reduce predation pressure on mosquito larvae, leading to more larvae surviving to adulthood, until temperatures exceeded the thermal tolerance of the larvae (Fig. 3.4c).

Our model's predictions are qualitatively consistent with patterns in mosquito larval abundance observed in natural rock pools (Fig. 3.5). Intuitively, mosquito larvae were less likely to be present in pools with dragonfly nymphs (Fig. 3.5a), and when they were present, larvae were less abundant (Fig. 3.5b). As we predicted, temperature and predator presence interactively influenced mosquito larval abundances, such that warmer pools with dragonfly nymphs still had higher mosquito larval abundances (Fig. 3.5b-c). However, we also observed positive instead of negative effects of warmer temperatures alone on mosquito larval abundances (Fig. 3.5b), contrary to experimental findings (Fig. 3.3b) and our model's predictions (Fig. 3.4c). This suggests that warmer conditions have positive benefits for *Ae. atropalpus* beyond the scope of our predictive model.

This positive effect of temperature on mosquito abundance observed in the field (Fig. 3.5b) was not observed under laboratory conditions (Fig. 3.3b). We suspect that this may be because during our experiment, mosquito larvae were kept at constant temperatures, which may be more thermally stressful for them (Kingsolver et al. 2015) and provided with food *ad libitum*. Studies on naturally occurring populations of *Ae. atropalpus* suggest that they are more abundant and have higher population growth rates in warmer pools (Byrd et al. 2019; Day et al. 2021). This may be in part because warmer conditions also spur the growth of food resources for mosquito larvae, such as plankton (Duchet et al. 2017), and *Ae. atropalpus* may be particularly sensitive to larval resource availability as compared to other mosquito species, due to the species' facultative autogeny (Hedeen 1953; O'Meara and Craig 1970; Armistead et al. 2008).

Taken collectively, our findings suggest that within our system, warming will increase the short-term abundance of *Ae. atropalpus* and its recruitment to adulthood because warmer pools yield higher densities of *Ae. atropalpus* and weaken the impacts of their predators. By using our pool temperature and mosquito abundance models in conjunction, we can predict the magnitude of this increase across the entire rock pool metapopulation under different warming scenarios. For example, if we assume that predator distributions across the pools remain the same and temperatures warm by approximately the same amount across all pools, we predict that even under modest warming (+2.5°C), landscape-level *Ae. atropalpus* larval abundances could increase by between 1.5-1.9 times the amount present under current conditions (accounting for the std. error of abundance estimates from the model). However, it remains unclear how this increase in recruitment will impact the long-term population dynamics of *Ae. atropalpus* and its predator *Pantala* spp., which we do not currently consider in our modeling framework.

While our findings provide evidence in favor of our model's predictions, as with any observational study we cannot definitively link the patterns in mosquito abundance we observed in the field to our model's underlying mechanisms. Importantly, our model provides an estimate of temperature-driven changes in short-term predation strength – specifically, it predicts the number of mosquito larvae that will survive to adulthood from a cohort of eggs laid simultaneously. By comparison, our field data consist of estimates of larval abundance during an unknown point in their development. These two quantities should be correlated but are likely not entirely equivalent.

Our findings may also depend on separate but adjacent temperature-sensitive processes that influence the interaction, such as prey growth rate. Predation rates often depend nonlinearly on prey body size (Brose et al. 2005, McCoy et al. 2011, Yodzis and Innes 2016), and warmer temperatures simultaneously speeds growth rates (in terms of body size) while shrinking the maximum body size that ectotherms attain (Atkinson 1994; Kingsolver and Huey 2008; Bideault et al. 2019). Preliminary data suggest that predation of *Ae. atropalpus* larvae may be strongly size-dependent – *E. simplicicollis and P. longipennis* nymphs can consume L1 *Ae. atropalpus* larvae (body length = 1.42mm) at greater than 10X the rate of L3 larvae (body length = 5.24mm; Fig. S3.2). Thus, size-dependent predation may be an important mechanism for our observed field patterns that our current model does not explicitly include but could in future iterations (see also McCoy et al. 2022).

Adult mosquitoes are also widely known to select sites for oviposition depending on factors such as larval resource availability, the presence of predators, and other abiotic conditions

(Kraus and Vonesh 2010; Yee et al. 2010; Silberbush and Blaustein 2011), including temperature in some cases (Zuharah and Lester 2010). Based on the zero-inflated component of our model, it is possible that *Ae. atropalpus* adults may avoid ovipositing in pools with dragonfly nymphs present (Fig. 3.5a), although anecdotally, we have not observed this in pilot studies conducted in laboratory settings. This also cannot be determined definitively from our findings here, because dragonfly nymphs have high feeding rates on *Ae. atropalpus* larvae (Fig. 3.3c-d; Davidson et al. 2021) and may simply extirpate larval populations from pools when they are present. By comparison, it is unlikely that adult *Ae. atropalpus* show preference for temperature when ovipositing in pools, because warmer pools were not more likely to have mosquito larvae. Additionally, we suspect that the high variability in temperature we observed in many pools (Fig. 3.2c) may make temperature an unreliable oviposition cue.

In the face of rising global temperatures, it is critical that we not only develop tools to monitor and predict how ecosystems will be impacted by warming, but also that we challenge our predictions and understanding of the issues with real data whenever possible. Here, we found evidence *in situ* in support of predictions made using short-term laboratory experiments and modeling informed by theory. This suggests that the effects of temperature on this stage-structured predator-prey interaction are strong enough to be observed despite the background noise and complexity of a natural system of rock pools. Further, our exploration of this modeling approach has identified potential gaps in our understanding of the temperature's effects on this interaction, such as the positive impacts warmer temperatures had on *Ae. atropalpus* abundance, and size-dependent predation's role as a potential mechanism for observed patterns in larval abundance. We stress that while controlled experiments and models are powerful tools for predicting the effects of climate change on species interactions, it is also critical that we treat these predictions as hypotheses to be tested before future warming occurs, and establish their importance within the spatiotemporal context of the ecosystems they occur in.

3.5. References

Amarasekare, P. (2015). Effects of temperature on consumer-resource interactions. *Journal of Animal Ecology*, *84*(3), 665–679. https://doi.org/10.1111/1365-2656.12320

Armistead, J. S., Nishimura, N., Escher, R. L., & Lounibos, L. P. (2008). Larval competition between Aedes japonicus and Aedes atropalpus (Diptera: Culicidae) in simulated rock pools. *Journal of Vector Ecology*, *33*(2), 238–246. https://doi.org/10.1016/j.bbi.2008.05.010

Barton, K. (2016) Package 'MuMIn'.

Begg, G. S., Cook, S. M., Dye, R., Ferrante, M., Franck, P., Lavigne, C., Lövei, G. L., Mansion-Vaquie, A., Pell, J. K., Petit, S., Quesada, N., Ricci, B., Wratten, S. D., & Birch, A. N. E. (2017). A functional overview of conservation biological control. *Crop Protection*, *97*, 145–158. https://doi.org/10.1016/j.cropro.2016.11.008

Bianchi, F. J. J. A., Booij, C. J. H., & Tscharntke, T. (2006). Sustainable pest regulation in agricultural landscapes: A review on landscape composition, biodiversity and natural pest control. *Proceedings of the Royal Society B: Biological Sciences*, *273*(1595), 1715–1727. https://doi.org/10.1098/rspb.2006.3530

Bideault, A., Loreau, M., & Gravel, D. (2019). Temperature Modifies Consumer-Resource Interaction Strength Through Its Effects on Biological Rates and Body Mass. *Frontiers in Ecology and Evolution*, *7*(February), 1–11. https://doi.org/10.3389/fevo.2019.00045

Brewer, M. J., Butler, A., & Cooksley, S. L. (2016). The relative performance of AIC, AICC and BIC in the presence of unobserved heterogeneity. *Methods in Ecology and Evolution*, *7*(6), 679–692. https://doi.org/10.1111/2041-210X.12541

Briere, J.-F., Pracros, P., le Roux, A.-Y., & Pierre, J.-S. (1999). A novel rate model of temperature-dependent development for arthropods. *Environmental Entomology*, *28*(1), 22–29.

Brooks, M. E., Kristensen, K., van Benthem, K. J., Magnusson, A., Berg, C. W., Nielsen, A., Skaug, H. J., Mächler, M., & Bolker, B. M. (2017). glmmTMB Balances Speed and Flexibility Among Packages for Zero-inflated Generalized Linear Mixed Modeling. In *The R Journal* (Vol. 2073, Issue 4859).

Brose, U., Dunne, J. A., Montoya, J. M., Petchey, O. L., Schneider, F. D., & Jacob, U. (2012). Climate change in size-structured ecosystems. *Proceedings of the Royal Society B: Biological Sciences*, *367*, 2903–2912.

Brose, U., Cushing, L., Berlow, E. L., Jonsson, T., Banasek-Richter, C., Bersier, L.-F., Blanchard, J. L., Brey, T., Carpenter, S. R., Blandenier, M.-F. C., Cohen, J. E., Dawah, H. A., Dell, T., Edwards, F., Harper-Smith, S., Jacob, U., Knapp, R. A., Ledger, M. E., Memmott, J., … Martinez, N. D. (2005). Body Sizes of Consumers and Their Resources. *Ecology*, *86*(9), 2545–2545. https://doi.org/10.1890/05-0379

Brown, J. H., Gillooly, J. F., Allen, A. P., Savage, V. M., & West, G. B. (2004). Toward a metabolic theory of ecology. *Ecology*, *85*(7), 1771–1789. https://doi.org/Doi 10.1890/03-9000

Burnham, K. P., & Anderson, D. R. (2004). Multimodel inference: Understanding AIC and BIC in model selection. *Sociological Methods and Research*, *33*(2), 261–304. https://doi.org/10.1177/0049124104268644

Byrd, B. D., Sither, C. B., Goggins, J. A., Kunze-Garcia, S., Pesko, K. N., Bustamante, D. M., Sither, J. M., Vonesh, J. R., & O'meara, G. F. (2019). Aquatic thermal conditions predict the presence of native and invasive rock pool Aedes (Diptera: Culicidae) in the southern Appalachians, U.S.A. *Journal of Vector Ecology*, *44*(1), 30–39.

Culler, L. E., Ayres, M. P., & Virginia, R. A. (2015). In a warmer Arctic, mosquitoes avoid increased mortality from predators by growing faster. *Proceedings of the Royal Society B: Biological Sciences*, *282*(1815), 20151549. https://doi.org/10.1098/rspb.2015.1549

Dallas, H. F., & Rivers-Moore, N. A. (2012). Critical Thermal Maxima of aquatic macroinvertebrates: Towards identifying bioindicators of thermal alteration. *Hydrobiologia*, *679*(1), 61–76. https://doi.org/10.1007/s10750-011-0856-4

Davidson, A. T., Hamman, E. A., McCoy, M. W., & Vonesh, J. R. (2021). Asymmetrical effects of temperature on stage-structured predator–prey interactions. *Functional Ecology*, *35*(5). https://doi.org/10.1111/1365-2435.13777

Day, C. A., Armstrong, E. G., & Byrd, B. D. (2021). Population growth rates of aedes atropalpus (Diptera: Culicidae) are depressed at lower temperatures where aedes japonicus japonicus (Diptera: Culicidae) are naturally abundant in rock pools. *Journal of Medical Entomology*, *58*(1), 493–497. https://doi.org/10.1093/jme/tjaa183

Dell, A. I., Pawar, S., & Savage, V. M. (2011). Systematic variation in the temperature dependence of physiological and ecological traits. *Proceedings of the National Academy of Sciences*, *108*(26), 10591–10596. https://doi.org/10.1073/pnas.1015178108

Dell, A. I., Pawar, S., & Savage, V. M. (2014). Temperature dependence of trophic interactions are driven by asymmetry of species responses and foraging strategy. *Journal of Animal Ecology*, *83*(1), 70–84. https://doi.org/10.1111/1365-2656.12081

Dormann, C. F., Calabrese, J. M., Guillera-Arroita, G., Matechou, E., Bahn, V., Bartoń, K., Beale, C. M., Ciuti, S., Elith, J., Gerstner, K., Guelat, J., Keil, P., Lahoz-Monfort, J. J., Pollock, L. J., Reineking, B., Roberts, D. R., Schröder, B., Thuiller, W., Warton, D. I., … Hartig, F. (2018). Model averaging in ecology: a review of Bayesian, information-theoretic, and tactical approaches for predictive inference. In *Ecological Monographs* (Vol. 88, Issue 4, pp. 485–504). Ecological Society of America. https://doi.org/10.1002/ecm.1309

Duchet, C., Segev, G. M., Spencer, O., Hayoon, M., & Gershberg, A. (2017). Effects of Flash Flooding on Mosquito and Community Dynamics in Experimental Pools. *Journal of Vector Ecology*, *42*(2), 254–263. https://doi.org/10.3376/038.042.0206

Englund, G., Öhlund, G., Hein, C. L., & Diehl, S. (2011). Temperature dependence of the functional response. *Ecology Letters*, *14*(9), 914–921. https://doi.org/10.1111/j.1461-0248.2011.01661.x

Estes, J. A., Terborgh, J., Brashares, J. S., Power, M. E., Berger, J., Bond, W. J., Carpenter, S. R., Essington, T. E., Holt, R. D., Jackson, J. B. C., Marquis, R. J., Oksanen, L., Oksanen, T., Paine, R. T., Pikitch, E. K., Ripple, W. J., Sandin, S. A., Scheffer, M., Schoener, T. W., … Wardle, D. A. (2011). Trophic downgrading of planet earth. *Science*, *333*(6040), 301–306. https://doi.org/10.1126/science.1205106

Fussmann, K. E., Schwarzmüller, F., Brose, U., Jousset, A., & Rall, B. C. (2014). Ecological stability in response to warming. *Nature Climate Change*, *4*(3), 206–210. https://doi.org/10.1038/nclimate2134

Hartig, F. (2022). *DHARMa: Residual Diagnostics for Hierarchical (Multi-Level / Mixed) Regression Models* (R package version 0.4.5).

Hedeen, R. A. (1953). The Biology of the Mosquito Aedes atropalpus Coquillett. *Journal of the Kansas Entomological Society*, *26*(1), 1–10.

Hoekman, D. (2010). Turning up the heat: temperature influences the relative importance of top-down and bottom-up effects in pitcher plant inquiline communities. *Ecology*, *91*(10), 100521032119033. https://doi.org/10.1890/10-0260

Jocqué, M., Vanschoenwinkel, B., & Brendonck, L. (2010). Freshwater rock pools: A review of habitat characteristics, faunal diversity and conservation value. *Freshwater Biology*, *55*(8), 1587–1602. https://doi.org/10.1111/j.1365-2427.2010.02402.x

Kingsolver, J. G., & Huey, R. B. (2008). Size, temperature, and fitness: Three rules. *Evolutionary Ecology Research*, *10*(2), 251–268.

Kingsolver, J. G., Arthur Woods, H., Buckley, L. B., Potter, K. A., MacLean, H. J., & Higgins, J. K. (2011). Complex life cycles and the responses of insects to climate change. *Integrative and Comparative Biology*, *51*(5), 719–732. https://doi.org/10.1093/icb/icr015

Kingsolver, J. G., Higgins, J. K., & Augustine, K. E. (2015). Fluctuating temperatures and ectotherm growth: Distinguishing non-linear and time-dependent effects. *Journal of Experimental Biology*, *218*(14), 2218–2225. https://doi.org/10.1242/jeb.120733

Kraus, J. M., & Vonesh, J. R. (2010). Feedbacks between community assembly and habitat selection shape variation in local colonization. *Journal of Animal Ecology*, *79*(4), 795–802. https://doi.org/10.1111/j.1365-2656.2010.01684.x

Lamoureux, J., Tiersch, T. R., & Hall, S. G. (2006). Pond heat and temperature regulation (PHATR): Modeling temperature and energy balances in earthen outdoor aquaculture ponds. *Aquacultural Engineering*, *34*(2), 103–116. https://doi.org/10.1016/j.aquaeng.2005.06.002

Leibold, M. A. (1996). A graphical model of keystone predators in food webs: trophic regulation of abundance, incidence, and diversity patterns in communities. *The American Naturalist, 147*(5), 784–812.

Lüdecke, D., Ben-Shachar, M., Patil, I., Waggoner, P., & Makowski, D. (2021). performance: An R Package for Assessment, Comparison and Testing of Statistical Models. In *Journal of Open Source Software* (Vol. 6, Issue 60, p. 3139). The Open Journal. https://doi.org/10.21105/joss.03139

McCoy, M. W., & Bolker, B. M. (2008). Trait-mediated interactions: Influence of prey size, density and experience. *Journal of Animal Ecology*, *77*(3), 478–486. https://doi.org/10.1111/j.1365-2656.2008.01372.x

McCoy, M. W., Bolker, B. M., Warkentin, K. M., & Vonesh, J. R. (2011). Predicting Predation through Prey Ontogeny Using Size-Dependent Functional Response Models. *The American Naturalist*, *177*(6), 752–766. https://doi.org/10.1086/659950

Nakagawa, S., & Schielzeth, H. (2013). A general and simple method for obtaining R2 from generalized linear mixed-effects models. *Methods in Ecology and Evolution*, *4*(2), 133–142. https://doi.org/10.1111/j.2041-210x.2012.00261.x

O’Connor, M. I. (2009). Warming Strengthens an Herbivore-Plant Interaction. *Ecology*, *90*(2), 388–398. https://doi.org/10.1890/08-0034.1

O’Meara, G. F., & Craig, G. B. (1970). Geographical variation in Aedes atropalpus (Diptera: Culicidae). *Annals of the Entomological Society of America*, *63*(5), 1392–1400. https://doi.org/10.1093/aesa/63.5.1392

Ohlberger, J. (2013). Climate warming and ectotherm body size - from individual physiology to community ecology. *Functional Ecology*, *27*, 991–1001. https://doi.org/10.1111/1365-2435.12098

Oksanen, L., Fretwell, S. D., Arruda, J., & Niemela, P. (1981). Exploitation Ecosystems in Gradients of Primary Productivity. *The American Naturalist*, *118*(2), 240–261.

Ortega, J. A., Gómez-Heras, M., Perez-López, R., & Wohl, E. (2014). Multiscale structural and lithologic controls in the development of stream potholes on granite bedrock rivers. *Geomorphology*, *204*, 588–598. https://doi.org/10.1016/j.geomorph.2013.09.005

Paine, R. T. (1980). Food Webs: Linkage, Interaction Strength and Community Infrastructure. *Journal of Animal Ecology*, *49*(3), 666–685.

Pelletier, J. D., Sweeney, K. E., Roering, J. J., & Finnegan, N. J. (2015). Controls on the geometry of potholes in bedrock channels. *Geophysical Research Letters*, *42*(3), 797–803. https://doi.org/10.1002/2014GL062900

Pepi, A., Grof-Tisza, P., Holyoak, M., & Karban, R. (2018). As temperature increases, predator attack rate is more important to survival than a smaller window of prey vulnerability. *Ecology*. https://doi.org/10.1002/ecy.2356

Petchey, O. L., Brose, U., & Rall, B. C. (2010). Predicting the effects of temperature on food web connectance. *Philosophical Transactions of the Royal Society B: Biological Sciences*, *365*(1549), 2081–2091. https://doi.org/10.1098/rstb.2010.0011

Power, A. G. (1996). Competition between Viruses in a Complex Plant-Pathogen System. *Ecology*, *77*(4), 1004–1010.

Price, C. A., Weitz, J. S., Savage, V. M., Stegen, J., Clarke, A., Coomes, D. A., Dodds, P. S., Etienne, R. S., Kerkhoff, A. J., Mcculloh, K., Niklas, K. J., Olff, H., & Swenson, N. G.

(2012). Testing the metabolic theory of ecology. *Ecology Letters*, *15*(12), 1465–1474. https://doi.org/10.1111/j.1461-0248.2012.01860.x

Quinn, B. K. (2017). A critical review of the use and performance of different function types for modeling temperature-dependent development of arthropod larvae. *Journal of Thermal Biology*, *63*(May 2016), 65–77. https://doi.org/10.1016/j.jtherbio.2016.11.013

Rall, B. C., Vucic-Pestic, O., Ehnes, R. B., Emmerson, M. C., & Brose, U. (2010). Temperature, predator–prey interaction strength and population stability. *Global Change Biology*, *16*, 2145–2157. https://doi.org/10.1111/j.1365-2486.2009.02124.x

Ren, H., Yuan, X., Yue, J., Wang, X., & Liu, H. (2016). Potholes of mountain river as biodiversity spots: Structure and dynamics of the benthic invertebrate community. *Polish Journal of Ecology*, *64*(1), 70–83. https://doi.org/10.3161/15052249PJE2016.64.1.007

Rogers, D. (1972). Random Search and Insect Population Models. *Journal of Animal Ecology*, *41*(2), 369–383.

Romero, G. Q., Gonçalves-Souza, T., Kratina, P., Marino, N. A. C., Petry, W. K., Sobral-Souza, T., & Roslin, T. (2018). Global predation pressure redistribution under future climate change. *Nature Climate Change*, *8*(12), 1087–1091. https://doi.org/10.1038/s41558-018-0347-y

Schenk, K., Suhling, F., & Martens, A. (2004). Egg distribution, mate-guarding intensity and offspring characteristics in dragonflies (Odonata). *Animal Behavior*, *68*, 599–606. https://doi.org/10.1016/j.anbehav.2003.12.010

Schiesari, L., Monteiro, A. S., Ilha, P., Pope, N., & Corrêa, D. T. (2018). The ecology of a system of natural mesocosms: Rock pools in the Atlantic Forest. *Freshwater Biology*, *March*, 1–11. https://doi.org/10.1111/fwb.13118

Schloerke, B., Cook, D., Larmarange, J., Briatte, F., Marbach, M., Thoen, E., Elberg, A., & Crowley, J. (2021). *GGally: Extension to "ggplot2"* (R package version 2.1.2).

Sentis, A., Hemptinne, J.-L. L., & Brodeur, J. (2012). Using functional response modeling to investigate the effect of temperature on predator feeding rate and energetic efficiency. *Oecologia*, *169*(4), 1117–1125. https://doi.org/10.1007/s00442-012-2255-6

Silberbush, A., & Blaustein, L. (2011). Mosquito females quantify risk of predation to their progeny when selecting an oviposition site. *Functional Ecology*, *25*(5), 1091–1095. https://doi.org/10.1111/j.1365-2435.2011.01873.x

Sohrabi, M. M., Benjankar, R., Tonina, D., Wenger, S. J., & Isaak, D. J. (2017). Estimation of daily stream water temperatures with a Bayesian regression approach. *Hydrological Processes*, *31*(9), 1719–1733. https://doi.org/10.1002/hyp.11139

Stunkle, C. R., Davidson, A. T., Shuart, W. J., McCoy, M. W., & Vonesh, J. R. (2021). Taxa-specific responses to flooding shape patterns of abundance in river rock pools. *Freshwater Science*, *40*(2). https://doi.org/10.1086/714597

Suhling, F., Suhling, I., & Richter, O. (2015). Temperature response of growth of larval dragonflies – an overview. *International Journal of Odonatology*, *18*(1), 15–30. https://doi.org/10.1080/13887890.2015.1009392

Tschumi, M., Ekroos, J., Hjort, C., Smith, H. G., & Birkhofer, K. (2018). Predation-mediated ecosystem services and disservices in agricultural landscapes. *Ecological Applications*, *28*(8), 2109–2118. https://doi.org/10.2307/26623300

Uiterwaal, S. F., & Delong, J. P. (2020). Functional responses are maximized at intermediate temperatures. *Ecology*. https://doi.org/10.1002/ecy.2975

Vasseur, D. A., & McCann, K. S. (2005). A mechanistic approach for modeling temperature-dependent consumer-resource dynamics. *American Naturalist*, *166*(2), 184–198. https://doi.org/10.1086/431285

Yee, D. A., Kneitel, J. M., & Juliano, S. A. (2010). Environmental correlates of abundances of mosquito species and stages in discarded vehicle tires. *Journal of Medical Entomology*, *47*(1), 53–62. https://doi.org/10.1603/033.047.0107

Yodzis, P., & Innes, S. (2016). Body Size and Consumer-Resource Dynamics. *The American Naturalist*, *139*(6), 1151–1175.

Zuharah, W. F., & Lester, P. J. (2010). Can adults of the New Zealand mosquito culex pervigilans (Bergorth) detect the presence of a key predator in larval habitats? *Journal of Vector Ecology*, *35*(1), 100–105. https://doi.org/10.1111/j.1948-7134.2010.00065.x

3.6. Figures and Tables

Fig. 3.1. A step-by-step process diagram illustrating the approach used by this study to produce and validate predictions about the effects of warming on stage-structured predator-prey interactions. These figures use our focal study system (stage-structured predation of mosquito larvae by dragonfly nymphs in riverine rock pools) as an example, but this approach is generic and could be applied to other predator-prey interactions (including those that are not stage-structured). Our approach uses a) a theoretical model that is b) parameterized by experimental results to c) yield predictions about how warming will change predation strength, and to what degree. We then compare our predictions against d) patterns of prey abundance across natural gradients of temperature and predation risk *in situ*. By identifying discrepancies between our model predictions and field observations, we can assess our predictions and identify targets for future research and/or model iterations. In this figure, we assume *a priori* knowledge of the thermal environment present *in situ*, while in the case of this study we first had to gather data to describe this.

Fig. 3.2. Temperature variation in rock pools on the south side of Belle Isle in the James River in Richmond, Virginia, USA. Panels a-c provide histograms showing the distribution of observed temperatures in rock pools, including a) the daily maximum temperature (°C), b) daily minimum temperature (°C), and c) coefficient of variation of temperature. Panel d provides a map of the rock pool system, with each point representing an individual rock pool. The symbology of each point represents the predicted daily maximum temperature of the pool, with cooler maximum temperatures in darker colors. The inset map shows the entire study site, and the main portion of the map displays a detailed subsection of the site.

Fig. 3.3. Experimentally measured effects of temperature on the development of *Ae. atropalpus* mosquito larvae and *Pantala* spp. dragonfly nymph foraging rates, used to parameterize the stage-structured model used by this study and Davidson et al. (2021) and predict the impacts of warming on stage-structured predator-prey interactions. Data shown here depict the effects of temperature on the a) development time (i.e., the number of days required for an individual to develop from hatching to adulthood) and b) mortality rate (shown here as the proportion of larvae that survived development to adulthood) of *Ae. atropalpus* mosquito larvae, as well as the functional response (i.e., the number of prey consumed in a 1hr period) of *Pantala* spp. dragonfly nymphs on *Ae. atropalpus* mosquito larval prey, shown as a function of c) initial prey density, color-coded by temperature in °C and d) temperature in °C, color-coded by initial prey density. Points represent individual observations, and the shaded areas in panels a) and b) represent 95% confidence intervals for prediction.

Fig. 3.4. Model predicted survivorship of a cohort of 300 *Ae. atropalpus* larvae in the presence of a single *Pantala* spp. dragonfly nymph, measured as proportional mortality (i.e., the proportion of the initial cohort that died before reaching adulthood) as a function of temperature (°C). Here, we illustrate the independent effects of a) dragonfly nymph predation and b) temperature alone on proportional mortality, while panel c) shows their combined effect. Thus, panel c) provides our prediction for the shape of the relationship between temperature and mosquito larval abundance *in situ*. Lines represent average larval survivorship across 3,000 replicated simulations, and shaded regions represent the 95% confidence interval of prediction.

Fig. 3.5. The interactive effects of temperature and predation on the a) presence and b) abundance of *Ae. atropalpus* mosquito larval prey, as modeled using a hurdle GLMM with a negative binomial error structure. Panel a) shows the influence of predator presence or absence

on the probability that a rock pool would contain any mosquito larvae, with error bars showing the 95% confidence intervals. Panel b) shows the interactive effects of predicted daily maximum pool temperature (°C) and predator presence (blue) or absence (yellow) on mosquito larvae where they were present in pools, presented on a log + 1 scale. The shaded regions in panel b) are 95% confidence intervals for prediction, and points represent observed mosquito abundances across the temperature gradient. Panel c) provides the difference between larval abundance where predators are present or absent (i.e., the lines in panel b) across a temperature gradient, expressed as a proportion (i.e., values above zero indicate greater larvae abundances in the absence of predators relative to their presence). Shaded areas represent the 95% confidence interval, as estimated using the delta method. As temperature increases, the difference in larval abundance between pools with and without predators grows smaller.

Fig. 3.1.

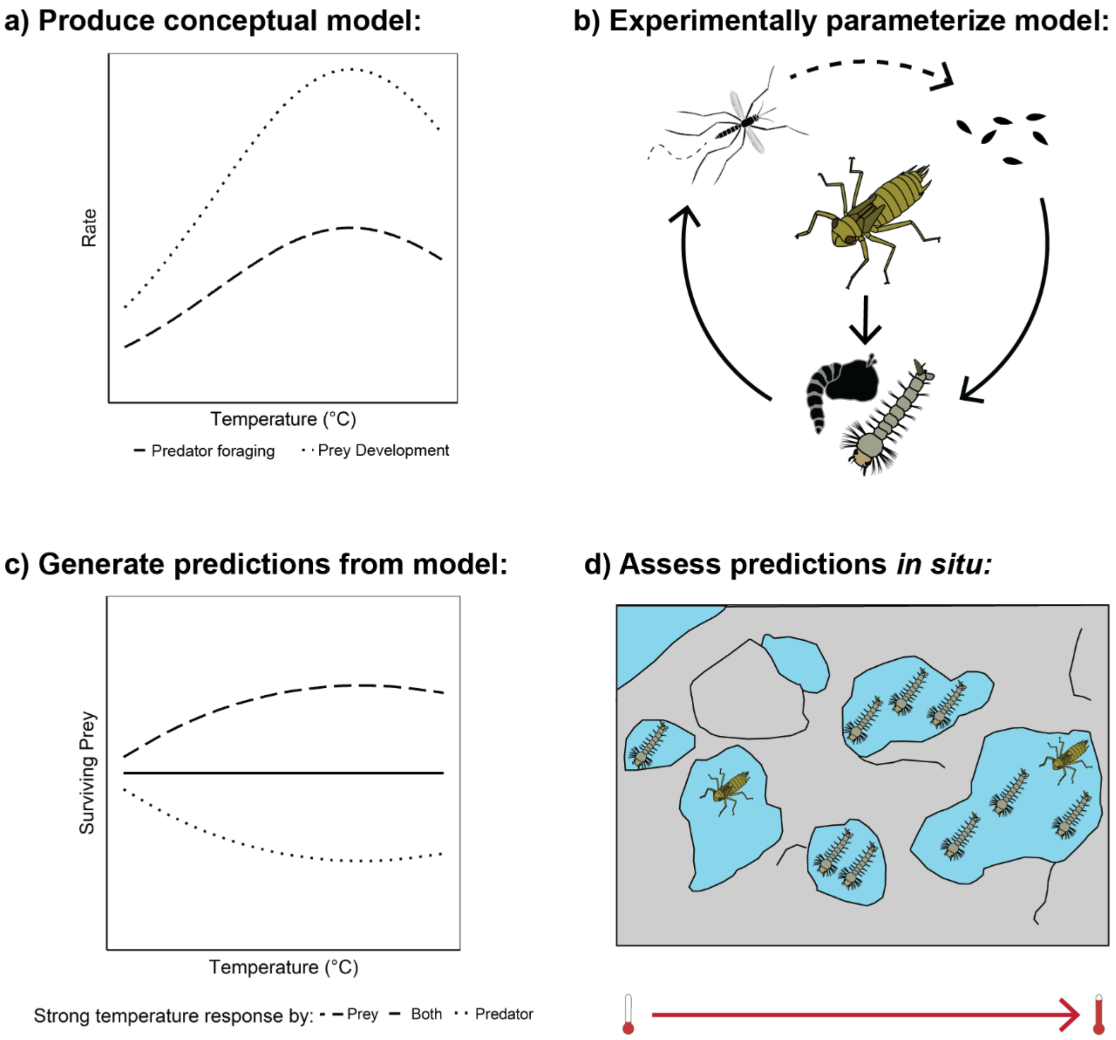
a) Produce conceptual model:
Rate
Temperature (°C)
Predator foraging
Prey Development
b) Experimentally parameterize model:
c) Generate predictions from model:
Surviving Prey
Temperature (°C)
Strong temperature response by:
Prey
Both
Predator
d) Assess predictions *in situ:*

Fig. 3.2.

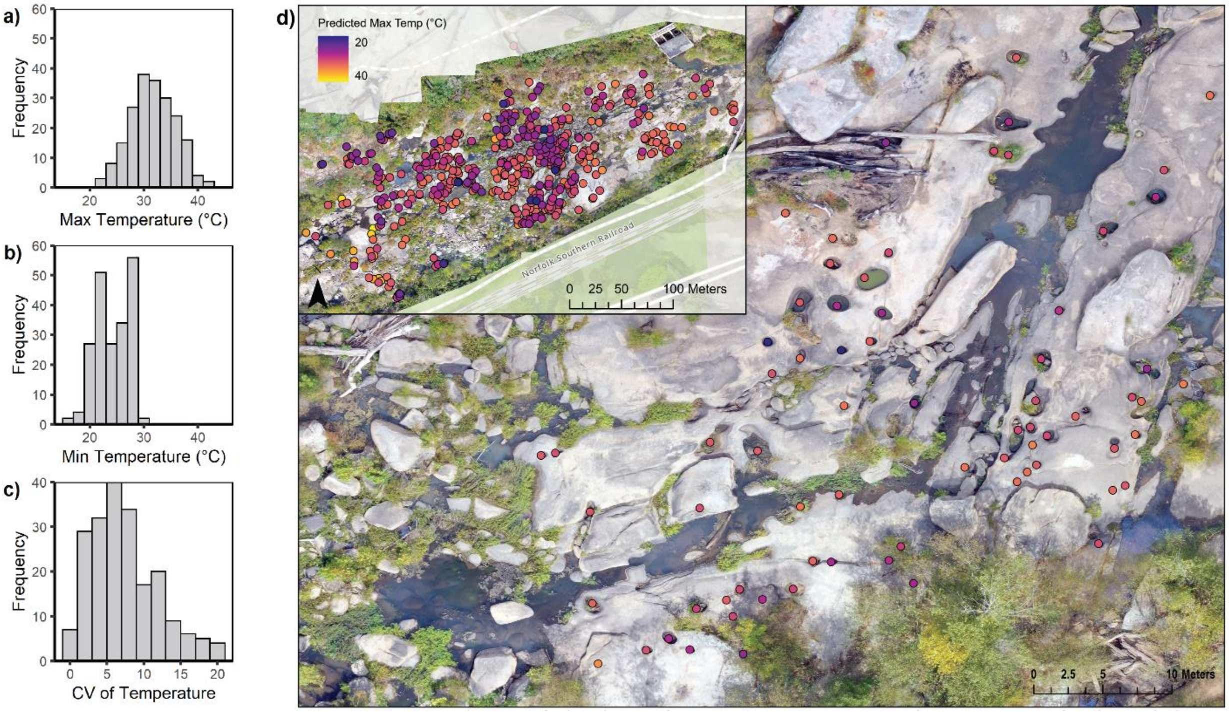
a)
Frequency
0
10
20
30
40
50
60
20
30
40
Max Temperature (°C)
b)
Frequency
0
10
20
30
40
50
60
20
30
40
Min Temperature (°C)
c)
Frequency
0
10
20
30
40
0
5
10
15
20
CV of Temperature
d)
Predicted Max Temp (°C)
20
40
Norfolk Southern Railroad
0 25 50 100 Meters
0 2.5 5 10 Meters

Fig. 3.3.

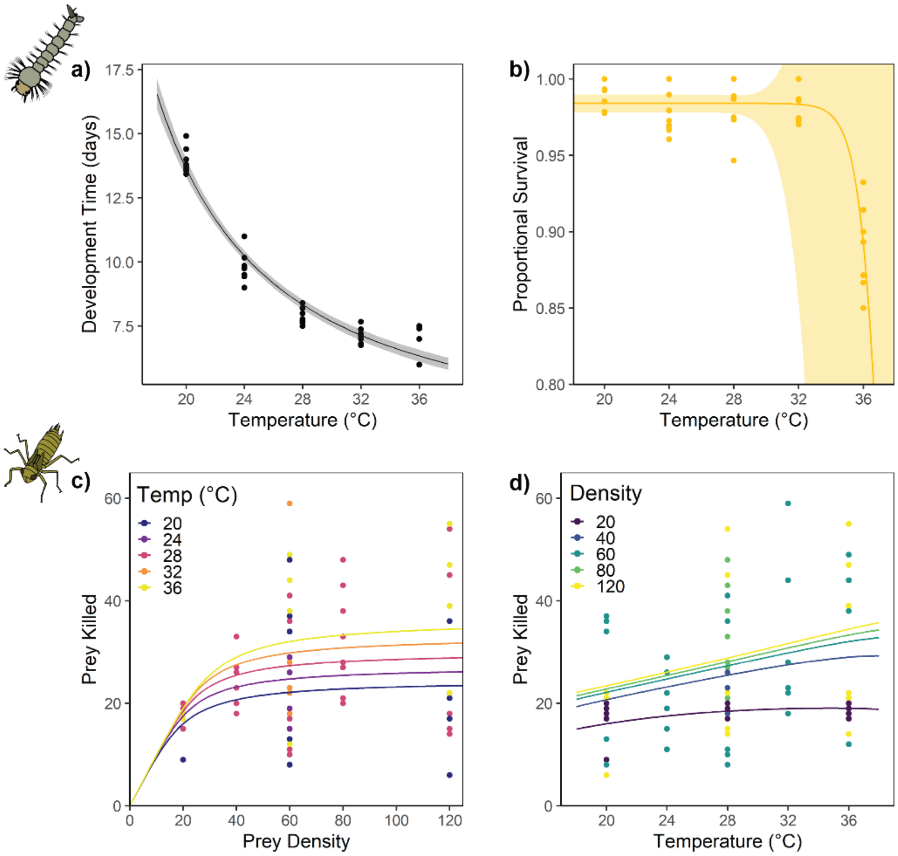
a)
Development Time (days)
17.5
15.0
12.5
10.0
7.5
20
24
28
32
36
Temperature (°C)
b)
Proportional Survival
1.00
0.95
0.90
0.85
0.80
20
24
28
32
36
Temperature (°C)
c)
Prey Killed
Temp (°C)
20
24
28
32
36
60
40
20
0
0
20
40
60
80
100
120
Prey Density
d)
Prey Killed
Density
20
40
60
80
120
60
40
20
0
20
24
28
32
36
Temperature (°C)

Fig. 3.4.

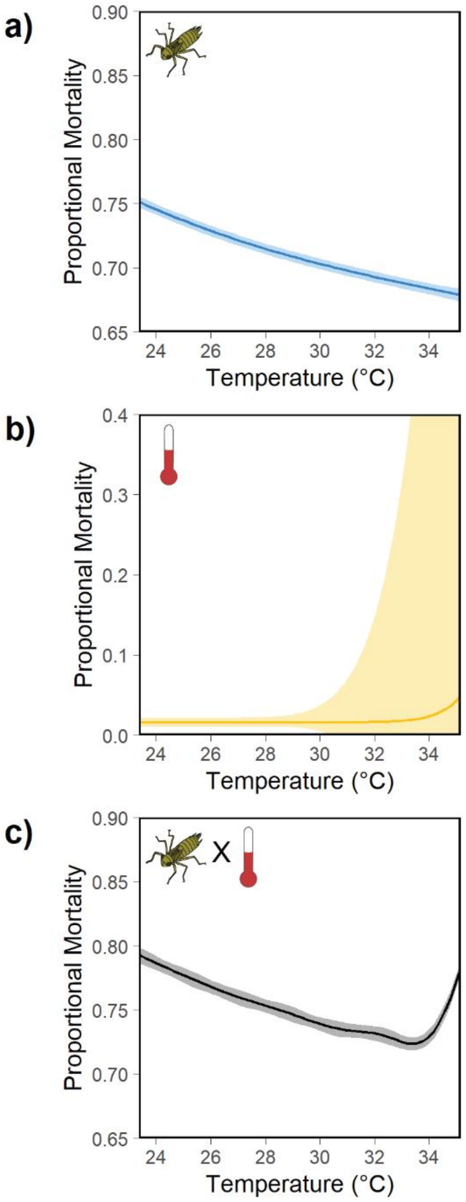
a)
0.90
0.85
0.80
0.75
0.70
0.65
Proportional Mortality
24
26
28
30
32
34
Temperature (°C)
b)
0.4
0.3
0.2
0.1
0.0
Proportional Mortality
24
26
28
30
32
34
Temperature (°C)
c)
X
0.90
0.85
0.80
0.75
0.70
0.65
Proportional Mortality
24
26
28
30
32
34
Temperature (°C)

Fig. 3.5.

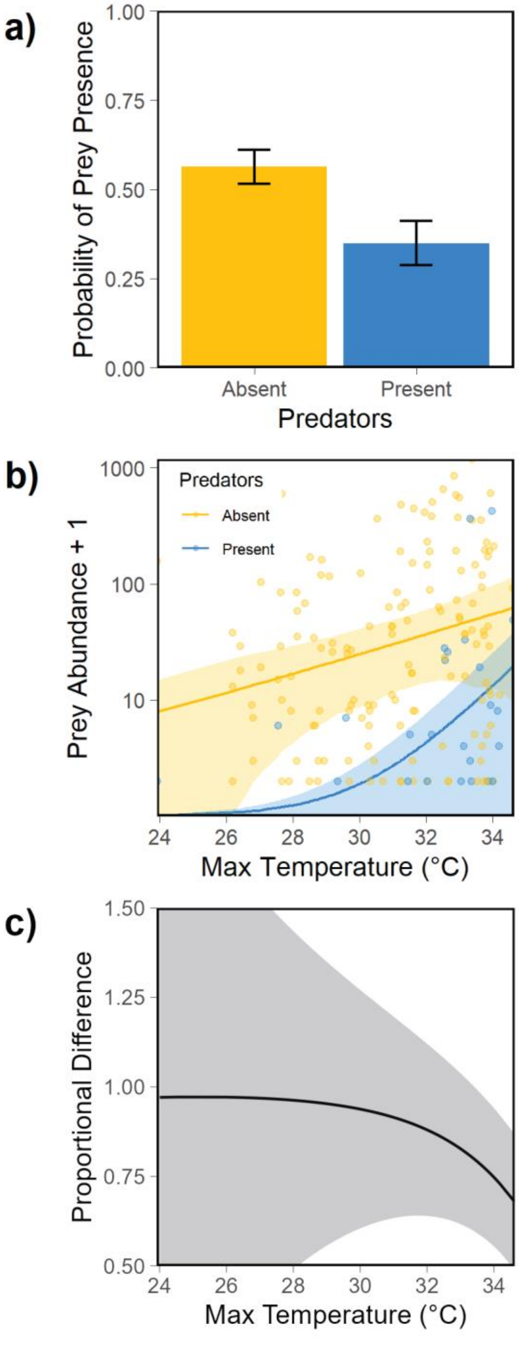
a)
1.00
0.75
0.50
0.25
0.00
Probability of Prey Presence
Absent
Present
Predators
b)
1000
100
10
Prey Abundance + 1
Predators
Absent
Present
24
26
28
30
32
34
Max Temperature (°C)
c)
1.50
1.25
1.00
0.75
0.50
Proportional Difference
24
26
28
30
32
34
Max Temperature (°C)

3.7. Supplementary Materials

Drivers of Dragonfly Nymph Distribution

Dragonfly nymphs occurred across the rock pool landscape mostly independently of temperature, and their presence and abundance were better captured by other variables such as pool shading and the number of days since the pool had been flooded (as described in Stunkle et al. 2021). We selected and averaged top models using the lowest AICc, based on the criterion that ΔAICc > 2.0. The final model included pool shading, the number of days since the pool had last flooded, and daily maximum temperature as fixed effects and sampling date as a random effect (Table S6). Dragonfly nymphs were more likely to be present in pools that were unshaded (zero-inflation model: coeff. estimate = 0.53, 95% CI: 0.23 to 0.83). When dragonfly nymphs were present, they were less abundant in shady pools (conditional model: coeff. estimate = -0.29, 95% CI: -0.65 to 0.07) or pools that had not flooded recently (conditional model: coeff. estimate = -0.24, 95% CI: -0.49 to 0.02), and slightly less abundant in warmer pools (conditional model: coeff. estimate = -0.12, 95% CI: -0.33 to 0.10).

Size-Dependent Predation of Mosquito Larvae

As part of a pilot study, we measured the feeding rates of two dragonfly nymph predators (*Erythemis simplicicollis* and *Pachydiplax longipennis*) on first (L1) and third (L3) instar *Ae. atropalpus* larvae. During this study, individual dragonfly nymphs were starved for a 24-hour period before being provided with either 300 L1 larvae (n = 10 per predator; avg. body length = 1.42mm) or 40 L3 larvae (n = 6 per predator; avg. body length = 5.24mm) and allowed to feed for 24 hours. To determine whether size-dependent differences in predator feeding rates were influenced by temperature, half of the predators were assigned to a low temperature treatment

(20°C) and half were assigned to a high temperature treatment (32°C). We manipulated temperatures and reared mosquito larvae in preparation for this study using environmental chambers (Percival Scientific Model I-30VL; access provided by the University of Richmond, Richmond, VA) set to a 14L:10D photoperiod, as in Davidson et al. 2021 and the remainder of this study. At the end of the 24-hour period, we recorded the number of larvae that had been eaten by the predator.

Data shown here are pooled across both predator and temperature treatments, to highlight the importance of mosquito larval body size for predator feeding rates (Fig. S2). While the L3 larvae were only 3.7X larger than the L1 larvae, differences in predator feeding rates depending on larval body size were disproportionately larger. On average, *E. simplicicollis* consumed 10.0X more L1 larvae than L3 larvae (263.0 ± 12.4 L1 larvae and 26.2 ± 5.7 L3 larvae, respectively). Similarly, *P. longipennis* consumed an average of 15.0X more L1 larvae than L3 larvae (281.1 ± 9.5 L1 larvae and 18.8 ± 3.9 L3 larvae, respectively).

Fig. S3.1. The response surface design used to collect data on the temperature-dependence of the functional response of *Pantala* spp. dragonfly nymphs, feeding on *Ae. atropalpus* mosquito larvae. Each number represents the number of replicates for the given temperature and prey density combination**.**

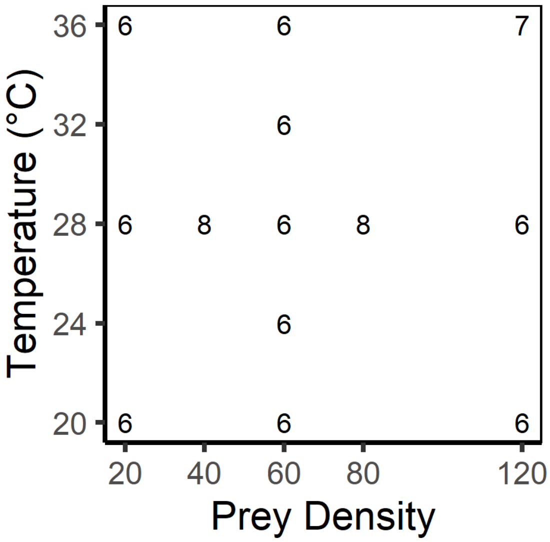

Fig. S3.2. Feeding rates of two species of dragonfly nymphs (*E. simplicicollis* and *P. longipennis*) on either first (L1) or third (L3) instar *Ae. atropalpus* mosquito larvae, measured as the number of larvae consumed in a 24-hour period. Data shown are pooled between both species of dragonfly nymph and both temperatures (20 and 32°C) tested, to illustrate average differences in feeding rates as a function of mosquito larval instar. For species-specific feeding rates and specific methods, see the description in the supplementary material.

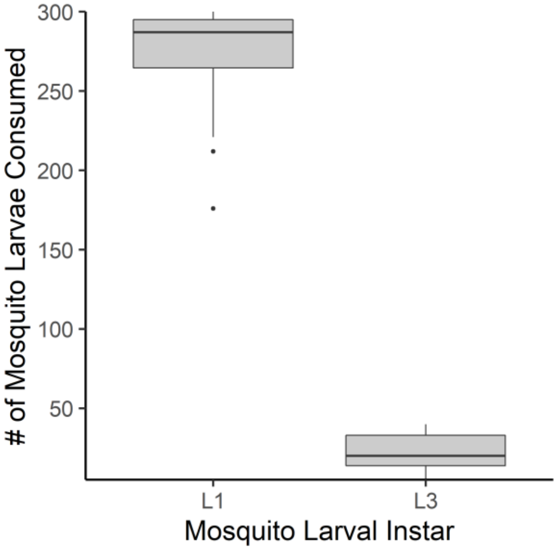

Table S3.1. Model selection table for models describing the abundance of dragonfly nymphs (*Pantala* spp.) in individual rock pools, as a function of predicted daily maximum temperature (°C), how shaded the pool was (%), and the number of days since the pool was last flooded. Only fixed effects are shown here, but all models include a sampling date-level random effect. For brevity, only the top ten models are presented here, with coefficient estimates provided for all included variables. Dashes indicate that the model did not include a particular variable.

Model	Days Since Last Flooded	Max Temp	% Shading	df	Log-Likelihood	AICc	ΔAICc	Weight
14	-0.23	-	-0.28	7	-370.9	756.1	0	0.18
10	-0.24	-	-	6	-372.0	756.2	0.10	0.17
16	-0.24	-0.13	-0.31	8	-370.0	756.5	0.43	0.15
13	-	-	-0.28	6	-372.3	756.8	0.77	0.12
9	-	-	-	5	-373.4	756.9	0.84	0.12
12	-0.25	-0.11	-	7	-371.4	757.1	1.06	0.11
15	-	-0.12	-0.31	7	-371.6	757.6	1.6	0.08
11	-	-0.09	-	6	-373.0	758.2	2.1	0.06
6	-0.23	-	-0.28	6	-379.0	770.2	14.1	0.01
2	-0.24	-	-	5	-380.0	770.3	14.2	0.01

Table S3.2. Model selection table for models describing the daily maximum temperature (°C) of individual rock pools. Fixed effects include pool depth (cm), shading (%), pool surface area (cm^2), and maximum river temperature on the day of sampling (°C). Only fixed effects are shown here, but all models include a pool-level random effect. For brevity, only the top ten models are presented here, with coefficient estimates provided for all included variables. Dashes indicate that the model did not include a particular variable.

Model	Depth	Max River Temp	% Shading	Surf. Area	Depth * Shade	Depth * Surf. Area	Shade * Surf. Area	Depth * Shade * Surf. Area	df	Log-Likelihood	AICc	ΔAICc	weight
8	-1.95	1.65	-1.39	-	-	-	-	-	6	-492.7	997.8	0	0.32
16	-1.94	1.65	-1.39	-0.08	-	-	-	-	7	-492.7	999.9	2.04	0.12
24	-1.93	1.65	-1.36	-	0.06	-	-	-	7	-492.7	1000.0	2.11	0.11
48	-1.97	1.64	-1.41	-0.178	-	0.34	-	-	8	-491.8	1000.3	2.43	0.10
112	-2.00	1.64	-1.27	0.03	-	0.43	0.73	-	9	-490.7	1000.4	2.52	0.09
80	-1.95	1.66	-1.28	0.09	-	-	0.54	-	8	-492.1	1000.9	3.02	0.07
256	-2.24	1.64	-1.23	-0.12	-0.50	-0.26	0.54	-1.59	11	-488.9	1001.1	3.23	0.06
32	-1.92	1.65	-1.37	-0.08	0.06	-	-	-	8	-492.7	1002.0	4.18	0.04
64	-1.93	1.64	-1.36	-0.19	0.14	0.36	-	-	9	-491.7	1002.3	4.45	0.03
128	-2.00	1.65	-1.27	0.03	-0.01	0.43	0.73	-	10	-490.7	1002.6	4.73	0.03

Table S3.3. Model selection table for models describing the daily minimum temperature (°C) of individual rock pools. NAs indicate that the random effect variances had some variance components equal to zero, which meant a conditional r^2 value could not be calculated. Fixed effects include pool depth (cm), shading (%), pool surface area (cm^2), and maximum river temperature on the day of sampling (°C). For brevity, only the top ten models are presented here, with coefficient estimates provided for all included variables. Dashes indicate that the model did not include a particular variable.

Model	Depth	Max River Temp	% Shading	Surf. Area	Depth * Shade	Depth * Surf. Area	Shade * Surf. Area	Depth * Shade * Surf. Area	df	Log-Likelihood	AICc	ΔAICc	Weight
16	0.52	2.72	-0.31	-0.34	-	-	-	-	6	-334.8	682.0	0	0.30
32	0.56	2.72	-0.26	-0.34	0.15	-	-	-	7	-334.0	682.6	0.62	0.22
48	0.53	2.73	-0.31	-0.32	-	-0.04	-	-	7	-334.7	683.9	1.95	0.11
80	0.52	2.72	-0.29	-0.31	-	-	0.08	-	7	-334.7	683.9	1.99	0.11
64	0.56	2.72	-0.26	-0.33	0.15	-0.03	-	-	8	-334.0	684.7	2.72	0.08
96	0.56	2.72	-0.26	-0.34	0.15	-	0.01	-	8	-334.0	684.7	2.79	0.08
112	0.52	2.73	-0.30	-0.31	-	-0.04	0.068	-	8	-334.6	686.0	4.03	0.04
128	0.56	2.72	-0.26	-0.33	0.15	-0.03	-0.01	-	9	-334.0	686.9	4.91	0.03
256	0.50	2.72	-0.25	-0.36	0.03	-0.20	-0.05	-0.41	10	-333.2	687.4	5.50	0.02
12	0.57	2.72	-	-0.32	-	-	-	-	5	-340.5	691.3	9.32	0.01

Table S3.4. Model selection table for models describing daily temperature variation (expressed as the coefficient of variation) in individual rock pools. Fixed effects include pool depth (cm), shading (%), pool surface area (cm^2), and maximum river temperature on the day of sampling (°C). Only fixed effects are shown here, but all models include a pool-level random effect. For brevity, only the top ten models are presented here, with coefficient estimates provided for all included variables.

Model	Depth	Max River Temp	% Shading	Surf Area	Depth * Shade	Depth * Surf. Area	Shade * Surf. Area	Depth * Shade *	df	Log-Likelihood	AICc	ΔAICc	Weight
8	-0.03	-0.02	-0.01	-	-	-	-	-	6	359.7	-706.9	0	0.23
16	-0.03	-0.02	-0.01	0.005	-	-	-	-	7	360.6	-706.6	0.37	0.19
48	-0.03	-0.02	-0.01	0.004	-	0.004	-	-	8	361.3	-705.8	1.13	0.13
80	-0.03	-0.02	-0.01	0.006	-	-	0.005	-	8	360.8	-704.9	2.03	0.08
24	-0.03	-0.02	-0.01	-	-0.001	-	-	-	7	359.7	-704.9	2.10	0.08
112	-0.03	-0.02	-0.01	0.006	-	0.005	0.008	-	9	361.8	-704.7	2.27	0.07
32	-0.03	-0.02	-0.01	0.005	-0.001	-	-	-	8	360.6	-704.5	2.45	0.07
64	-0.03	-0.02	-0.01	0.004	-0.001	0.004	-	-	9	361.3	-703.6	3.31	0.04
96	-0.03	-0.02	-0.01	0.007	-0.003	-	0.006	-	9	361.0	-703.0	3.90	0.03
128	-0.03	-0.02	-0.01	0.006	-0.002	0.005	0.009	-	10	361.9	-702.6	4.29	0.03

Table S3.5. Log-transformed estimates for models describing the temperature dependence of the functional response of *Pantala* spp. dragonfly nymphs fed on *Ae. atropalpus* mosquito larvae. See Eqn. 2-3 for more information about the specific parameters fit and their role in the models.

Parameter	Estimate	SE	p value
b	-2.32	0.115	< 0.001
h_0	-15.3	0.717	< 0.001
E_h	-1.65	0.0974	< 0.001

Table S3.6. Model selection table for models describing the abundance of *Ae. atropalpus* mosquito larvae in individual rock pools, as a function of predicted daily maximum temperature (°C), the presence or absence of predatory dragonfly nymphs (*Pantala* spp.), and the number of days since the pool was last flooded. Only fixed effects are shown here, but all models include a sampling date-level random effect. For brevity, only the top ten models are presented here, with coefficient estimates provided for all included variables. (+) and (-) symbols for categorical variables indicate their presence or absence in the model, respectively.

Model	Days Since Flooded	Dragonfly Presence	Max Temp	Days * Dragonflies	Days * Max Temp	Dragonflies * Max Temp	Days * Dragonflies * Max Temp	df	Log-Likelihood	AICc	ΔAICc	Weight
167	-	+	0.47	-	-	+	-	9	-1056.4	2131.4	0	0.34
168	0.14	+	0.51	-	-	+	-	10	-1056.1	2132.9	1.48	0.16
176	0.06	+	0.49	+	-	+	-	11	-1055.3	2133.4	2.01	0.12
135	-	+	0.57	-	-	-	-	8	-1058.7	2133.9	2.48	0.10
184	0.17	+	0.52	-	0.07	+	-	11	-1056.0	2134.8	3.40	0.06
136	0.14	+	0.61	-	-	-	-	9	-1058.4	2135.3	3.94	0.05
192	0.07	+	0.49	+	0.02	+	-	12	-1055.3	2135.5	4.14	0.04
256	0.07	+	0.48	+	0.04	+	+	13	-1054.8	2136.7	5.28	0.02
152	0.23	+	0.62	-	0.13	-	-	10	-1058.0	2136.7	5.31	0.02
144	0.10	+	0.59	+	-	-	-	10	-1058.1	2136.9	5.55	0.02

4. Detection of emergent multiple predator effects in a warming world

4.1. Introduction

Predators play a fundamental role in regulating food webs by both consuming prey species and through a variety of nonconsumptive pathways, such as inducing changes in prey behavior, morphology, physiology, and development (Werner and Peacor 2003; Preisser et al. 2007; Cardinale et al. 2012). However, understanding and predicting the influence of predators on food web dynamics remains challenging, particularly when multiple predator species share a common prey species (Sih et al. 1998; McCoy et al. 2012). This is because predator species can have interactive effects on prey such that their combined effects on prey survival often cannot be predicted from their independent effects on prey (Sih et al. 1998). For example, prey avoidance of one predator species can increase their exposure across space and/or time to another predator species (i.e., risk enhancement; Soluk and Collins 1988; Swisher et al. 1998). Alternatively, processes such as competition between predators or intraguild predation can reduce the overall risk of predation that prey face (i.e., risk reduction; Crumrine and Crowley 2003; Vance-Chalcraft and Soluk 2005; Griffen and Byers 2006).

These types of emergent multiple predator effects (MPEs) are thought to be common in nature (Sih et al. 1998; McCoy et al. 2022) and understanding and predicting them is critical for understanding food web dynamics. However, detecting future MPEs under climate change may be especially challenging due to the numerous pathways by which temperature can modify predator-prey interactions. Temperature has well-known nonlinear effects on the rate at which predators attack, subdue, and digest their prey (Englund et al. 2011; Sentis et al. 2012; Uszko et al. 2017), and thus under warming conditions the feeding rates of any given predator species may already differ from what would be predicted under current conditions. Further, there is evidence that warming can affect the presence, magnitude, and direction (i.e., whether risk is enhanced or reduced) of emergent MPEs by altering the range, behavior, and diet of predator species (Barton and Schmitz 2009; Cuthbert et al. 2021; Liu et al. 2023). Thus, climate change may have profound impacts on ecosystem structure and function that cannot be predicted or understood without a fundamental understanding of how temperature impacts different predator species and their interactions with other predators and their prey.

One of the most widely used approaches to detect emergent MPEs is the multiplicative risk model (MRM; Soluk and Collins 1988; Sih et al. 1998). The MRM provides a null expectation for prey survival in the presence of two or more predator species, and past research has used deviations from its predictions as evidence of risk enhancement or reduction between predator species. However, subsequent research has highlighted the fact that the MRM is poorly equipped to handle nonlinear determinants of predator foraging, such as prey density or body size (McCoy et al. 2011; Sentis and Boukal 2018; McCoy et al. 2022). Bias introduced by failing to account for these processes can lead to incorrect estimates of predation risk, which can result in false positives in the detection of emergent MPEs (McCoy et al. 2022). Accounting for nonlinear determinants of predation rate is especially important in the case of density-dependent predation, because the relationship between predator foraging rates and prey density is nonlinear in the vast majority of cases (i.e., best captured by a Type II or III functional response; Holling 1989; Rogers 1972; Jeschke et al. 2004).

To address this and similar problems, recent studies have suggested that predation rates should be mechanistically modeled using the functional response (Holling 1959; Sentis and Boukal 2018; McCoy et al. 2022), which can be modified to account for prey depletion (Rogers 1972), prey body size (Vucic-Pestic et al. 2010; McCoy et al. 2011), temperature (Englund et al. 2011; Sentis et al. 2012), and other nonlinear determinants of predation risk. For example, McCoy et al.'s (2022) generalized functional response (GFR) framework suggested that size-dependent predation risk can lead the MRM to falsely detect either risk enhancement or reduction depending on the form of the relationship between prey body size and predator foraging rates. Because temperature can also affect predator foraging rates in a nonlinear fashion (Englund et al. 2011; Sentis et al. 2012; Uszko et al. 2017), it is likely that temperature is another factor that can produce bias in the detection of emergent MPEs by models like the MRM. However, the consequences of ignoring temperature-dependence in the MRM have not been quantified, and it is thus far unclear how failing to account for temperature-dependent predation risk might bias its ability to detect emergent MPEs.

Here, we extend the GFR to consider temperature-dependent predation risk and explore how temperature can impede our ability to detect and predict emergent MPEs under a changing climate using models like the MRM. We adapted the GFR by modeling core components of the functional response (attack rate and handling time) as nonlinear functions of temperature and compared its predictions and the MRM's against experimentally measured prey survival in the presence of two predator species. We demonstrate that the MRM and GFR can produce contradictory expectations about the presence of emergent MPEs, emphasizing the limitations of the MRM for detecting MPEs under a changing climate. Further, our research adds to a growing body of research (Barton and Schmitz 2009; Cuthbert et al. 2021; Liu et al. 2023) suggesting that risk reduction or enhancement by multiple predator species can vary across a temperature gradient.

4.2. Methods

We focused on a two predator-one prey interaction, specifically, predation of North American rock pool mosquito larvae (*Aedes atropalpus*) by eastern pondhawk dragonfly nymphs (*Erythemis simplicicollis*; see also Davidson et al. 2021) and adult predacious diving beetles (*Laccophilus maculosus*).

To test for emergent MPEs across a thermal gradient, we compared experimentally measured predation rates of *Ae. atropalpus* mosquito larvae by this two-predator assemblage to predictions yielded by both the multiplicative risk model (MRM) and a modified version of the generalized functional response (GFR) framework described in McCoy et al. (2022). Both models provide a “null expectation” for predation in the absence of predator-predator interactions – i.e., differences between their predictions and experimentally measured prey survival in the presence of both predator species suggest risk enhancement or reduction when both predator species are present. However, the GFR allows for incorporation of important nonlinear determinants of predator foraging rates, such as prey density and temperature, which are likely to bias predictions generated using the MRM (McCoy et al. 2012; McCoy et al. 2022). Thus, we subsequently compared detection of emergent MPEs by both models and directly compared predation estimates produced by both models to assess the degree of bias the MRM introduces by failing to account for density- and temperature-dependent predation.

4.2.1. Prey Survival in One- and Two-Predator Assemblages

We used an additive design to determine *Ae. atropalpus* larval predation risk in the presence of either 1) one adult *L. maculosus*, 2) one *E. simplicicollis* nymph, or 3) one individual of each predator species present. We crossed these predator treatments with three temperature treatments (20, 25, and 30 °C), for a total of 9 treatment combinations, replicated 4-6 times each (total n = 54). We used a single prey density of 80 *Ae. atropalpus* larvae across all treatments.

Because prey body size is also known to have nonlinear effects on predator foraging rates (Werner and Gilliam 1984; Vonesh and Bolker 2005; McCoy et al. 2011), we restricted the size of mosquito larvae prey to third instars only. To do so, we hatched *Ae. atropalpus* larvae prior to the experiment from rehydrated eggs and reared them to third instar on a diet of brewer's yeast and liver powder provided *ad libitum*. Larvae were kept at a constant temperature of 28 °C in environmental chambers (Percival Scientific Model I-V30L) with a 14L:10D photoperiod, in larval rearing trays filled with 600 mL of water and a stocking density of ~1000 larvae per tray (see also Davidson et al. 2021). While the larvae developed, we collected late instar *E. simplicicollis* nymphs (mean head capsule width ± SE = 4.03 ± 0.10 mm) and adult *L. maculosus* from local ponds. We held individuals of both predator species in the laboratory at room temperature (~22°C) and fed them to satiation on a diet of live brine shrimp (*Artemia* spp.) before fasting them for 48 h prior to the experiment.

We conducted the experiment in 950 mL deli cups, filled to a standardized volume of 800 mL of deionized water. To provide habitat complexity, we added four small (<4 cm diameter) river rocks and a 10-cm tall plastic aquarium plant to each cup. We added these cups to the environmental chamber that corresponded to their temperature treatment 24 h before the experiment ran, to allow the temperatures in the cups to equilibrate before the study organisms were added. The day of the experiment, we placed the mosquito larvae into the deli cups at their assigned densities and left both the larvae in the deli cups, and the predators in separate, individual 150 mL cups, in the environmental chambers to acclimate for 1 h before the experiment ran. After that hour had passed, we added the predators to their assigned deli cups with the mosquito larvae and allowed them to feed for 6 h before removing the predators and counting the number of surviving mosquito larvae in each cup. These data were subsequently used to compare against expected values for predation calculated using both the GFR and MRM, and to directly calculate expected values for predation using the MRM.

4.2.2. Detecting MPEs Using the MRM

To predict prey survival in two-predator assemblages using the MRM, we used data from the two-predator feeding trials described above. We estimated the expected number of mosquito larvae that would be consumed in the two-predator treatment in the absence of emergent MPEs by using the additive form of the MRM (Sih et al. 1998; Vonesh and Osenberg 2003; McCoy et al. 2012):

$$(1) \qquad S_{ij} = \frac{S_i * S_j}{S_c}$$

where S_{ij} is the predicted proportion of prey that survive in the presence of both predator species, S_i and S_j are the observed proportion of prey that survive in the presence of each predator alone, and S_c is prey survival in the absence of predators (assumed here to be 1 due to low background mortality and short experimental duration; see Davidson et al. 2021).

To carry over measurement error in estimating S_i and S_j to the MRM's expected values for prey survival, we randomly resampled pairs of values for S_i and S_j from distributions defined by the observed means and standard deviations of each value. We then used these values to predict expected prey survival under the MRM by solving Eqn. 1 for a total of 500 replicates. We assessed whether the MRM detected an emergent MPE during our experiment by comparing these simulated expected values to observed levels of prey survival during the experiment. We considered an emergent MPE to have been detected by the MRM if the expected value for prey survival did not overlap with the 95% confidence interval for observed prey survival. Specifically, if observed prey survival was greater than we would expect from the MRM, this suggests risk reduction in the presence of both predators. Similarly, if observed prey survival was less than we would expect as estimated by the MRM, this suggests that the presence of both predators enhances prey risk.

4.2.3. Detecting MPEs Using the GFR

Using the GFR framework to detect MPEs requires measuring both predators' functional responses in isolation. To do so, we measured the foraging rates of both species separately on *Ae. atropalpus* larvae across a set of constant temperatures (20, 24, 28, 32, and 36 °C) over a 24 h period, with a 14L:10D photoperiod. We crossed these temperature treatments with a range of prey densities (10, 20, 30, 40, or 80 mosquito larvae for *L. maculosus*; and 10, 20, 40, 60, and 80 mosquito larvae for *E. simplicicollis*) using a response surface design to reduce the number of experimental treatments needed to fit the functional response (McCoy and Bolker 2008; Fig. S4.1).

We conducted this experiment in the same venues used in the feeding trials described above, consisting of a 950 mL deli cup filled to 800 mL of deionized water, four small (<4 cm diameter) river rocks, and one plastic plant. Prior to the experiment, mosquito larvae and predators were prepared using the same protocols for rearing, predator fasting, and acclimation described above. We assigned each cup one predator species (either *E. simplicicollis* or *L. maculosus*), temperature, and prey density as described above.

After allowing all experimental organisms to acclimate using the protocol outlined above, we added the predators to their assigned deli cups with the mosquito larvae and allowed them to feed for a full 24 h. At the end of the 24 h period, we removed the predator from each deli cup and counted the remaining mosquito larvae in each cup.

Using these data, we described each predator species' foraging rate by fitting a Type II functional response, accounting for prey depletion (Rogers 1972), that depended upon both prey density and temperature. Specifically, we modeled prey consumption as:

$$(2) \qquad N = N_0 - \frac{W(ahN_0 e^{-a(t-hN_0)}}{ah}$$

where N is the number of prey eaten after time t (24 h), N_0 is the initial number of prey, a is the attack rate, h is the handling time, and W is the Lambert's W function (McCoy and Bolker 2008).

We incorporated temperature as a nonlinear driver of predator feeding rates by modeling attack rate and handling time using the following equations (Sentis et al. 2012; Davidson et al. 2021). Attack rate (a) is described as a unimodal function of temperature in Celsius (T) as:

$$(3) \qquad a = b(T - T_{min})(T_{max} - T)^{1/2}$$

where b is a fitted species-specific constant, and T_{min} and T_{max} are the predator's lower and upper thermal bounds for activity, respectively (Briere et al. 1999; Sentis et al. 2012; Davidson et al. 2021). We modeled handling time (h) as a power function of temperature in Celsius (T) and predator body mass in mg (M) as:

$$(4) \qquad h = h_0 M^{b_h e^{Eh/k(T+273.15)}}$$

where h_0 is a species-specific fitted constant, b_h is an allometric scaling constant (0.75; Brown et al. 2004), E_h is the activation energy for the rate-limiting enzyme-catalyzed biochemical rate of metabolism (eV) and k is Boltzmann's constant (8.62×10^{-5} eV/K; i.e., the Arrhenius equation; Brown et al. 2004).

We used the following estimates for the lower and upper temperature thresholds for activity of our predator species. For *E. simplicicollis*, we estimated T_{min} as 10 °C (the approximate temperature at which growth stops for most Odonate nymphs; Suhling et al. 2015) and T_{max} as 42.2 °C (the median CT_{max} for Libellulid dragonfly nymphs; Dallas and Rivers-Moore 2012). For *L. maculosus,* we estimated T_{min} as 6.4 °C and T_{max} as 41.6 °C (from two congeneric species; Hidalgo-Galiana et al. 2021). We estimated the biomass of both predator species by taking the wet mass of a subsample of 25 individuals of each predator species after fasting them for a 24-48 h after the experiment ran. Mean *E. simplicicollis* nymph wet mass was 114.2 ± 7.5 mg (M ± SE), while mean adult *L. maculosus* wet mass was 23.5 ± 1.1 mg.

Using these functional response estimates, we applied the GFR to estimate prey consumption in the presence of both predators by integrating the sum of both predators' functional responses (Eqn. 2) over the 6 h duration of the experiment described above. As with our approach for propagating error in the MRM, we incorporated error in estimating the functional response parameters by randomly resampling values for b, h_0, and E_h in Eqn.s 3-4 from distributions defined by their means and standard deviations in these calculations, for a total of 500 simulated replicates. As before, we assessed whether the GFR detected an emergent MPE during our experiment by comparing simulated expected prey survival to observed levels prey survival during the experiment and looking for the presence or absence of overlap in their 95% confidence intervals.

4.2.4. *Estimating Bias*

By ignoring nonlinear determinants of predation risk such as prey depletion and temperature, the MRM can produce biased estimates of predation by assemblages consisting of multiple predators (McCoy et al. 2012; Sentis and Boukal 2017; McCoy et al. 2022). To estimate this bias, we conducted a series of pairwise comparisons between the GFR and MRM's estimates of prey survival at each temperature and the mean expected number of prey killed across all temperatures under the MRM and GFR (i.e., ignoring temperature-dependent predation; $\mathrm{GFR}_{\mathrm{TI}}$ and $\mathrm{MRM}_{\mathrm{TI}}$). These comparisons serve to estimate to the amount of bias introduced by ignoring density-dependence and depletion (i.e., the GFR's estimates vs. the MRM's), temperature-dependence alone (i.e., the GFR's estimates vs. the $\mathrm{GFR}_{\mathrm{TI}}$'s), and both density- and temperature-dependence (i.e., the GFR's estimates vs. the $\mathrm{MRM}_{\mathrm{TI}}$'s).

4.3. Results

4.3.1. *Detection of MPEs by the MRM and GFR*

The number of prey killed in two-predator assemblages only increased at the warmest experimental temperature (observed mean at 30°C = 27.3, 95% CI: 23.4 to 31.2). The number of prey killed at 20 and 25°C was lower by comparison and did not differ substantially between the two temperatures (observed mean at 20°C = 22.3, 95% CI: 20.0 to 24.7; and observed mean at 25°C = 20.3, 95% CI: 18.5 to 22.1). Relative to the cooler temperatures, the number of prey consumed was 1.2-1.3X greater at 30°C.

In single predator assemblages, the number of prey killed by *E. simplicicollis* increased strongly with temperature, from 7.8 ± 2.0 (mean ± std. error) at the lowest temperature (20°C) to 16.0 ± 2.6 at the highest temperature (30°C). However, predation by *L. maculosus* increased only modestly with temperature across the same range, from 11.3 ± 1.2 at 20°C to 13.8 ± 2.0 at 30°C (Fig. 4.1). This finding was mirrored in the functional response experiments (Fig. 4.2), where *E. simplicicollis* (Fig. 4.2a, c) displayed a stronger response to temperature than *L. maculosus* (Fig. 4.2b, d). In the functional response experiments, *E. simplicicollis* consumed approximately 81.3% more mosquito larvae at 20°C relative to 36°C (at $N_0 = 80$), while *L. maculosus* only consumed 54.8% more across the same thermal gradient (at $N_0 = 80$; Fig. 4.2).

Using these observed values, we produced expected values for the number of prey killed by both predators using the MRM. The MRM detected prey risk enhancement at 20°C (Fig. 4.3; expected mean = 18.0), but risk reduction at 25°C (expected mean = 22.7). At 30°C, the MRM's expected number of prey killed did not differ from the observed number of prey killed (expected mean = 27.0).

We estimated prey survival using the GFR by first fitting separate temperature-dependent functional response models for both predators (Fig. 4.2; Table 4.1). By applying the GFR using those functional response models, the GFR detected slight risk enhancement, but only at 20°C (Fig. 3; expected mean = 17.4). The GFR's expected values for the number of prey killed did not differ from the observed number of prey killed at either 25°C (expected mean = 21.9) or 30°C (expected mean = 23.9).

4.3.2. Bias Introduced by Ignoring Prey Depletion and Temperature

Both the magnitude and direction of bias introduced by ignoring temperature- and density-dependent predation varied depending upon which of these relationships was unaccounted for. When prey density and depletion were unaccounted for (i.e., GFR vs. MRM; Fig. 4.4a), the MRM's predictions were biased towards overestimating predation (i.e., detecting risk reduction) at each temperature relative to the GFR, and the degree of bias increased at the warmest temperatures (Fig. 4.4a). When temperature-dependence alone was unaccounted for (i.e., GFR vs. $\mathrm{GFR}_{\mathrm{TI}}$; Fig. 4.4b), the direction of bias varied with temperature such that at the coolest temperature (20°C) the mean expected number of prey killed under the GFR overestimated predation (i.e., detecting risk reduction), while at warmer temperatures (25 and 30°C) it underestimated predation (i.e., detecting risk enhancement; Fig. 4.4b). When both temperature-dependence and prey depletion were unaccounted for (i.e., GFR vs. $\mathrm{MRM}_{\mathrm{TI}}$; Fig. 4.4c), the MRM performed similarly to $\mathrm{GFR}_{\mathrm{TI}}$, but it was more strongly biased towards overestimating the number of prey killed at all but the very warmest temperature (i.e., detecting risk reduction at all but 30°C; Fig. 4.4c).

4.4. Discussion

Predicting how predator-prey interactions and other community-level processes will change under a changing climate remains challenging due to the myriad ways in which environmental temperature can affect organisms. Temperature can impact the rate at which predators forage for, attack, and consume prey, as well as the behavior and spatiotemporal range of predators and their prey, which may fundamentally change how, when, and even whether they interact with one another (Rall et al. 2010; Jochum et al. 2012; Lurgi et al. 2012). Understanding how climate change will impact predation is especially challenging when multiple predator species share a common prey, because the combined effects of multiple predators on a single prey are often not easily predicted from their independent effects on that prey (Sih et al. 1998). Thus, it is critical that we develop tools to better understand and predict the occurrence of emergent multiple predator effects (MPEs) under a changing climate.

Our findings add to a growing body of evidence that simple and widely used models such as the multiplicative risk model (MRM) fail to accurately predict the combined impact of two or more predators on shared prey, because they fail to account for fundamentally predictable nonlinear determinants of predation, such as prey depletion, body size, or temperature (McCoy et al. 2012; Sentis and Boukal 2018; McCoy et al. 2022). Specifically, we found that failing to account for both prey depletion and temperature caused the MRM to detect emergent MPEs at two out of three experimental temperatures. At the coolest temperatures (20°C), the MRM detected risk enhancement between *E. simplicicollis* dragonfly nymphs and adult *L. maculosus* diving beetles feeding on *Ae. atropalpus* mosquito larvae, while at intermediate temperatures (25°C) the MRM suggested that slight risk suppression occurred (Fig. 4.3). By comparison, the generalized functional response (GFR) framework, which does account for prey depletion and temperature, only detected risk enhancement at the coolest temperatures (20°C; Fig. 4.3).

Our findings corroborate recent studies that suggest that the occurrence of emergent MPEs can vary with temperature (Barton and Schmitz 2009; Cuthbert et al. 2021; Liu et al. 2023). While prey risk was enhanced at cool temperatures in mixed predator assemblages, this risk enhancement was not detected at warmer temperatures. While we did not determine the mechanism behind risk enhancement in this study, we suspect that the presence of actively foraging adult *L. maculosus* may have increased encounters between mosquito larvae and *E.*

simplicicollis nymphs, which are generally sit-and-wait predators (Corbet 1960; Pritchard 1965; Larson et al. 2000; Bofill and Yee 2019). However, at warmer temperatures this effect may have been overridden by increased competition between the two predators, particularly by *E. simplicicollis*, which appears to be more sensitive to temperature (Fig. 4.3) and may switch to active foraging strategies at warmer temperatures (e.g., Hirvonen and Ranta 1996). Alternatively, this temperature-driven change in predation risk could be mediated by prey behavior – *Ae. atropalpus* are generally considered a warm-adapted species (Byrd et al. 2019; Day et al. 2021) and thus may simply be more active with tasks such as foraging for food at warmer temperatures, regardless of predation risk. In either case, our findings suggest that when increasing temperatures reduce risk enhancement between multiple predators and/or increases risk suppression (via increased competition), greater predator diversity may limit the effects of climate change on overall predation strength.

In our simulations, we found that failing to account for density- and temperature-dependent predation had varying consequences for the detection of MPEs, depending on which processes were ignored. When density-dependence and prey depletion alone were ignored (i.e., GFR vs. MRM), the MRM was more likely to overestimate predation relative to the GFR, biasing towards the detection of risk reduction (Fig. 4.4a). When temperature-dependence was ignored but prey depletion was accounted for (i.e., GFR vs. $\mathrm{GFR}_{\mathrm{TI}}$; Fig. 4.4b), model bias varied with temperature, such that predation was overestimated at low temperature (i.e., risk suppression at 20°C; Fig. 4.4b) but underestimated at intermediate and high temperatures (i.e., risk enhancement at 25 and 30°C; Fig. 4.4b). By ignoring both density- and temperature-dependence (i.e., GFR vs. $\mathrm{MRM}_{\mathrm{TI}}$; Fig. 4.4c), model predictions were similar to simulations without temperature-dependence alone but were more strongly biased towards overestimating predation (i.e., risk suppression at all but 30°C; Fig. 4.4c). Taken collectively, these findings suggest that failing to properly account for nonlinear determinants of predation rates can lead to false conclusions about the occurrence, magnitude, and direction (i.e., suppression or enhancement) of emergent MPEs, particularly across temperature gradients.

Overall, the MRM produced higher estimates for predation across all temperatures relative to the GFR, with model estimates diverging most at the warmest temperature considered (30°C; Fig. 4.3). This may be in part because the MRM does not account for prey depletion (McCoy et al. 2011; Sentis and Boukal 2018; McCoy et al. 2022), and temperature-dependent increases in overall predation rates likely caused greater depletion at warmer temperatures. While the GFR and MRM both did not detect an MPE at 30°C, the MRM's estimate was closer to the observed number of prey killed in mixed predator assemblages than the GFR's. However, it is important to note that depending on the shape of the relationship between predation rates and any factors that might modify it (e.g., temperature here; prey size in McCoy et al. 2012, McCoy et al. 2022), the MRM can predict either higher or lower risk than would otherwise be expected (McCoy et al. 2022). Additionally, our model simulations suggest that the MRM is more likely to overestimate predation at warmer temperatures (Fig. 4.4c). Thus, the MRM's failure to account for these types of nonlinear modifiers of predation rate may lead to both false positive and negative detection of MPEs.

While our findings already highlight the importance of accounting for nonlinear processes when detecting emergent MPEs, they may still under-emphasize the importance of using models like the GFR framework over the MRM for these purposes. For example, it is important to remember that our MPE experiment was conducted over a very short time frame (6 h), and the bias introduced by prey depletion is stronger over longer experimental durations

(McCoy et al. 2022). Additionally, experimental detection of emergent MPEs is commonly done by comparing the 95% confidence intervals between observed and expected prey survival in the presence of multiple predators (e.g., Sih et al. 1998; McCoy et al. 2012; Sentis and Boukal 2018). However, from a statistical standpoint, the 95% confidence interval for a simple categorical model like the MRM will naturally tend to be smaller than the prediction intervals for a more complex regression-style model like the GFR (Dormann et al. 2018). Thus, the MRM may also be statistically biased towards detecting MPEs.

While use of the GFR framework lacks the experimental and computational simplicity of the MRM, our study adds to a growing body of research that suggests that the MRM may falsely attribute to MPEs what can instead be explained by known nonlinear determinants of predation risk. Despite this, the MRM has been cited in over 1350 studies, and its inferences remain influential in the field of predator-prey ecology (McCoy et al. 2022). The GFR allows for easy incorporation of modifier-dependent predation risk introduced by prey density, body size, and other processes (McCoy et al. 2012; Sentis and Boukal 2018; McCoy et al. 2022), and its use may be especially important in understanding and predicting MPEs under a changing climate. By making use of functional response models, the GFR can draw on a large body of theoretical and mechanistic models that describe the effects of these variables on predation (e.g., Rogers 1972; McCoy et al. 2011; Sentis et al. 2012), allowing more accurate forecasting and detection of emergent MPEs in nature.

4.5. References

Barton, B. T., & Schmitz, O. J. (2009). Experimental warming transforms multiple predator effects in a grassland food web. *Ecology Letters*, *12*(12), 1317–1325. https://doi.org/10.1111/j.1461-0248.2009.01386.x

Bofill, C. E., & Yee, D. A. (2019). An army of one: predaceous diving beetle life history stages affect interactions with shared mosquito prey. *Hydrobiologia*, *827*(1), 201–209. https://doi.org/10.1007/s10750-018-3765-y

Briere, J.-F., Pracros, P., le Roux, A.-Y., & Pierre, J.-S. (1999). A novel rate model of temperature-dependent development for arthropods. *Environmental Entomology*, *28*(1), 22–29.

Brown, J. H., Gillooly, J. F., Allen, A. P., Savage, V. M., & West, G. B. (2004). Toward a metabolic theory of ecology. *Ecology*, *85*(7), 1771–1789. https://doi.org/Doi 10.1890/03-9000

Byrd, B. D., Sither, C. B., Goggins, J. A., Kunze-Garcia, S., Pesko, K. N., Bustamante, D. M., Sither, J. M., Vonesh, J. R., & O'meara, G. F. (2019). Aquatic thermal conditions predict the presence of native and invasive rock pool Aedes (Diptera: Culicidae) in the southern Appalachians, U.S.A. *Journal of Vector Ecology*, *44*(1), 30–39.

Cardinale, B. J., Duffy, J. E., Gonzalez, A., Hooper, D. U., Perrings, C., Venail, P., Narwani, A., Mace, G. M., Tilman, D., Wardle, D. A., & Kinzig, A. P. (2012). Biodiversity loss and its impact on humanity. *Nature*, *486*(7401), 59–67. https://doi.org/10.1038/nature11148.Access

Corbet, P. S. (1999). Dragonflies: Behavior and Ecology of Odonata. Cornell University Press

Crumrine, P. W., & Crowley, P. H. (2003). Partitioning components of risk reduction in a dragonfly-fish intraguild predation system. *Ecology*, *84*(6), 1588–1597. https://doi.org/10.1890/0012-9658(2003)084[1588:PCORRI]2.0.CO;2

Cuthbert, R. N., Wasserman, R. J., Dalu, T., & Briski, E. (2021). Warming mediates intraspecific multiple predator effects from an invasive crustacean. *Marine Biology*, *168*(3). https://doi.org/10.1007/s00227-021-03840-z

Dallas, H. F., & Rivers-Moore, N. A. (2012). Critical Thermal Maxima of aquatic macroinvertebrates: Towards identifying bioindicators of thermal alteration. *Hydrobiologia*, *679*(1), 61–76. https://doi.org/10.1007/s10750-011-0856-4

Davidson, A. T., Hamman, E. A., McCoy, M. W., & Vonesh, J. R. (2021). Asymmetrical effects of temperature on stage-structured predator–prey interactions. *Functional Ecology*, *35*(5). https://doi.org/10.1111/1365-2435.13777

Day, C. A., Armstrong, E. G., & Byrd, B. D. (2021). Population growth rates of Aedes atropalpus (Diptera: Culicidae) are depressed at lower temperatures where Aedes japonicus japonicus (Diptera: Culicidae) are naturally abundant in rock pools. *Journal of Medical Entomology*, *58*(1), 493–497. https://doi.org/10.1093/jme/tjaa183

Dormann, C. F., Calabrese, J. M., Guillera-Arroita, G., Matechou, E., Bahn, V., Bartoń, K., Beale, C. M., Ciuti, S., Elith, J., Gerstner, K., Guelat, J., Keil, P., Lahoz-Monfort, J. J., Pollock, L. J., Reineking, B., Roberts, D. R., Schröder, B., Thuiller, W., Warton, D. I., … Hartig, F. (2018). Model averaging in ecology: a review of Bayesian, information-theoretic, and tactical approaches for predictive inference. In *Ecological Monographs* (Vol. 88, Issue 4, pp. 485–504). Ecological Society of America. https://doi.org/10.1002/ecm.1309

Englund, G., Öhlund, G., Hein, C. L., & Diehl, S. (2011). Temperature dependence of the functional response. *Ecology Letters*, *14*(9), 914–921. https://doi.org/10.1111/j.1461-0248.2011.01661.x

Griffen, B. D., & Byers, J. E. (2006). Intraguild predation reduces redundancy of predator species in multiple predator assemblage. *Journal of Animal Ecology*, *75*, 959–966. https://doi.org/10.1111/j.1365-2656.2006.01115

Hidalgo-Galiana, A., Ribera, I., & Terblanche, J. S. (2021). Geographic variation in acclimation responses of thermal tolerance in South African diving beetles (Dytiscidae: Coleoptera). *Comparative Biochemistry and Physiology -Part A : Molecular and Integrative Physiology*, *257*. https://doi.org/10.1016/j.cbpa.2021.110955

Hirvonen, H., & Ranta, E. (1996). Prey to predator size ratio influences foraging efficiency of larval Aeshna juncea dragonflies. *Oecologia*, *106*(3), 407–415. https://doi.org/10.1007/BF00334569

Holling, C. S. (1959). The components of predation as revealed by a study of small-mammal predation of the european pine sawfly. *The Canadian Entomologist*, *91*(5), 293–320.

Jeschke, J. M., Kopp, M., & Tollrian, R. (2004). Consumer-food systems: Why type I functional responses are exclusive to filter feeders. *Biological Reviews of the Cambridge Philosophical Society*, *79*(2), 337–349. https://doi.org/10.1017/S1464793103006286

Jochum, M., Schneider, F. D., Crowe, T. P., Brose, U., & O'Gorman, E. J. (2012). Climate-induced changes in bottom-up and top-down processes independently alter a marine ecosystem. *Philosophical Transactions of the Royal Society B: Biological Sciences*, *367*, 2962–2970. https://doi.org/10.1098/rstb.2012.0237

Larson, D. J., Y. Alarie & R. E. Roughley, 2000. Predaceous Diving Beetles Coleoptera: Dytiscidae of the Nearctic Region. NCR Research Press, Ottawa.

Liu, D., Zhu, B., Liang, Q., Zhang, H., Dong, S., & Wang, F. (2023). High temperatures enhance the strength of multiple predator effects in a typical crab-clam system. *Marine Pollution Bulletin*, *188*. https://doi.org/10.1016/j.marpolbul.2023.114670

Lurgi, M., López, B. C., & Montoya, J. M. (2012). Novel communities from climate change. *Philosophical Transactions of the Royal Society B: Biological Sciences*, *367*, 2913–2922. https://doi.org/10.1098/rstb.2012.0238

McCoy, M. W., & Bolker, B. M. (2008). Trait-mediated interactions: Influence of prey size, density and experience. *Journal of Animal Ecology*, *77*(3), 478–486. https://doi.org/10.1111/j.1365-2656.2008.01372.x

McCoy, M. W., Stier, A. C., & Osenberg, C. W. (2012). Emergent effects of multiple predators on prey survival: The importance of depletion and the functional response. *Ecology Letters*, *15*(12), 1449–1456. https://doi.org/10.1111/ele.12005

McCoy, M. W., Bolker, B. M., Warkentin, K. M., & Vonesh, J. R. (2011). Predicting Predation through Prey Ontogeny Using Size-Dependent Functional Response Models. *The American Naturalist*, *177*(6), 752–766. https://doi.org/10.1086/659950

McCoy, M. W., Hamman, E., Albecker, M., Wojdak, J., Vonesh, J. R., & Bolker, B. M. (2022). Incorporating nonlinearity with generalized functional responses to simulate multiple predator effects. *PeerJ*, *10*, e13920. https://doi.org/10.7717/peerj.13920

Preisser, E. L., Orrock, J. L., & Schmitz, O. J. (2007). Predator hunting mode and habitat domain alter nonconsumptive effects in predator-prey interactions. *Ecology*, *88*(11), 2744–2751. https://doi.org/10.1890/07-0260.1

Pritchard, G. (1965). Prey capture by dragonfly larvae (Odonata: Anisoptera). *Canadian Journal of Zoology*. 43(2): 271-289. https://doi.org/10.1139/z65-026

Rall, B. C., Vucic-Pestic, O., Ehnes, R. B., Emmerson, M. C., & Brose, U. (2010). Temperature, predator–prey interaction strength and population stability. *Global Change Biology*, *16*, 2145–2157. https://doi.org/10.1111/j.1365-2486.2009.02124.x

Rogers, D. (1972). Random Search and Insect Population Models. *Journal of Animal Ecology*, *41*(2), 369–383.

Sentis, A., & Boukal, D. S. (2018). On the use of functional responses to quantify emergent multiple predator effects. *Scientific Reports*, *8*(1), 11787. https://doi.org/10.1038/s41598-018-30244-9

Sentis, A., Hemptinne, J.-L. L., & Brodeur, J. (2012). Using functional response modeling to investigate the effect of temperature on predator feeding rate and energetic efficiency. *Oecologia*, *169*(4), 1117–1125. https://doi.org/10.1007/s00442-012-2255-6

Sentis, A., Gémard, C., Jaugeon, B., & Boukal, D. S. (2017). Predator diversity and environmental change modify the strengths of trophic and nontrophic interactions. *Global Change Biology*, *23*(7), 2629–2640. https://doi.org/10.1111/gcb.13560

Sih, A., Englund, G., & Wooster, D. (1998). Emergent impacts of multiple predators on prey. *Trends in Ecology and Evolution*, *13*(9), 350–355. https://doi.org/10.1016/S0169-5347(98)01437-2

Soluk, D. A., & Collins, N. C. (1988). *Synergistic Interactions between Fish and Stoneflies: Facilitation and Interference among Stream Predators* (Vol. 52, Issue 1). https://www.jstor.org/stable/3565987

Suhling, F., Suhling, I., & Richter, O. (2015). Temperature response of growth of larval dragonflies – an overview. *International Journal of Odonatology*, *18*(1), 15–30. https://doi.org/10.1080/13887890.2015.1009392

Swisher, B. J., Soluk, D. A., & Wahl, D. H. (1998). *Non-Additive Predation in Littoral Habitats: Influences of Habitat Complexity* (Vol. 81, Issue 1). https://www.jstor.org/stable/3546464

Uszko, W., Diehl, S., Englund, G., & Amarasekare, P. (2017). Effects of warming on predator-prey interactions -- a resource-based approach and a theoretical synthesis. *Ecology Letters*, *20*(4), 513–523. https://doi.org/10.1111/ele.12755

Vance-Chalcraft, H. D., & Soluk, D. A. (2005). Multiple predator effects result in risk reduction for prey across multiple prey densities. *Oecologia*, *144*(3), 472–480. https://doi.org/10.1007/s00442-005-0077-5

Vonesh, J. R., & Bolker, B. M. (2005). Compensatory larval responses shift trade-offs associated with predator-induced hatching plasticity. *Ecology*, *86*(6), 1580–1591. https://doi.org/10.1890/04-0535

Vonesh, J. R., & Osenberg, C. W. (2003). Multi-predator effects across life-history stages: Non-additivity of egg- and larval-stage predation in an African treefrog. *Ecology Letters*, *6*(6), 503–508. https://doi.org/10.1046/j.1461-0248.2003.00470.x

Vucic-Pestic, O., Rall, B. C., Kalinkat, G., & Brose, U. (2010). Allometric functional response model: Body masses constrain interaction strengths. *Journal of Animal Ecology*, *79*(1), 249–256. https://doi.org/10.1111/j.1365-2656.2009.01622.x

Werner, E. E., & Gilliam, J. F. (1984). The Ontogenetic Niche and Species Interactions in Size-Structured Populations. *Annual Review of Ecology and Systematics*, *15*, 393–425.

Werner, E. E., & Peacor, S. D. (2003). A review of trait-mediated indirect interactions in ecological communities. In *Ecology* (Vol. 84, Issue 5, pp. 1083–1100). Ecological Society of America. https://doi.org/10.1890/0012-9658(2003)084[1083:AROTII]2.0.CO;2

4.6. Figures and Tables

Fig. 4.1. The mean number of *Ae. atropalpus* mosquito larvae killed in a 6 h period by either one *E. simplicicollis* dragonfly nymph (red), one adult *L. maculosus* diving beetle (dark blue), or one of each predator species (green). Error bars represent the standard error of the mean.

Fig 4.2. The functional response of a) *E. simplicicollis* nymphs and b) adult *L. maculosus* diving beetles feeding on *Ae. atropalpus* larvae, as a function of initial prey density (a-b) and temperature (c-d). Data were measured at a range of constant temperatures from 20°C to 36°C. Functional responses were fit accounting for depletion, with attack rate and handling time modeled as functions of temperature as described in Eqn. 2-4.

Fig. 4.3. Expected values for the number of *Ae. atropalpus* mosquito larva prey killed during a 6 h period by a mixed predator assemblage of one *Erythemis* nymph and one adult *Laccophilus* diving beetle, as calculated using the GFR approach (gold) or MRM (light blue), as compared to mean observed values from the experiment (green). Error bars represent the 95% confidence interval for the observed values. While the MRM detected risk enhancement at 20°C and slight suppression at 25°C, the GFR only detected risk enhancement at 20°C.

Fig 4.4. A comparison between the expected number of *Ae. atropalpus* mosquito larva prey killed in a six-hour period by a mixed assemblage of one *Erythemis* nymph and one adult *Laccophilus* diving beetle, as calculated using the GFR and the MRM. In panel a), the MRM's predictions (light blue) are shown alongside the GFR's predictions (gold) across all temperatures, to show the consequences of ignoring density-dependent predation and prey depletion when detecting emergent MPEs. In panel b), the GFR's predictions (solid line, gold) across all temperatures are shown as compared to the mean expected number of prey killed under the GFR (blue dashed line), to show the consequences of ignoring temperature-dependence alone. Last, in panel c), the GFR's predictions (solid line, gold) are shown alongside the mean expected number of prey killed under the MRM (dotted line), to show the consequences of ignoring both temperature- and density-dependence.

Table 4.1. Log-transformed parameter estimates for models describing the temperature-dependence of the functional response of *E. simplicicollis* dragonfly nymphs and adult *L. maculosus*. Functional response equations are given in Eqns 2-4.

Fig. 4.1.

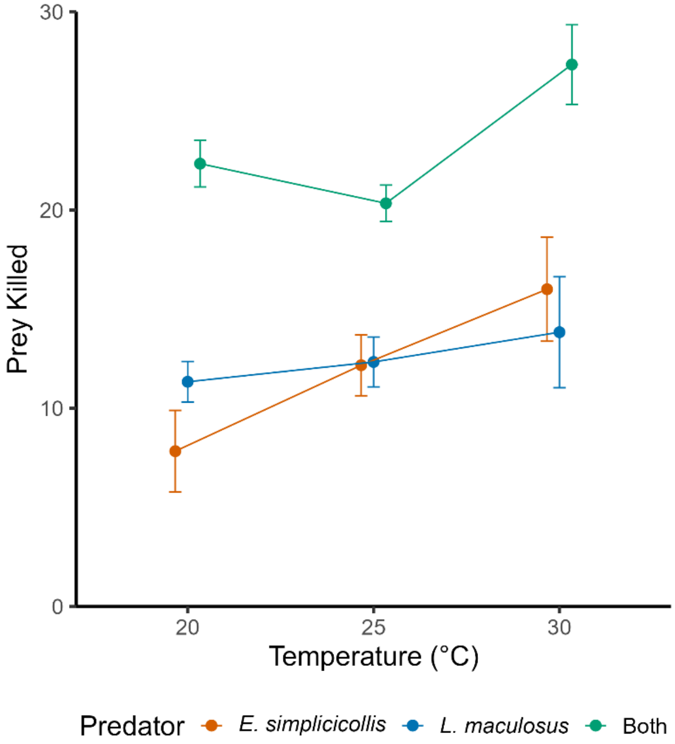

30
20
10
0
Prey Killed
20
25
30
Temperature (°C)
Predator
E. simplicicollis
L. maculosus
Both

Fig. 4.2.

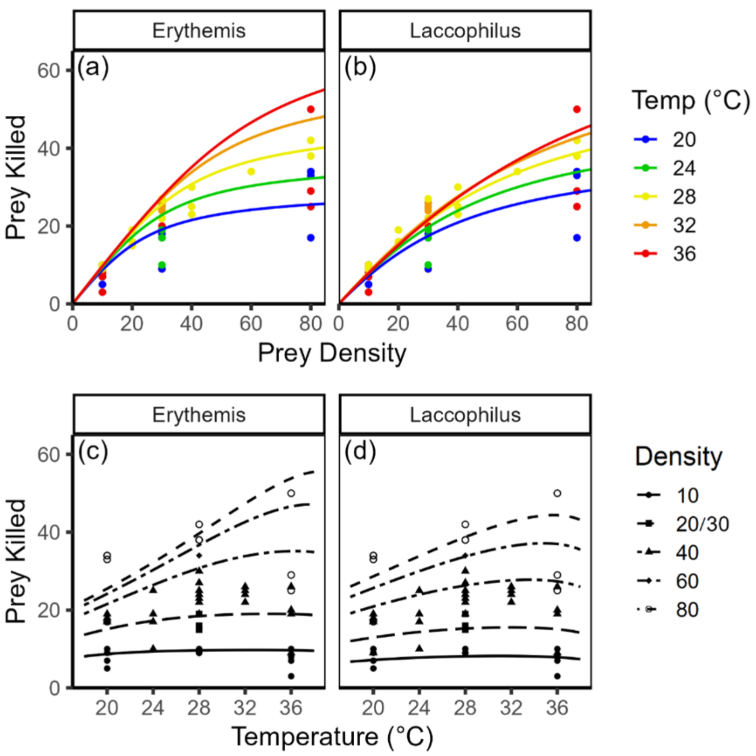
Erythemis
Laccophilus
(a)
(b)
Prey Killed
Prey Density
0
20
40
60
80
Temp (°C)
20
24
28
32
36
Erythemis
Laccophilus
(c)
(d)
Prey Killed
Temperature (°C)
20
24
28
32
36
Density
10
20/30
40
60
80

Fig. 4.3.

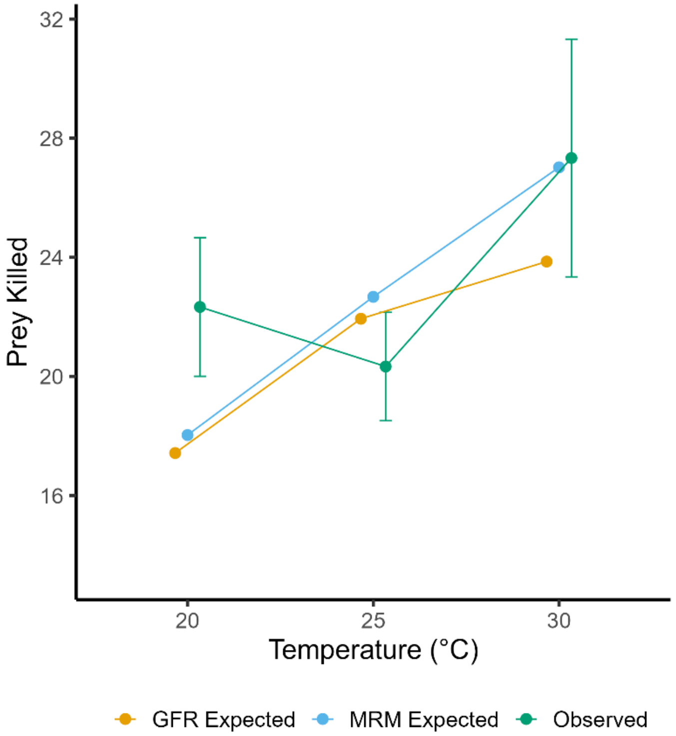
Prey Killed
32
28
24
20
16
20
25
30
Temperature (°C)
GFR Expected
MRM Expected
Observed

Fig. 4.4.

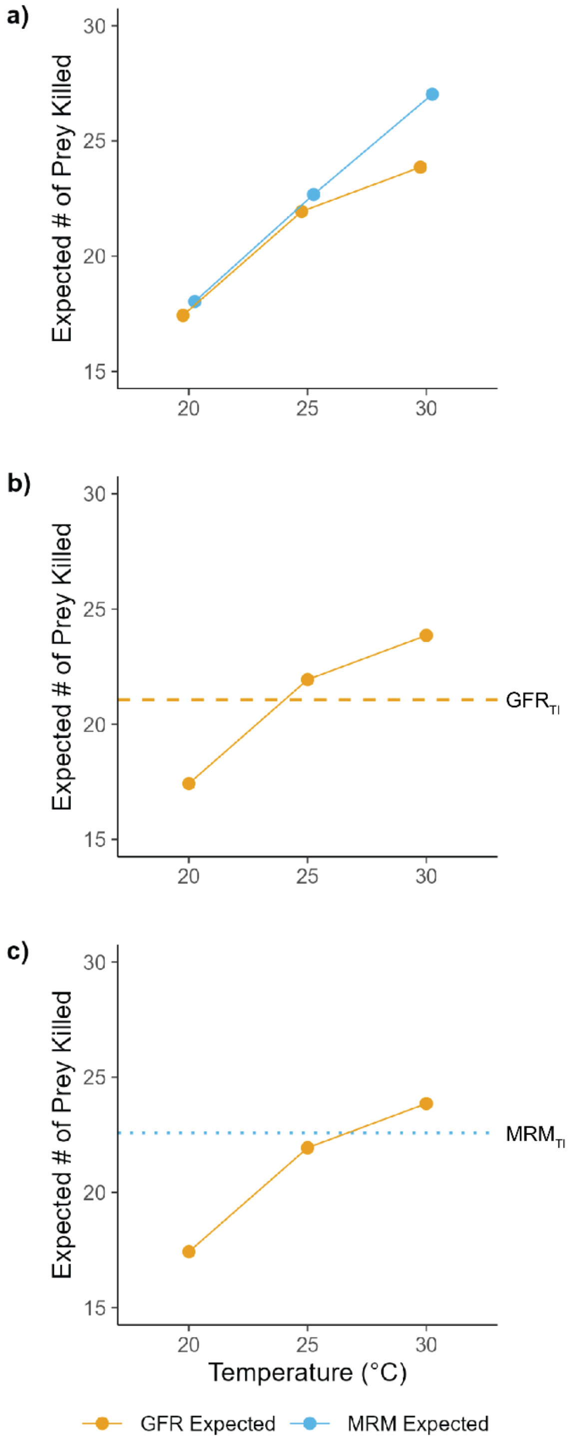
a)
b)
c)
Expected # of Prey Killed
30
25
20
15
20
25
30
GFR_TI
MRM_TI
Temperature (°C)
GFR Expected
MRM Expected

Table 4.1.

Predator	Parameter	Estimate	Std. Error	*p* value
E. simplicicollis	*b*	-2.791	0.116	<0.001
	h0	-25.0	0.493	<0.001
	E_h	-0.785	0.028	<0.001
L. maculosus	*b*	-3.717	0.081	<0.001
	h0	-20.373	2.187	<0.001
	E_h	-1.018	0.155	<0.001

4.7. Supplementary Materials

Fig. S4.1. The response surface design used to collect data on the temperature-dependence of the functional response for a) *E. simplicicollis* nymphs and b) adult *L. maculosus* diving beetles, feeding on *Ae. atropalpus* mosquito larvae.

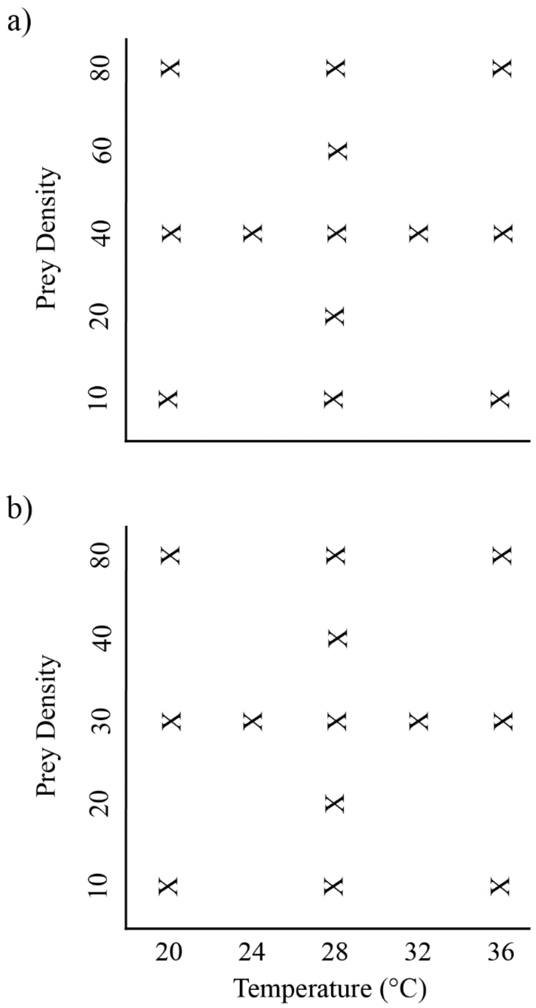

Vita

Andrew T. Davidson was born on April 9, 1991 in Memphis, Tennessee. He attended Florida State University and received his B.S. in Biological Sciences in 2013. He then subsequently began graduate studies in 2014, attending Florida Atlantic University and receiving his M.S. in Biological Sciences in 2016. He briefly worked as a research assistant during the spring and summer of 2017 before beginning studies at Virginia Commonwealth University during fall of the same year. He received his Ph.D. in Integrative Life Sciences from Virginia Commonwealth University in 2023.